SORPTION OF TETRACYCLINE ANTIBIOTICS ON NATURAL AND MODIFIED ZEOLITE

by

Aslı Ş. Şalcıoğlu

M.S. in Marine Biology, Istanbul University, 2000

Submitted to the Institute of Environmental Sciences in partial fulfillment of

the requirements for the degree of

Master of Science

in

Environmental Sciences

Boğaziçi University

2007

ACKNOWLEDGMENTS

I would like to express sincere thanks to my advisor, Prof. Dr. Işıl Balcıoğlu for her guidance, support, and patience with me. I thank for her all she has done for me.

I would also like to thank my dissertation committee, Prof. Dr. Orhan Yenigün and Prof. Dr. Naz Zeynep Atay for their suggestions and advice.

I thank Dr. Gülhan Özkosemen for metal analysis. I also thank for Gökhan Çaylı, for his technical assistance with Infrared Spectrophotometer. I would like to thank for Aslı Çakır for X-ray Diffraction Analysis and Sinan Şen for his technical guidance with Scanning Electron Microscopy Analysis.

I am thankful to Assoc. Prof. Ayşen Erdinçler for permission using centrifuge. I also thank research assistance Aslı Aköz for her guidance using centrifuge.

Lastly and most importantly, I would like to thank my mother for her loving support and patience with me.

ABSTRACT

Antibiotics found in different compartments of environment are classified as emerging pollutants due to their potential for forming resistance and their bacterial toxicity. Animal farming and aquaculture facilities are two potential sources for antibiotic pollution in the environment.

In this study, the adsorption of widely used antibiotic, oxytetracycline (OTC) onto sodium (Na) and hexadecyltrimethylammonium (HDTMA) modified zeolite was investigated. Adsorption studies were carried out at different OTC concentrations, initial solution pH, and adsorbent doses.

The adsorption isotherm data were fitted to the Freundlich model. The adsorption capacities of Na and HDTMA-modified zeolite were found as 2.5 x 10^{-1} $mg^{1-n}L^{n}/g$ at pH 6.5 and $3x10^{-1}mg^{1-n}L^{n}/g$ at pH 8, respectively. HDTMA-modified zeolite exhibited stronger pH dependence and 90 per cent antibiotic removal was achieved at pH 8 with 30 mg/L OTC. The adsorption capacity of Na-zeolite did not change significantly in the pH range of 2-10 and it exhibited a maximum OTC adsorption of 88 per cent at pH 6.5. The simplified kinetic models including pseudo-first order, pseudo-second, and intraparticle diffusion equations were selected to determine adsorption model.

The effect of various ions on the adsorption of OTC onto zeolite was also investigated. While the presence of calcium, magnesium, phosphate, chloride, and sulfate ions decreased the sorption of OTC onto Na and HDTMA-modified zeolite, bicarbonate ion promoted the adsorption of OTC on HDTMA-modified zeolite. NH_4^+ and OTC simultaneously removed from water by Na-zeolite.

The obtained results show that both types of zeolites can be considered as a potential adsorbent for tetracycline antibiotics.

ÖZET

Son yıllarda çevrenin birçok kompartımanda bulunan antibiyotikler direnç oluşturma potensiyelleri ve bakteriyel toksisiteleri nedeniyle kirletici olarak sınıflandırılırlar. Hayvan ve su ürünleri yetiştiriciliği çevredeki antibiyotik kirlililiğine neden olan iki potansiyel kaynaktır.

Bu çalışmada hayvancılıkta yaygın bir şekilde kullanılan oksitetrasiklin (OTC) antibiyotiğinin sodyum ve hekzadesiltrimetilammonyum (HDTMA) ile modifiye edilmiş zeolitte adsorpsiyonu incelenmiştir. Adsorpsiyon çalışmaları farklı OTC konsantrasyonları, çözelti pH'ı ve adsorbent dozu ile yapılmıştır.

Adsorpsiyon isoterm verileri Freundlich modeline uygulanmıştır. Na-zeolitin ve HDTMA-zeolitin adsorbsiyon kapasiteleri sırasıyla pH 6.5'da 2.5 x 10^{-1} ($mg^{1-n}L^{n}/g$) ve pH 8'de $3x10^{-1}$($mg^{1-n}L^{n}/g$) olarak bulunmuştur. HDTMA-zeolit pH'a kuvvetli bir bağlılık göstermiştir ve pH 8'de % 90'lik maksimum antibiyotik giderimi 30 mg/L OTC ile elde edilmiştir. Na-zeolitin adsorpsiyon kapasitesi pH 2 ve 10 arasında çok fazla değişmemiştir ve pH 6.5'da % 88'lik maksimum OTC adsorbsiyonu elde edilmiştir. Yalancı-birinci ve -ikinci derece kinetik modeller ve partiküllerarası difüzyon denklemleri adsorpsiyon modelini tanımlamak için seçilmiştir.

Çeşitli iyonların OTC adsorpsiyonuna etkisi de araştırılmıştır. Kalsiyum, magnezyum, fosfat, klorür, ve sülfat iyonları OTC'nin Na ve HDTMA-zeolitte adsorpsiyonunu azalttırmıştır, bikarbonat iyonları ise OTC'nin HDTMA-zeolitte adsorpsiyonunu arttırmıştır. Amonyum iyonları ve OTC birlikte Na zeolit tarafından sudan giderilmiştir.

Elde edilen sonuçlar, iki tip zeolitin OTC antibiyotiği için potansiyel adsorbent olduğunu göstermektedir.

TABLE OF CONTENTS

LIST OF FIGURES

LIST OF TABLES

LIST OF SYMBOLS/ABBREVIATIONS

Symbol	Explanation	Units used
BCD	Butryl CoA Dehydrogenase	
C	Intercept	
C_o	Initial concentration	(mg/L)
C_t	Concentration time t	(mg/L)
CAS	Chemical Abstracts Service	
CEC	Cation Exchange Capacity	
CTC	Chlortetracycline	
DDTMA	Dodecyltrimethylammonium	
DF	Dilution Factor	
ECEC	External Cation Exchange Capacity	
EDAX	Energy Dispersive X-ray spectroscopy	
FTIR	Fourier Transform Infrared	
HDTMA	Hexadecyltrimethylammonium	
ICEC	Internal Cation Exchange Capacity	
K_d	Distribution coefficient	(L/kg)
K_f	Freundlich adsorption capacity constant	($mg^{1-n} L^n g$)
K_L	Energy of adsorption	(L/mg)
K_{oc}	Organic carbon normalized sorption coefficient	(L/kg)
K_{ow}	Octanol water partition coefficient	
k_p	Intraparticle diffusion model rate constant	($mg/g\ min^{1/2}$)
k_1	Pseudo-first order model rate constant	(1/min)
k_2	Pseudo-second order model rate constant	(min g/mg)
m	Weighed mass of mineral	(g)
MW	Molecular Weight	(g/mole)
n	Freundlich adsorption intensity	
OECD	Organization for Economic Co-operation and Development	
OTC	Oxytetracycline	
pK_a	Acid dissociation constant	

q_e	Equilibrium adsorbed concentration	(mg/g)
q_t	Adsorbed concentration time t	(mg/g)
R	Correlation coefficient	
SEM	Scanning Electron Microscopy	
$t^{1/2}$	Intraparticle diffusion model plot	(min)
TC	Tetracycline	
UV	Ultraviolet	
V	Volume	(L)
W	Weight	(g)
XRD	X-ray Diffraction	

INTRODUCTION

In recent years, antibiotics in the environment have become an increasing concern due to their impact on public health and the environment. Recent studies have shown that antibiotics were determined at low concentrations in soil (Rabolle and Spliid, 2000), ground water (Hirsch et al., 1999), and surface water (Spaepen et al., 1997). Although antibiotics generally present in low concentrations in the environment their continual input leads to development of antibiotic resistance bacteria (Chee-Sanford et al., 2001) that threats public health. In addition to this, antibiotics are accumulated in some aquatic (Delepee et al., 2004) and terrestrial organisms (Le Bris and Pouliquen, 2004) and exert toxic effects. It has also been reported that antibiotics can be taken up by plants and have adverse effects on plant growth (Batchelder, 1981).

Antibiotics are introduced into environment by different sources. Sewage treatment plant effluents, waste from industrial activities, animal feeding operations, and aquacultural activities constitute the sources. Among them, manure is the major source of antibiotic pollution in environment, as most of the antibiotics used in veterinary medicine end up in manure. It is known that about 75 per cent of antibiotics administered can be excreted in animal feces (Magnussen et al., 1991).Animal manure can be used as fertilizer in agricultural fields. Antibiotics present in the manure may leach into groundwater or surface water via run off depending on their mobility in the soil system and affect terrestrial and aquatic organisms.

In order to eliminate spreading of antibiotics in the environment they should be controlled at source. Adsorption can be used as promising technology for the antibiotics excreted from the animal body, since sorption may ultimately influence the fate of antibiotics in the environment. Zeolite can be used as an adsorbent in pollution control due to their availability, low cost, high cation exchange capacity, and high surface area. In order to enhance the adsorption capacity of zeolite for organic pollutants various surfactants are used for the modification of its surface (Haggerty and Bowman, 1994).

Adsorption of a widely used antibiotic, OTC onto raw, Na, and HDTMA-modified zeolite was investigated in this study. In order to evaluate adsorption data, various parameters such as equilibrium time, pH, adsorbent dosage, and initial OTC concentration were investigated. Effect of various ions on OTC sorption was also conducted to indicate the competition between OTC and ions onto zeolite considering their concentrations in natural and polluted water. Identification of crystalline phases of zeolite was characterized by X-ray diffraction pattern. Spectral shifts in characteristic functional groups of zeolite and OTC were determined by FTIR. Surface of zeolite was investigated by SEM.

2. THEORETICAL BACKGROUND

2.1. Occurrence of Antibiotics in the Environment

The occurrence of antibiotics in the environment is of ecotoxicological concern because of potential ecosystem alteration (Kümmerer, 2001). Prolonged exposure to low doses of antibiotics leads to the selective proliferation of resistant bacteria, which could transfer the resistance genes to other bacterial species. Antibiotics have a wide range of uses in both human and veterinary medicine.

From the late 1980s, occurrence of human derived antibiotics in different environmental compartments has been reported. Later, it was found that animal feeding operations and aquaculture facilities are the other sources of antibiotics. Until now, numerous studies have been documented to report occurrence of human used antibiotics in environment and measured concentration was generally less than 1 μg/L with few exception (Farre et al., 2001; Golet et al., 2002; Heberer, 2002; Miao and Koenig, 2002, Barreiro and Lores, 2003; McArdell et al., 2003; Stamatelatou et al., 2003; Vanderford et al., 2003; Cahill et al., 2004; Gobel et al., 2004; Gross et al., 2004; Kolpin et al., 2004; Wiegel et al., 2004; Glassmeyer et al., 2005). However, significantly higher concentration of veterinary antibiotics up to 46 mg/kg (Martinez-Carbollo et al., 2007) has been detected in manure and thus manure amended soil contains high amount of antibiotics such as 100 μg/g in soil (Accinelli et al., 2007). Antibiotics are also detected in other natural sources such as 246 μg/kg in sediment (Lalumera et al., 2004); 20 μg/L in fauna (Pathak and Gobal, 2005); and 1233 ng/g in plants (Migliore et al., 2003).

2.1.1. Emissions of Antibiotics to the Environment

Antibiotics can enter the environment by a number of different pathways. Effluents of sewage treatment plant and pharmaceutical industry, waste from confined animal feeding operations and manure can be a source for antibiotic pollution (Figure 2.1) (Kuımar et al., 2005).

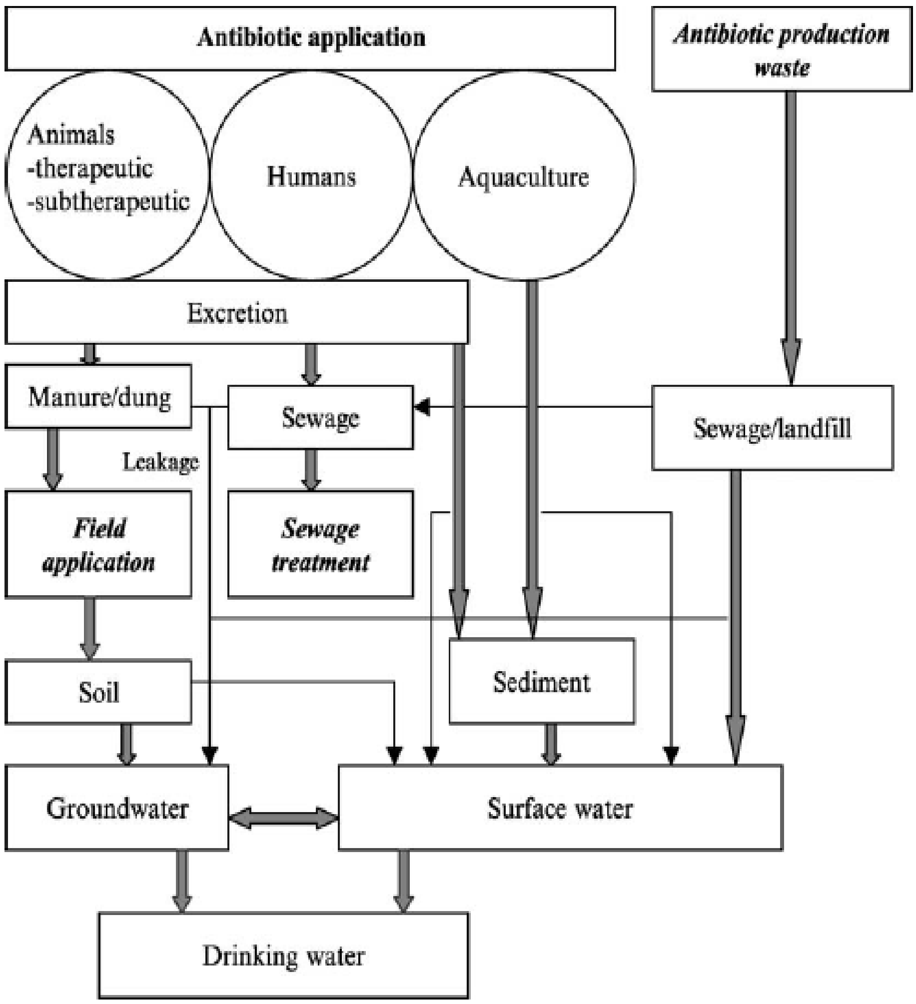

Figure 2.1. Principal routes of antibiotics in the environment (Kumar et al., 2005).

Antibiotics used in human treatment can enter the environment either by excretion or disposal of surplus drugs into sewage system. In general, antibiotics are adsorbed by organism after intake and then subjected to metabolic reactions. However, significant proportion of administered antibiotic is excreted with urine and feces and discharge into sewage treatment plants (Kumar et al., 2005). Several investigations have shown that various antibiotics including tetracycline, sulfamethoxazole, tylosin, and erythromycin are not eliminated completely in sewage treatment plants (Zwiener and Frimmel, 2000; Mc Ardell., et al 2003; Kumar et al., 2005; Batt et al., 2006). Many conventional wastewater treatment plants are not designed and operated to remove very low concentrations of antibiotics. During sewage treatment, it is likely that many organic compounds, including antibiotics are sorbed onto sludge or residues remain in treated effluent. Hence, they may release directly into surface water, sorbed in sediments or leach into groundwater depending upon the physicochemical properties of antibiotics.

Effluents of manufacturing operations and accidental spillage in pharmaceutical industry may also increase concentration of antibiotics in the environment (Boxall et al., 2004).

In the livestock production, large quantities of antibiotics are used to improve animal health care and increase production. A significant portion of the administered antibiotics is excreted in an unmetabolized form. The amount of antibiotics excretion varies with the type of antibiotic, the dosage level, and the age of the administered animal (Sarmah et al., 2006). Animal manure containing excreted antibiotics is frequently applied to agricultural fields, where antibiotics may potentially contaminate environment (Chui et al., 1990; Magnussen et al., 1991; Boxall et al., 2004). It is possible for these antibiotics to leach groundwater from soil amended with manure or reach surface water bodies through surface runoff (Hirsch et al., 1999; Meyer et al., 2000).

In aquaculture facilities, antibiotics enter the environment as a result of leaching from feces and uneaten antibiotic feed. It has been estimated that a minimum 75 per cent of the antibiotics in feed used in aquaculture systems are released to the surrounding environment and accumulate in the sediment (Diaz-Cruz et al., 2003). Presence of antibiotic in sediment favors the development of bacterial resistance which gives rise to infections. Sediments act as a reservoir for both the compounds and resistance bacteria. (Bjorklund and Bylund, 1991; Hustvedt et al., 1991; Bjorklund et al., 1991; Sarter et al., 2007). Presence of residual feed additives may also taken up by wild fish and crustaceans and exert toxic effects (Bjorklund et al., 1990; Samuelsen et al., 1992; Ervik et al., 1994; Capone et al., 1996; Pathak and Gobal, 2005).

2.1.2. Environmental Loads of Antibiotics

In the different environmental compartments some monitoring studies for human and veterinary antibiotics are discussed below.

<u>2.1.2.1. Soil</u> Excess use of antibiotics in animal feeding operations inevitably leads to residual concentrations in excrements (Thiele-Bruhn, 2003; Boxall et al., 2004; Martinez-Carbollo et al., 2007). It is not surprising to find residues of antibiotics either as metabolite or parent compound in manure and subsequently in agricultural fields (Hamscher et al., 2002). Generally, tetracyclines are widely used in livestock production and they were detected in the top few centimeters of the soil column. Obtained results indicate that tetracycline is highly sorbed on the soil (Boxall et al., 2004).

<u>2.1.2.2. Surface water</u> As a result of inefficient sewage treatment and intensive livestock production waste treatment, antibiotics are found in surface water. Chlortetracycline was analyzed as 0.5 μg/L in surface water from areas associated with intensive swine and poultry production (Meyer et al., 2000). Residues of chloramphenicol were detected by German researchers at 0.06-0.56 μg/L (Hirsch et al., 1999). Eryhtromycin was also detected in surface water in the U.S. (Kolpin et al., 2002) and the maximum reported concentration was 1.7 mg/L.

<u>2.1.2.3. Plants</u> When antibiotics release into environment through manure application, they may end up on arable land and can be taken up by plants. Batchelder (1981) tested the effects of OTC on pinto bean plants in aerated nutrient media and showed that relatively low antibiotic concentrations can effect the plant growth and development. Boxall et al. (2004) showed that bioaccumulation of sulfamethoxine antibiotics by roots and stems of plant species at much higher dose levels (13-2000 mg/kg). In a separate study, Migliore et al. (2003) found that uptake of enrofloxacin on crop plants induce toxic effects on plant roots.

<u>2.1.2.4. Groundwater</u> Groundwater contamination by antibiotics are determined generally as a result of agricultural usage of antibiotics. There are some reports of veterinary antibiotics being detected in groundwater (Hirsch et al., 1999; Lindsey et al., 2001; Sarmah et al, 2006). In an extensive monitoring study conducted in Germany, sulfamethazine concentrations were detected from 0.08 to 0.16 μg/L (Lindsey et al., 2001)

<u>2.1.2.5. Sediment</u> In order to prevent infections in intensive fish farming antimicrobial agents are distributed directly to the water or added to feed resulting in high local

concentrations in the water compartment and the adjoining sediments. Using tetracycline antibiotics in aquaculture has been extensively researched since it is widely used in aquaculture for treatment diseases (Bjorklund et al., 1990; Coyne et al., 1994; Capone et al., 1996). It has been reported that OTC concentration detected from 0.05 to16 µg/g on Baltic Sea sediment (Bjorklund et al., 1990). Capone et al. (1996) reported the presence of OTC residues ranging from 0.2 to 2 µg/g on subsurface sediments. OTC has also been found in wild fauna such as 0.1µg/g in oysters (Bjorklund et al., 1990; Capone et al., 1996) and 30 µg/L in fish liver (Pathak and Gopal, 2005).

2.2. Environmental Fate of Antibiotics

Once antibiotics released into the environment, they can be transported and distributed among the major environmental compartments (soil, surface waters, sediment and biota). The resulting concentration in these compartments can be described by a number of factors and processes including dosage of the compounds, the physicochemical properties of substances, degradation in manure and slurry, environmental conditions including soil type and climatic factors (Samuelsen, 1989). Persistence of antibiotics in the terrestrial environment is a key factor in determining their adverse environmental impact and depends on its photostability, its binding and adsorption capacity, its degradation rate, and leaching in water. While strongly sorbing antibiotics tend to accumulate in soil or sediment, highly mobile antibiotics tend to leach into groundwater and be transported with groundwater, drainage water, and surface water (Kumar et al., 2005). Sorption of antibiotics in soil is characterized by distribution coefficients and the sorption coefficient of many neutral hydrophobic organic chemicals has been shown to vary, depending on the organic carbon content of the sorbent (Schawarzenbach et al., 1993). For such compounds, organic carbon-normalized sorption coefficient, K_{oc}, is recommended. Another consideration that favors the use of K_{oc} as a measure of the sorption in environmental risk assessment is the strong correlation between this coefficient and the octanol water partition coefficient (Jacobsen and Berglind, 1988). Data are available on the sorption behavior of antibiotics in soils and sediments (Table 2.1).

Table 2.1. Sorption data for veterinary antibiotics to soil or soil constituents.

Compound	**Test matrix**	* **K_d (L/kg)**	** **K_{oc} (L/kg)**	**References**
Tetracycline	Soil organic matter	1620	-	Sithole and Guy (1987b)
	Clay loam soil	>400	40,000	Tolls (2001)
Oxytetracycline	Marine sediment	0.3	17	Pouliquen and Le-Bris (1996)
	Sandy loam soil	1,030	93,300	Rabolle and Spliid (2000)
Floroquinoline	Sandy loam soil	285	40,714	Nowara et al.(1997)
Metronidazole	Sandy loam soil	0.67	42	Rabolle and Spliid (2000)
Olaquindox	Sandy loam soil	1.67	104	Rabolle and Spliid (2000)
Enrofloxacin	Loamy sand	5,610	100,000	Nowara et al.(1997)
Sulfamethazine	Clay loam soil	0.6	60	Tolls (2001)
Sulfachloro pyridazine	Sandy loam soil	0.9		Boxall et al.(2002)
Ciprofloxacin	Sandy loam soil	427	61,000	Nowara et al.(1997)
Tylosin	Sandy loam soil	62.3	5,660	Rabolle and Spliid (2000)
	Clay loam soil	516-7,740	1,290-266,000	Sarmah et al. (2006)

*K_d = Distribution coefficient
**K_{oc} = Organic carbon-normalized coefficient

Antibiotic compounds with K_d values greater than 1000 L/kg are strongly bound to soils and are less mobile, while antibiotic compounds with K_d values lower than 2 L/ kg are loosely bound to soil and can be transported to either ground or surface waters. Strongly bound antibiotics, on the other hand, are more likely to be transported with sediments in surface runoff. The mobility of antibiotics further increases if these compounds are bound organic carbon in manure or soil (Kumar et al., 2005).

Sorption of antibiotics on soil and sediment is affected by several factors such as organic carbon, clay content, particle size and surface area. Some studies can explain sorption behaviour of antibiotics.

Pouliquen and Le-Bris (1996) confirmed that sorption coefficient of OTC on marine sediment was much lower than sandy loam soil that contain significant portion of silt and clay.

Nowara et al. (1997) indicated that the sorption of quinoline group antibiotics was strongly related with the particle size of the soil.

Rabolle and Spliid (2000) found that sorption of OTC on sandy soil depends on organic carbon content. It was also found that sorption of tylosin group antibiotics were related cation exchange, hydrophobic partitioning, and hydrogen bonding.

Tolls (2001) determined that surface interactions of tetracycline with clay minerals were responsible for the strong sorption to soils.

Boxall et al. (2002) investigated the sorption behavior of sulfonamide antibiotics in sandy loam soil and soil manure mixture in order to assess the likely potential for these compounds to pollute surface and groundwater. Sorption coefficients K_d was found ranging from 0.9 to 1.81 L/kg. Sulfonamide would be highly mobile in the environment.

Sarmah et al. (2006) reported tylosin adsorption on high clay content soil. They found that cation exchange, organic carbon and clay content are responsible for tylosin sorption on soil.

Environmental fate of veterinary antibiotics is explained by degradation rates. Number of studies were performed to explain degradation of antibiotics (Loke et al., 2002; Ingerslev and Halling Sorensen 2001; Sarmah et al., 2006).

Gavalchin and Katz (1994) studied degradation range of veterinary antibiotics (streptomycin, tylosin and chlortetracycline) as a function of temperature in a sandy soil.

Their study showed that degradation of these antibiotics varied according to their chemical structure and temperature under field conditions. Degradation is also likely to be affected humidity, rainfall, and nature of soil properties.

Kay et al. (2004) found that tylosin rapidly degraded in manure and soil. They also found that combination of manure and soil rapidly increased degradation.

Degradation of veterinary and human antibiotics in water can also occur via photodegradation and hydrolysis. Several studies are available in the literature (Oka et al., 1989; Sarmah et al., 2006).

Kühne et al. (2000) reported significant reduction in the concentration of tetracycline under laboratory study in liquid swine manure. It was found that degradation was very fast due to higher pH values in manure. In addition beyond pH 6 the oxidation processes play a major role in the degradation of tetracycline.

Degradation of tylosin antibiotic was also observed in swine manure under laboratory condition (Paesen et al., 1995). It was reported that the rate of decomposition of tylosin antibiotic depended largely on pH, buffer type, concentration and ionic strength of the compound.

2.3. Classification of Veterinary and Human Antibiotics

Antibiotics can be classified in several ways. The most common method classifies them according to their chemical structure as antibiotics sharing the same or similar chemical structure will generally show similar patterns of antibacterial activity, effectiveness, toxicity (Table 2.1) (Thiele-Bruhn, 2003). A number of physical and chemical processes are responsible for the antibiotics moving into the environment. Sorption, leaching, and degradation are the three important processes in the soil-water system. These processes are driven by physicochemical properties of antibiotics such as molecular weight, structure, size, solubility, pK_a, and log K_{ow} values. Ranges of physicochemical properties of important antibiotic compound classes (Thiele-Bruhn, 2003) are listed in Table 2.2.

Table 2.2. Representative antibiotics and typical ranges of physicochemical properties.

Compound Class	Molecular Weight (g/mol)	Water Solubility (mg/L)	log K_{ow}	pK_a
Tetracyclines	444.5-527.6	230-52,000	-1.3 -0.05	3.3 /7.7/ 9.3
Sulfonamides	172.2 -300.3	7.5 – 1,500	-0.1 -1.7	2 -3 /4.5 -10.6
Aminoglycosides	332.4- 615.6	10,000 -500,000	-8.1- -0.8	6.9-8.5
β- Lactams	334.4- 470.3	22-10,100	0.9-2.9	2.7
Macrolides	687.9-916.1	0.45-15	1.6-3.1	7.7-8.9
Florquinolones	229.5-417.6	3.2-17790	-1.0- 1.6	8.6
Imidazoles	171.5- 315.3	6.3- 407	-0.02-3.9	2.4
Polyethers	670.9- 751	2.2×10^{-6} -3.1×10^{-3}	5.4 -8.5	6.4
Glycopeptides	1450.7	> 1,000	-	5.0
Quinoxaline derivatives	263.3	1.0×10^{6}	-2.2	10

2.4. Properties of Tetracycline Antibiotics

The tetracyclines (TCs) are broad-spectrum antibacterials widely used in veterinary medicine. They are active against a range of organisms such as myco-plasma and *Chlamydia*, as well as a number of gram-positive and gram-negative bacteria. Tetracycline (TC), oxytetracycline (OTC) and chlortetracyclines (CTC) are widely used in animal feeding to maintain health and improve growth efficiency in many countries. These chemicals are characterized by a partially conjugated four-ring structure with a carboxyamide functional group (Mitscher, 1978). The molecule of tetracycline has several ionizable functional groups, and the charge of the molecule depends on the solution pH (Sarmah et al., 2006) (Figure 2.2). pK_a values of tetracyclines are represented in Table 2.3.

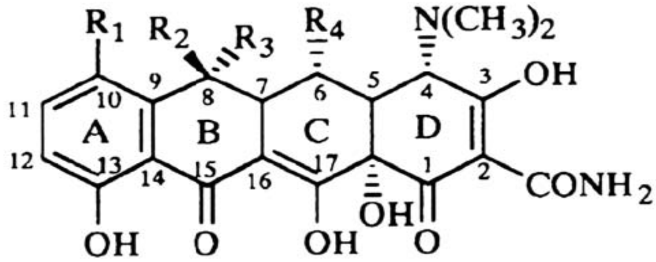

	R_1	R_2	R_3	R_4
Tetracycline (TC)	H	CH_3	OH	H
Chlortetracycline (CTC)	Cl	CH_3	OH	H
Oxytetracycline (OTC)	H	CH_3	OH	OH

Figure 2.2. Molecular structure of tetracycline antibiotics.

Table 2.3. pK_a values of tetracycline antibiotics.

	pK_{a1}	pKa_2	pKa_3	References
Tetracycline (TC)	3.57	7.49	9.88	(Figueroa et al., 2004)
Chlortetracycline (CTC)	3.3	7.7	9.7	(Figueroa et al., 2004)
Oxytetracycline (OTC)	3.6	7.52	9.88	(Tavares and McGuffin, 1994)

An examination of their pK_a values (Table 2.3) suggest that TC, OTC and CTC have similar pH dependent speciation, which is also consistent with their structural relationship. There are three distinct acidic functional groups for tetracycline: tricarbonyl methane (pK_{a1} 3.3); dimethyl ammonium cation (pK_{a3} 9.6); and phenolic diketone (pK_{a2} 7.7). The multiple ionizable functional groups present in TCs suggest that at environmentally relevant pH values, they may exist as a cation below pH 3.3 (+ 0 0), zwitterions between pH 3.3 and 7.7 (+ - 0), and as a net negatively charged ion above pH 7.7 (+ - -) (Figueroa et al., 2004; Sassman and Lee, 2005). The speciation diagram of OTC is presented in Figure 2.3.

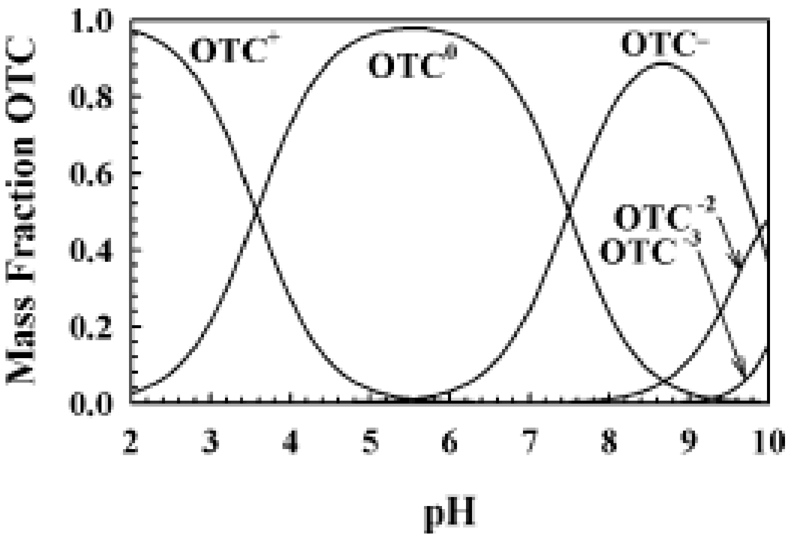

Figure 2.3. Speciation of OTC as a function of pH (Figueroa et al., 2004).

The speciation diagram is calculated for OTC, but it is similar for tetracycline and chlortetracycline due to closeness of pK_a values all these compounds. It can be envisaged from these ionization schemes that in the pH regime of environmental interest (pH 4–8), zwitterionic OTC species would be dominated and reach maximum concentration at pH 5.5.

TCs are relatively stable in acidic media, but not in alkaline conditions and form salts in both media (Halling-Sorensen et al., 2002). The free base and the various salts are very stable in the dried form. Aqueous solution is stable at neutral pH values. At pH 2.5, one per cent solution of OTC will maintain potency for at least 30 days at 25°C and for five days at 37°C. At pH 9, OTC loses two per cent of its potency in two hours and eight per cent in 24 hours. Stability is both a function of pH and temperature in water. Aqueous solutions of the hydrochloride at pH 1 to 2.5 are stable for at least 30 days at 25°C; solutions stored between pH 3 and 9 show no detectable loss of potency when stored at 5°C for at least 30 days (Mitscher, 1978). Tetracyclines are reported to degrade when exposed to sunlight or near UV wavelengths forming biologically inactive compounds such as peroxide, a hydroperoxide, and hydro compounds, and the epimer β-deoxytetracycline. The extent and rates of decomposition have not been established (http://www.fda.gov/cvm/FOI/038-439_EA.pdf).

2.4.1. Sorption of Tetracycline Group Antibiotics

Sorption of tetracycline group antibiotics on soil, clay, and sediments were investigated in several studies.

Porubcan et al. (1978) examined the adsorption of tetracycline on montmorillonite surface. The results of the study indicated that tetracycline was adsorbed by cation exchange mechanism at low pH values where the positively charged species predominate and complexation with divalent interlayer cations has contributed significantly to adsorption at higher pH values where negatively charges species exist. The obtained results were confirmed by X-ray and FTIR analyses.

Sorption of tetracycline on humic acids was detected by Sithole and Guy (1987b). Humic acid has significant contribution to the adsorption of tetracycline depending upon the pH. It was suggested that sorption of OTC was caused by three different mechanisms with the interaction of organic matter: Binding to divalent cations, ion exchange reactions, and hydrogen bonding between acidic groups in the humic acid and the polar groups of tetracycline.

Pouliquen and Le-Bris (1996) investigated the presence of OTC in sediments. It was found that OTC was most likely to form complexes with mineral cations and organic matter. Higher organic matter content of sediment resulted in higher sorption of OTC. It was also found that size of sediment particles influenced the sorption rate of tetracycline.

Rabolle and Spliid (2000) studied sorption and mobility of OTC on soil. They found that OTC was strongly sorbed on soil and exhibited high distribution coefficient, K_d value of OTC was found 1026 L/kg.

Loke et al. (2002) determined sorption of OTC on manure. It was found that sorption of OTC to manure was influenced by ionic binding to divalent metal ions such as Mg^{2+} and Ca^{2+} as well as other charged compounds in the matrix.

Figueora et al. (2004) investigated the sorption of zwitterionic forms of OTC on montmorillonite. It was found that OTC sorption was accompanied by proton uptake and decreased with increasing ionic strength and sorption was more favorable on acidic clay. They also found that calcium salts promoted OTC sorption at alkaline pH's likely by a surface bridging mechanisms.

Kulshtrestha et al. (2004) studied sorption on native, Na, and HDTMA-modified montmorillonite surface. They found that OTC sorption was decreased with increasing pH on native and Na-montmorillonite as a result of cation exchange reactions. However, OTC sorption was increased on HDTMA-modified montmorillonite as the pH increased.

Jones et al. (2005) reported the factors that influenced sorption of OTC on soil. They determined that soil texture and iron oxide content influenced the extent of OTC sorption on soils with organic carbon content ranged from 0 to four per cent.

Sorption of OTC on iron oxides and iron oxide rich soils were conducted by Figueroa and Mackay (2005). They found that OTC sorption increased with increasing pH. Moreover, surface complexation mechanism was important for OTC sorption. Gu and Karthikeyan (2005) achieved similar results for the sorption of tetracycline on aluminum and iron hydrous oxides surface. It was also found that ligand promoted dissolution increased sorption of tetracycline on hydrous oxides surfaces.

2.4.2. Complexation of Tetracycline Antibiotics with Metal Ions

Tetracycline group antibiotics form reversible complexes with a number of chemical species, due to their β–dicetone group, dicarbonyl system and amino-alcohol group, which are their chromophoric groups, shown in Figure 2.4 (Buckley and Smyth, 1986). Metal tetracycline complexes are important because they are thought to be linked to the mode of action of antibiotics.

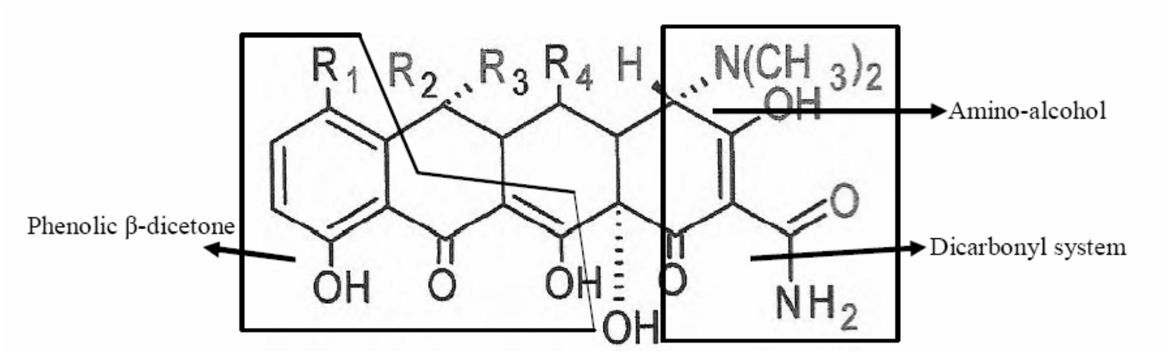

Figure 2.4. Metal coordination and chromophoric groups of TCs.

TCs complex readily with Fe^{3+}, Fe^{2+}, Cu^{2+}, Ni^{2+}, Co^{2+}, Zn^{2+}, Mn^{2+}, Mg^{2+}, Ca^{2+}, Be^{2+}, Al^{3+} among metal ions. This complexing is further supported by the observed dramatic changes in UV spectral bands from the chromophoric regions of TC upon interaction with complexing agents. Multiple species of chelated TCs can co-exist in solution. The number and kind of species can change depending on pH or type of metal.

The complex deprotonation pattern of tetracycline as well as large numbers of possible chelation sites has led to extensive studies on the complexation of various tetracyclines derivatives with several divalent metal ions in aqueous and organic environments using magnetic resonounce spectroscopy (Williamson and Everett, 1975) circular dichroism spectroscopy (Newman and Frank, 1976; Machado et al., 1995), absorption and fluorescence spectroscopy (Wessels et al., 1998).

Buckley and Smyth (1986) explained that metal combination with tetracycline must be on the β–dicetone moiety. Studies also shown that different metals can not form different type complexes but rather 1:2 or 2:1 metal antibiotic complexes at different concentrations. 1:2 or 2:1 metal antibiotic complexes have also been reported at high pH. They are also reported that tetracycline forms stable complexes with trivalent ions such as Al^{3+} and Fe^{3+}.

Lunestand and Goksayr (1990) reported the reducing antibacterial effect of oxytetracyline in the presence of Mg^{2+} and Ca^{2+}.

Wessels et al. (1998) used steady state absorption and emission, circular dichroism, and time of flight secondary ion mass spectroscopic measurements for the determination of tetracycline and anhydrotetracycline complexes formed with $Mg^{2+}$and Ca^{2+}ions. The results of the study revealed that Ca^{2+} formed a 1:2 ligand metal complex with tetracycline. However, Mg^{2+} formed both 1:2 and 1:1 complex with tetracyclines. The results also showed that Mg^{2+} led to increase in fluorescence intensity and observed changes in absorption spectra. In contrast to tetracycline Mg^{2+} formed 2:2 ligand metal complex with anhydrotetracycline.

Tongaree et al. (1999b) found that solubility of OTC increased in the presence of $Mg^{2+}$and Ca^{2+}. They also found that chelation increased with increasing pH

Schmitt and Schneider (2000) investigated $Mg^{2+}$and Ca^{2+} complexation with OTC at pH 7 and 8.5. Both ions resulted in bathochromic shift of the long wavelength absorption band of OTC at pH 7 and 8.5. They also found that chelation reactions increased with pH.

2.5. Adsorption of Pollutants by Zeolites

Zeolites of the clinoptilolite type are hydrated aluminosilicate minerals with cage like structure that offers large internal and external surface areas (Perraki et al., 2005). Zeolites are generally environmentally benign substances, natural, inert, nontoxic, and highly porous structure and their structure is ideal for sorption and ion exchange processes. However, ion exchange properties are not as effective as activated carbon. They are widely used in agriculture, aquaculture, and animal husbandry operations. Zeolites can also be used improving physical properties of soil and for the treatment of contaminated soil and wastewater pollution control. For the adsorption of contaminants, zeolites have been used in removing inorganic and organic pollutants like ammonia (Booker et al., 1996; Karadağ et al., 2006; Wang et al., 2006), heavy metals (Cincotti et al; 2001) and azo dyes (Armağan et al., 2003).

The cation exchange poperties of natural zeolites can be exploited to modify their surface in order to retain anions and nonpolar organics. Generally long chain cationic surfactants like hexadecyltrimetylammonium chloride (HDTMA-Cl), hexadecyltrimetylammonium bromide (HDTMA-Br), and dodecyltrimethylammonium bromide (DDTMA) and oleylemine have been used for modification of zeolite surface (Bowman, 2003). Hexadecyltrimethylammonium (HDTMA) is a long chain cationic surfactant that possesses a permanent positive charge. The resulting modified zeolite is capable of simultaneous sorption of anions, cations and nonpolar organic molecules from water.

2.5.1. Adsorption Studies with Raw Zeolites

While most of the sorption studies on raw zeolite were performed by inorganics relatively few studies were conducted with sorption of organics.

The adsorption mechanism of reactive azo dyes by natural zeolite has been examined (Armağan et al., 2003). The results of adsorption experiments indicated that the natural zeolite has limited adsorption capacity of reactive dyes.

Adsorption of quinoline group antibiotics onto natural zeolite was investigated (Ötker and Balcıoğlu, 2005). It was found that adsorption of quinoline group antibiotics on natural zeolite pH dependent. In addition, the presence of ammonium ion enhanced the adsorption of quinoline group antibiotics.

Haidouiti (1997) used natural zeolites as a soil additive to reduce the uptake of mercury by plants. It was determined that using natural zeolites at application rates of one, two, and five per cent by soil weight caused reduction in mercury concentrations of up to 58 per cent in plant root, as compared with controls no added zeolites.

Nickel removal by natural clinoptilolite was observed in the presence of NH_4OH solutions (Iznega et al., 2002). It was found that NH_4OH solutions were both provoked by nickel solution cycles and increased nickel ion removal capacity of zeolite.

Fluoride sorption was investigated by Mexican clinoptilolite (Diaz-Nava et al., 2002). It was found that fluoride retention was not influenced by the cations (Na^+, Ca^{2+}, La^{2+} and Eu^{2+}), initial pH or the particle size of the zeolite mineral.

Simultaneous removal of metals with Cu^{2+}, Fe^{3+}, and Cr^{3+} on natural zeolite with anions such as SO_4^{2-} and HPO_4^{2-} were examined by Inglezakis et al. (2003). It was observed that Cu^{2+} uptake was significantly decreased in the presence of $SO_4^{2-}$and HPO_4^{2-}. The observed effect was less significant for Fe^{3+}, and Cr^{3+} in the presence of SO_4^{2-} and HPO_4^{2-}, respectively. This could possibly be due to metal-anion complex formation.

Wang et al. (2006) investigated ammonia removal using natural Chinese clinoptilolite, and found that ammonia adsorption increased with decreasing clinoptilolite particle size and increased with increasing initial ammonia concentration.

Removal of ammonium ion by Turkish clinoptilolite was conducted by Karadağ et al. (2006). They found that pseudo second order kinetic model provided excellent kinetic data. Intraparticle diffusion also influenced the ammonium uptake. Thus, there was a significant potential for the natural Turkish clinoptilolite as an adsorbent for ammonium removal.

Jorgensen and Weatherley (2003) examined ammonia removal from wastewater by ion exchange in the presence of organic compounds. It was found that the presence of organic compounds increased the uptake of ammonia onto clinoptilolite due to surface tension changes.

2.5.2. Adsorption Studies with Surfactant Modified Zeolites

Several studies were performed for sorption of anions and nonpolar organics by surfactant modified zeolites.

Haggerty and Bowman (1994) investigated sorption of inorganic oxyanions like sulfate, selenate and chromate on organozeolite. Hexadecyltrimetylammonium bromide (HDTMA-Br) was used for surface modification of zeolite surface. The result of the study determined that sorption was maximized when the zeolite external cation exchange has been fully satisfied by HDTMA. Surface precipitation with HDTMA-anion complex may influence the removal of inorganic anions from aqueous solution.

Li and Bowman (1997) studied the effect of selected counterions (Cl^-, Br^-, and HSO_4^-) on the sorption of HDTMA on clinoptilolite and they also conducted sorption of chromate by HDTMA-zeolite. It was found that HDTMA sorption capacity on zeolite was greatest when Br^- was used as counterion. However, chromate sorption capacity was highest when HSO_4^- was used as counterion. It was also found that the sorption of chromate on HDTMA-zeolite results from combination of entropic, columbic, and hydrophobic effects.

Li and Bowman (1998) also conducted sorption of perchlorethylene on surfactant modified zeolite. They confirmed that sorption of perchlorethylene depended on surfactant molecule configuration and fractional organic carbon content. Above monolayer coverage, increasing fractional organic carbon resulted in further increase in the perchlorethylene sorption coefficient.

Li et al. (1999) used zerovalent iron pellets which were modified with cationic surfactants hexadecyltrimetylammonium bromide (HDTMA-Br) to increase chromate sorption on zeolite. They determined that chromate sorption by modified zeolite with zerovalent iron pellets was higher than that of zeolite with zerovalent iron pellets.

Vujakoviç et al. (2000) conducted adsorption of sulfate, dihydrogen phosphate, and hydrogen chromate by surfactant modified zeolite. Oleylamine was used as cationic surfactant for the modification of zeolite surface. Two types of anion adsorbents were used. Oleylamine was adsorbed on H clinoptilolite as strong adsorbents. However, oleylamine was adsorbed by Ca and Na-clinoptilolites as a weak anion adsorbent. They confirmed that excess oleylamine did not significantly influence the anion adsorption, and sulfate and dihydrogen phosphate adsorption process were slower than hydrogen chromate adsorption.

Li et al. (2000) studied adsorption of ionizable organic solutes (phenol and aniline) by surfactant modified zeolite. It was found that phenol sorption on surfactant modified zeolite increased with solution pH. However, decreasing pH resulted in reduced aniline sorption due to repulsion of aniline from surfactant modified zeolite treated to bilayer covarege.

Kurama et al. (2002) investigated the effect of chemical modification on the sorption capacity of natural zeolite. It was found that ion exchange with H^+ has a great influence on the effective pore volume and surface area of the zeolite. They also concluded that acid treated samples with increasing Si/Al ratio offer advantageous for the adsorption of nonpolar organics.

Armağan et al. (2003) investigated the removal of reactive azo dyes by modified zeolite from aqueous solution. It was found that in contrast to natural zeolite azo dyes were effectively adsorbed by HDTMA-zeolite.

Tamoseviç-Canoviç et al. (2003) investigated mycotoxins (aflotoxin B_1, zeralenone, ochratoxin A and ergopeptine alkaloids) adsorption by surfactant modified zeolite. Octadecyldimethyl benzyl ammonium chloride and dioctadecyldimethyl ammonium chloride cationic surfactant were used as modification zeolite surface. The results of the study showed that all the organozeolites effectively adsorbed aflotoxin B_1, zeralenone, ochratoxin A, and ergopeptine alkaloids. In contrast to Tamoseviç-Canoviç et al. (2003), Dakoviç et al. (2005) stated that aflotoxin adsorption was reduced by modified zeolite. They indicated that zeolite did not have hydrophobic interactions with octadecyldimethyl benzyl ammonium chloride.

Toxic nonionic organic contaminants, aniline and nitrobenzene adsorption by organozeolite were conducted by Ersoy and Çelik (2004). It was confirmed that partitioning mechanism was responsible for adsorption of nonionics. The effectiveness of the partitioning mechanism was connected hydrophobic properties of the nonionic organic contaminants.

Li (2004) studied chromate adsorption on modified zeolite. The results of the study indicated that chromate sorption decreased as the solution pH and ionic strength increased.

Riviera and Farias (2005) investigated the adsorption of (sulfamethoxazole) on surfactant modified clinoptilolite. Three kinds of surfactants (cationic, anionic and nonionic) were used for modification of zeolite. It was determined that modified zeolite adsorbed a considerable amount of sulfamethoxazole.

3. MATERIALS AND METHODS

3.1. Materials

3.1.1. Natural Zeolite

Natural zeolite was used as an adsorbent and provided by Ultra A.Ş., İzmir. Prior to use in adsorption experiments, the zeolite was sieved to a size range of 0.8-2 mm (10-20 mesh size).

3.1.2. Oxytetracycline hydrochloride

Hydrochloride salt of oxytetracycline was used in the adsorption experiments since this form is quite soluble in water (solubility = 6.9 g/L) (http://www.fda.gov/cvm/FOI/038-439_EA.pdf). Oxytetracycline hydrochloride, OTC ($C_{22}H_{24}N_{2}0_{9}$. HCl, 95 % purity) was used as received from Sigma Aldrich. Fresh stock solution (1.2 mM) of OTC was prepared in deionized water. Working solutions of OTC was prepared by diluting the stock solution with deionized water. Chemical structure of OTC (Sassman and Lee, 2005) is represented in Table 3.1.

Table 3.1. Chemical structure of OTC.

Antibiotic	**Structure**	**Molecular Weight**	**CAS Number**
Oxytetracyline hydrochloride (OTC)	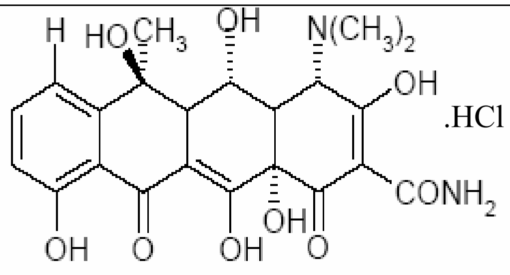	496.9	79-57-2

3.1.3. Hexadecyltrimethylammonium bromide

Hexadecyltrimethylammonium bromide (HDTMA-Br), ($C_{19}H_{42}$ Br N, 99% purity) was purchased from Sigma Aldrich used for modification of the zeolite surface. Chemical structure of HDTMA-Br (Haggerty and Bowman, 1994) is presented in Table 3.2.

Table 3.2. Chemical structure of HDTMA.

Surfactant	Structure	Molecular Weight	CAS Number
Hexadecyltrimethylammonium bromide (HDTMA-Br)	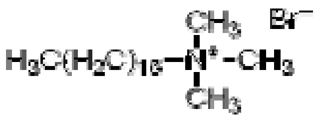	364.45	57-09-0

3.1.4. Phosphate Buffer Solutions

Phosphate buffer solutions were used to adjust the pH of OTC suspension in pH effect and isotherm experiments. In order to prepare the phosphate buffer solutions at different pH values, all phosphate components given in Table 3.3 were dissolved in 200 mL deionized water. pH of each buffer solutions was measured by a WTW 330 pH meter and WTW Sen Tix 41 combined pH electrode.

Table 3.3. Composition of phosphate buffer solutions.

pH	KH_2PO_4 (g/L)	Na_2HPO_4 (g/L)	Na_3PO_4 (g/L)
5	5.168	0.210	-
5.8	4.189	1.102	-
6.5	2.170	2.848	-
7.4	0.428	4.404	-
8	0.122	4.680	-
10.5	-	4.497	0.348

3.1.5. Other chemicals

All other chemicals used in the study were reagent grade and are listed below.

Table 3.4. Chemical reagents.

Name	Formula	Experiment	Supplier
Sodium hydroxide	NaOH (pellet)	pH adjustment	Riedel de Haen
Hydrochloric acid	HCl	pH adjustment	Riedel de Haen
Ammonium chloride	NH_4Cl	NH_4^+ effect	Riedel de Haen
Magnesium chloride	$MgCl_2$. $6H_20$	Mg^{2+} effect	Merck
Calcium chloride	$CaCl_2$(anhydrous)	Ca^{2+} effect	Baker
Sodium hydrogen phosphate	Na_2HPO_4 .12 H_20	PO_4^{3-}effect	Merck
Potassium dihydrogen phosphate	KH_2PO_4	Phosphate buffer	Riedel de Haen
Sodium phosphate	Na_3PO_4	Phosphate buffer	Merck
Sodium sulphate	Na_2SO_4 (anhydrous)	SO_4^{2-} effect	Riedel de Haen
Sodium chloride	NaCl	Cl^- effect	Riedel de Haen
Sodium hydrogen carbonate	$NaHCO_3$	HCO_3^-effect	Merck
Sodium acetate	CH_3COONa	CEC	Riedel de Haen
Acetic acid	CH_3COOH	CEC	Riedel de Haen

3.2. Methods

3.2.1. Mineral Preparation

3.2.1.1. Preparation of Raw Zeolite. The sieved zeolite was washed with deionized water by shaking at 110 rpm and 25°C (Julabo Shake Temperature SW 22) for two hours and subsequently dried at room temperature. The resulting material was called raw zeolite.

3.2.1.2. Preparation of Na-Zeolite. 2000 mL of 2 M CH_3COONa /CH_3COOH (Riedel de Haen) buffer (pH=5) was added to one kg of sieved natural zeolite. The suspension was mixed at 110 rpm and 25 °C for 24 hours on a shaker. After settling, the supernatant was decanted and then the zeolite was washed thoroughly with deionized water followed by air drying. The resulting material was labelled Na-zeolite.

3.2.1.3. Preparation of HDTMA-modified Zeolite. HDTMA-Br was used to prepare organomodified zeolite. 10 grams of Na-zeolite was mixed with 50 mL of 0.08 M HDTMA-Br at 110 rpm and 25 °C for 24 hours (Haggerty and Bowman, 1994). After shaking period, zeolite was rinsed with deionized water for several times and air dried.

3.2.2. Batch Adsorption Tests

Batch adsorption tests were performed at various concentrations of OTC by using raw, Na, and HDTMA-modified zeolite. A volume of 10 mL OTC solution at desired concentration was placed in a glass stoppered 100 mL conical flask. An accurately weighed zeolite was then added to the solution. The pH of suspension was adjusted to desired value by the addition of 0.1 M NaOH or 0.1 M HCl. A series of conical flasks, which were wrapped with aluminum foil, was shaken at 110 rpm on the shaking water bath at 25 ^{o}C for predetermined contact time. Control flasks containing no sorbent were assembled in the same manner to account for possible OTC losses at different pH values. Each run was done at least in duplicate. After equilibration, zeolite particles were separated from the suspension by centrifugation (Nuve NF 1205) at 4000 x g for one hour and subsequently filtered through a 0.45 µm membrane filter (Sartorius Minisart). The filtrate was analyzed for the OTC concentration. The amount of OTC adsorbed on zeolite was calculated by a mass balance relationship. The experimental parameters included zeolite dosage, initial OTC concentration, pH, and equilibration time. Additionally, competitive adsorption experiments were carried out with different cations and anions at pH 6.5 and 8.

3.2.3. Analytical Methods

3.2.3.1. Determination of Cation Exchange Capacity (CEC). Total cation exchange capacities of raw, Na, and HDTMA-zeolite were determined by the sodium acetate method (http://www.epa.gov/epaoswer/hazwaste/test/pdfs/9081.pdf). The procedure for the CEC determination involved: (1) saturation of the zeolite by Na^+ ions, (2) extraction of Na^+ ions by NH_4^+ ions, and (3) analysis of the extract for Na^+ ions. Four grams of pretreated zeolite was placed in a 50 mL conical-bottom plastic centrifuge tube. The mineral was exchanged through four successive 10 min saturations with 33 mL of 1N CH_3COONa solution (pH 8.2). After centrifugation at 4000 x g (Hettich Universal 16 A) for 10 min, the clear supernatant was decanted. The mineral was then washed through three successive 10 min rinses with 33 mL of isopropyl alcohol (Sigma Aldrich) and centrifuged (4000x g, 10 min). Na saturated mineral was subjected to three successive 10 min extractions with 33 mL of 1 N CH_3COONH_4 solution (pH 7) to replace Na^+ ions by NH_4^+ ions. CH_3COONH_4 solution was prepared by diluting glacial acetic acid (Riedel de Haen) and concentrated ammonium hydroxide (Riedel de Haen) in deionized water. After centrifugation (4000 x g, 10 min) the clear supernatant was transferred to a 100 mL volumetric flask and diluted to 100 mL with 1 N CH_3COONH_4 solution. Exchangeable Na^+ ions were analyzed from the ammonium acetate extract by atomic absorption spectroscopy (Perkin Elmer A Analyst 300). Equation 3.1 describes the calculation of cation exchange capacity (http://www.epa.gov/epaoswer/hazwaste/test/pdfs/9081.pdf).

$$\text{CEC (meq /100 g)} = \frac{[Na] \times V \times DF \times 100}{m \times MV} \tag{3.1}$$

[Na] = Na^+ concentration (mg/L)
V = Volume of extract (L)
DF = Dilution factor
m = Weighed mass of mineral (g)
MW = Molecular weight of sodium (23 g/mole =23 mg/meq)

<u>3.2.3.2. Determination of External and Internal Cation Exchange Capacity of Zeolite.</u> The procedure for external (ECEC) and internal (ICEC) cation exchange capacity determination involved (1) saturation of the mineral with Na^+ ions, (2) extraction of external Na ions by HDTMA cations, (3) extraction of internal Na^+ ions by NH_4^+ ions, and (4) analysis of both extracts for Na^+ions (Ming and Dixon, 1987; Haggerty and Bowman, 1994). Four grams of pretreated zeolite was placed in a 50 mL conical-bottom plastic

centrifuge tube. The mineral was exchanged through four successive 10 min saturations with 40 mL of 1N CH_3COONa solution (pH 8.2). After centrifugation (4000 x g, 10 min) the clear supernatant was decanted. Excess interstitial Na ions were removed by one 10 min rinse with 40 mL of deionized water, followed by three successive 10 min rinses with 33 mL of isopropyl alcohol and centrifuged (4000 x g, 10 min). External exchangeable Na^+ ions were removed by one 24 h extraction and two successive 15 min extractions with 30 mL of 0.1 N HDTMA-Br solution. After centrifugation, all three clear supernatants were decanted into a 100 mL volumetric flask and diluted to 100 mL with 0.1 N HDTMA–Br solution. The ICEC Na^+ ions were removed by three successive 15 min extractions with 30 mL of 1 N CH_3COONH_4 solution (pH 7). After centrifugation (4000 x g, 10 min) all three clear supernatants were transferred to a 100 mL volumetric flask and diluted to 100 mL with 1 N CH_3COONH_4 solution. Dilution technique and calculation procedure were identical to the CEC methodology.

$$\text{ECEC (meq /100 g)} = \frac{[Na] \times V \times DF \times 100}{m \times MV} \qquad (3.2)$$

$$\text{ICEC (meq /100 g)} = \frac{[Na] \times V \times DF \times 100}{m \times MV} \qquad (3.3)$$

3.2.3.3. Ammonium Determination. Before and after equilibration, NH_4^+ concentration in solution was determined by Nessler Method with a portable HACH DR/2010 spectrophotometer. The analysis was performed according to the procedure described in the manual of HACH DR/2010. Adsorbed NH_4^+ amount was calculated from these measurements. All reagents and chemicals were supplied by HACH company.

3.2.3.4. Phosphate Determination. PO_4^{3-} concentration was measured by PhosVer 3 Method with Hach DR/2010 spectrophotometer according to the procedure described in manual. Adsorbed phosphate was calculated from the difference between the initial phosphate concentration and the concentration of phosphate that remained in the supernatant solution.

3.2.3.5. Spectrophotometric Analysis of Antibiotics. The concentration of OTC in the solution phase was quantified by UV/Vis spectrophotometer (Schimadzu Model 1208) at a wavelength corresponding to the maximum absorbance. UV absorbance spectra of OTC at different pH values and in the presence of Ca^{2+} and Mg^{2+} ions were recorded between 200-450 nm at 0.5 nm intervals. Ionization and complexation interactions of OTC led to a spectral shift in absorbance. Therefore at each condition separate calibration curve was prepared at the maximum absorbance wavelength (Appendix A Figure A.1, 2, 3, 4). Initial and final antibiotic concentrations were found using these calibration curves. In accordance with the Lambert- Beer Law the absorbance values were found linear to concentrations of OTC and dilutions were undertaken when absorbance exceeded 0.9. Presence of HDTMA-Br in solution did not interfere with the OTC determination.

3.2.3.6. Scanning Electron Microscopy (SEM) Analysis. Surfaces of the Na and HDTMA-modified zeolites were investigated by scanning electron microscopy, SEM (Philips XL-30 ESEM-FEG/EDAX microscope). For SEM analysis, the zeolite samples were mounted directly on the holders and analysis was performed at 20-25 kV electron beam accelerating voltage. Magnification of the samples was selected at 1500, 3000 and 6000x. Surface elemental composition of zeolite samples was obtained by energy dispersive X-ray spectroscopy (EDAX).

3.2.3.7. FTIR Analysis. Before and after adsorption, the infrared spectra of OTC and zeolite samples were registered using a (Perkin-Elmer FTIR Spectrophotometer Model 1600) FTIR spectrophotometer at room temperature. The zeolite samples were prepared using the KBr pressed pellet technique. Two to four mg of zeolite and OTC samples were mixed with approximately 150 mg of KBr. The mixture was milled to a fine powder using a mortar and pestle and made into a fragile pellet using a high pressure compression machine. This pellet was used for FTIR analysis. The FTIR spectra were set to scan in the region of 4000-400 $cm^{-1}$with a resolution of 2 cm^{-1}.

3.2.3.8. X-ray Diffraction Analysis. The crystalline phases of zeolite were determined by X-ray diffraction (XRD) analysis with a Rigaku-D/Max-2200 Ultima X-Ray diffractometer with CuKα radiation generated at 40 kV, 40 mA and a scanning rate of $2°min^{-1}$.

4. RESULTS AND DISCUSSION

4.1. X-ray Diffraction Analysis of Raw, Na, and HDTMA-modified Zeolite

Components of the zeolites were investigated by X-ray diffraction analysis. Figure 4.1 displays the XRD patterns for raw, Na, and HDTMA-modified zeolite samples.

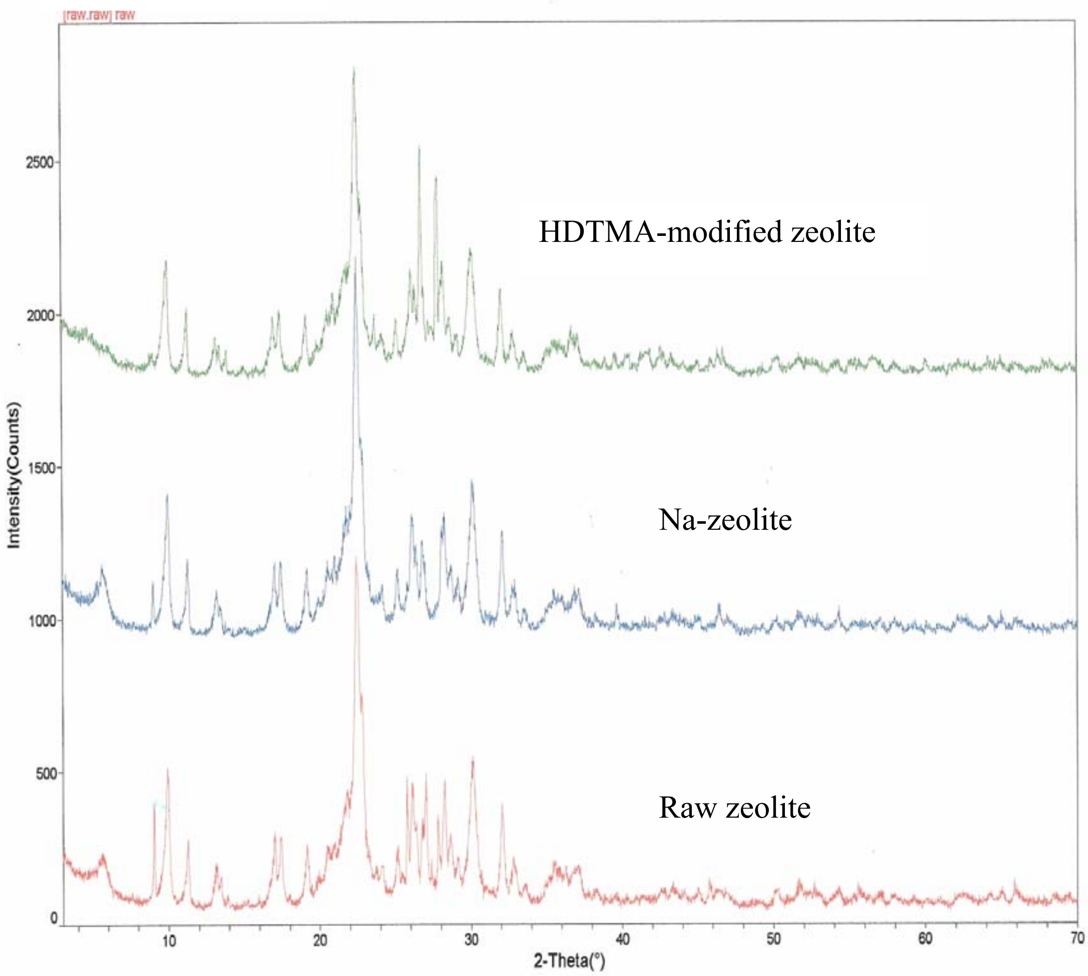

Figure 4.1. XRD patterns of raw, Na and HDTMA-modified zeolite

According to X-ray diffraction patterns of raw, Na, and, HDTMA-modified zeolite, the most intense diffraction peaks belong to clinoptilolite–Ca (KNa_2Ca_2 (Si_{29} Al_{17}) O_{72}24 H_2O) at 2θ = 22.459° for raw, 22.520° for Na zeolite and 22.461° for HDTMA-modified zeolite (Figure 4.1). Other mineral phases (magadite, zeolite Rho) were also found in minor amounts.

It can be seen in the Figure 4.1, the most intense peaks of raw zeolite were detected at 2θ = 22.459° (100 per cent), 22.800° (62 per cent), 25.781° (45 per cent), 27.037° (33 per cent), 30.122° (39 per cent), and 27.816° (26 per cent). Their relative intensities and corresponding interlayer spacing are presented in Appendix B Table B.1.

Modification of zeolite with Na resulted in slight changes in the position of diffraction peaks. Some peaks disappeared at 2θ = 25.781°, 27.037° and 27.816° and new small peaks were appeared at 2θ = 39.646° (6 per cent), 42.819° (3.5 per cent), and 43.378° (4 per cent). However, no significant changes in interlayer spacing were detected (Appendix B Table B.2).

According to X-ray diffraction analysis of HDTMA-modified zeolite, some peaks disappeared at 2θ = 17.076° (19 per cent), and 22.899° (45 per cent). New peaks were appeared at 2θ = 23.275° (9 per cent), 23.716° (18 per cent), 27.820° (68 per cent), 35.643° (10 per cent), and 46.704°(10 per cent) . Their interlayer spacing was almost remained constant (Appendix B Table B.3).

4.2. Cation Exchange Capacities of Raw and Modified Zeolites

Zeolites normally provide a number of different intra-crystalline environments for cations in the crystalline network. These cations then have different exchange properties for each environment and pre-treatment is recommended in order to reach a final homoionic or near homoionic state of the zeolites to improve their effective exchange capacities. As can be seen in Table 4.1 treatment of raw zeolite with Na^+ did not improve total cation exchange capacity of zeolite. On the other hand, external cation exchange capacity of Na-zeolite increased two fold.

Clinoptiolite has negative charge as a result of isomorphic substitution of Si^{4+} with Al^{3+} in the crystal lattice. Cations can interact with the zeolite via ion exchange on the negatively charged internal and external surfaces. However, the rigid cage-like structure of zeolite is too small for the HDTMA cation to access the interior exchange. Thus positively charged head of HDTMA attaches itself to negatively charged external surfaces of zeolite and this resulted in a change in the CEC of zeolite. Surface modification of Na-zeolite with HDTMA led to a decrease in total cation exchange capacity of zeolite while it improves its external cation exchange capacity (Table 4.1).

Table 4.1. CEC and ECEC of raw and modified zeolites.

Zeolite	**CEC (meq/100g)**	**ECEC (meq/100g)**
Raw zeolite	62.3	11.1
Na-zeolite	61.9	20.7
HDTMA-modified zeolite	47.2	31.7

4.3. Effect of Contact Time on Sorption

The kinetics of sorption that describes the solute uptake rate governing the contact time of the sorption reaction is one of the important characteristics that define the efficiency of sorption. Hence, a series of contact time experiments for raw, Na, and HDTMA-modified zeolites have been carried out with 0.06 mM (29.8 mg/L) initial OTC concentration and 40 g/L zeolite at pH 6.5 and 8 by increasing the contact time up to 32 h (1920 min) (Figure 4.2). Amount of adsorbed OTC, q_t (mg/g), onto the zeolite was calculated by mass balance relationship,

$$q_t = \frac{(C_0 - C_t)V}{W} \qquad (4.1)$$

where C_0 and C_t are initial and at time =t liquid phase concentrations of OTC (mg/L) ,V is the volume of solution (L), and W is the weight of zeolite used (g).

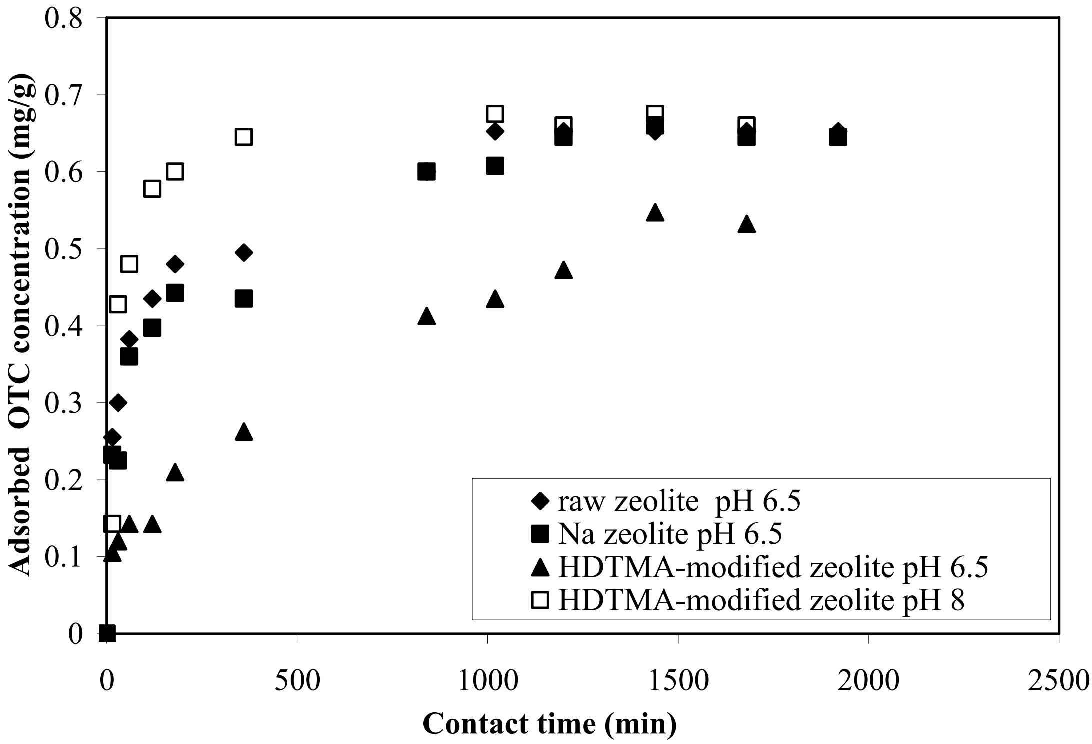

Figure 4.2. Effect of contact time on OTC uptake ([OTC] = 0.06 mM; [zeolite] =40 g/L; pH=6.5 and pH=8; 25º C).

As observed from Figure 4.2, raw and Na-zeolite exhibited similar performance for the adsorption of OTC at pH 6.5 whereas HDTMA-modified zeolite has lower adsorption capacity at this pH. Figure 4.2 also shows that adsorption of OTC onto raw, Na, and HDTMA-modified zeolite could be characterized by three distinct phases: the first phase indicated the fast sorption of OTC within two h contact time, the second one showed a gradual equilibrium, and the third one indicated the final equilibrium. Actually, this trend is typical for the adsorption of tetracycline group antibiotics on clay minerals (Sithole and Guy, 1987a). After 17 h contact time, OTC adsorption leveled off and q_t values of OTC obtained by raw, Na, and HDTMA-modified zeolite were 0.65 and 0.66, and 0.55 mg/g, respectively. Unlike the sorption at pH 6.5, fast sorption of OTC by HDTMA modified zeolite was achieved within 30 min contact time at pH 8. After 17 h, OTC sorption by HDTMA-modified zeolite reached to the equilibrium and the maximum OTC sorption was 0.68 mg/g. The contact time of 24 h appeared to be sufficient to reach equilibrium for three different zeolites therefore contact time was maintained at 24 h for performing the following experiments. The time required to attain this state of equilibrium is termed the equilibrium time and the amount of adsorbed OTC at the equilibrium time reflects the maximum adsorption capacity of the adsorbents under those operating conditions. At this point, the amount of OTC being adsorbed onto the adsorbent would be in a state of dynamic equilibrium with the amount of the OTC desorbing from the adsorbent. However, desorption of OTC were not detected under applied experimental conditions.

In order to study the rate-determining step for the adsorption of OTC, three kinetic models were tested to fit experimental data obtained from batch adsorption experiments: the pseudo first order kinetic model proposed by Lagergren (Ho and Chiang, 2001), the pseudo-second order kinetic model described by Ho and McKay (Ho and McKay, 1999), and intraparticle diffusion model given by Weber and Morris (Ru et al., 2007).

The pseudo first order model (eq. 4.2) assumes that the rate of adsorption is directly proportional to difference in saturation concentration and the amount of solid uptake with time.

$$\frac{dq_t}{dt} = k_1(q_e - q_t) \qquad (4.2)$$

where k_1 is the rate constant of pseudo-first order adsorption (1/min) and q_e and q_t are the amounts of sorbate adsorbed per unit mass of adsorbent (mg/g) at equilibrium and time t, respectively. After integration by applying the initial conditions, q_t=0 at t=0 and equilibrium condition, equation 4.3 is obtained.

$$\log(q_e - q_t) = \log q_e - \frac{k_1}{2.303}t \qquad (4.3)$$

The equilibrium adsorption, q_e is required to fit the data. In many cases, the pseudo-first order equation of Lagergren does not fit well whole range of contact time and is generally applicable over the initial stage of adsorption process (Aksu and Tezer, 2000; Chiou and Li, 2002).

On the other hand, the pseudo-second order equation (eq. 4.4) is based on adsorption equilibrium capacity.

$$\frac{dq}{dt} = k_2 (q_e - q_t)^2 \qquad (4.4)$$

Integrating the equation for boundary conditions, t=0 to t=t and q_t=0 to q_t=q_e gives following equation:

$$\frac{t}{q_t} = \frac{1}{k_2 q_e^{\ 2}} + \frac{t}{q_e} \qquad (4.5)$$

where k_2(min g/mg) is the rate constant of second order adsorption. $k_2q_e^2$ is the initial sorption rate (mg/g min). In the case of the pseudo-second order kinetics whole range of adsorption can be predicted and there is no need to know any parameter of adsorption beforehand (Ho and Mckay, 1999).

To identify the mechanism of adsorption, intraparticle diffusion model (eq. 4.6) was also applied to obtained adsorption data. This model suggests that the sorption process is controlled by the internal diffusion with a minor effect of the external diffusion (Khraisheh et al., 2002).

$$q_t = k_p \sqrt{t} + C \qquad (4.6)$$

where q_t (mg/g) is the concentration of organics sorbed at time t and k_p (mg/g min$^{1/2}$) is the rate constant for intraparticle transport and C is the intercept. The linearized forms of the pseudo first and second order models for OTC adsorption on three types of zeolites are presented in Figures 4.3 and 4.4, respectively. Both log (q_e-q_t) and t/q_t were calculated from the kinetic data for each type of zeolite and are plotted against time. First order equation was applied to the data obtained within 1200 min contact time whereas whole data was used for second order model.

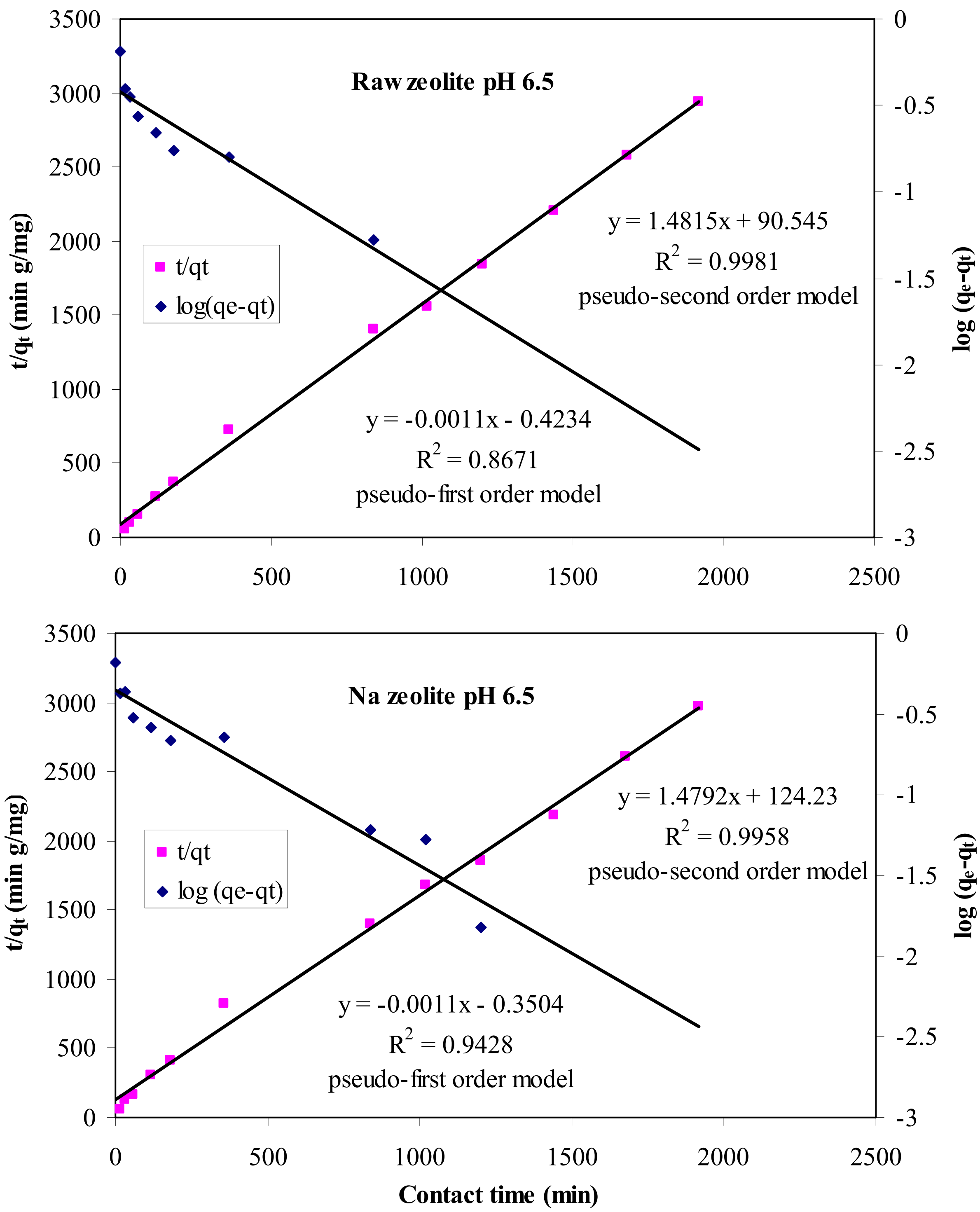

Figure 4.3. Pseudo-first and pseudo-second order plots for OTC adsorption on raw and Na-zeolite at pH 6.5.

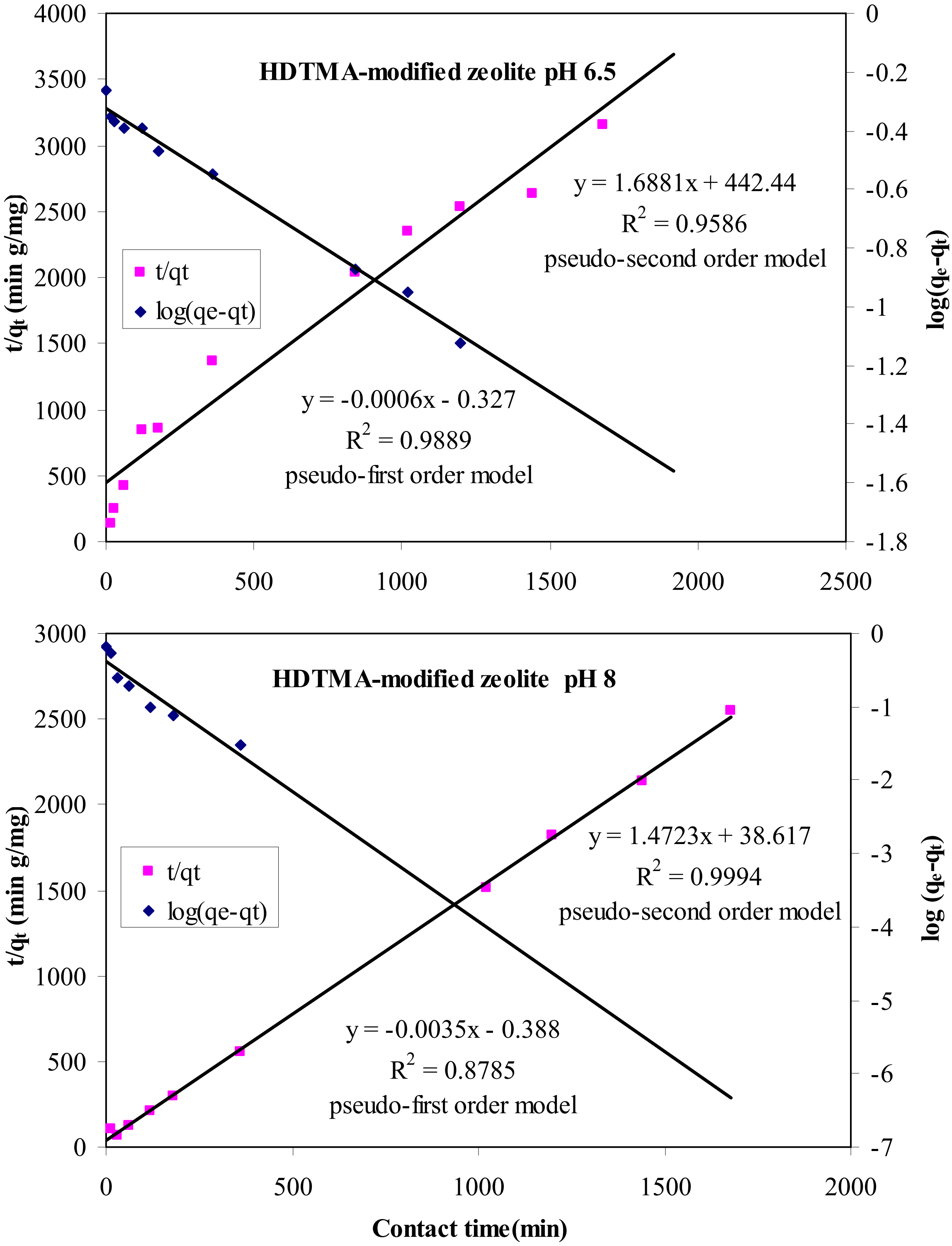

Figure 4.4. Pseudo-first and pseudo-second order plots for OTC adsorption on the HDTMA-modified zeolite at pH 6.5 and 8.

Pseudo-first and pseudo-second order OTC adsorption rate constants and experimental and calculated q_e values of three different types of zeolites are tabulated in Table 4.2 together with correlation coefficients.

Table 4.2. Comparison of the pseudo-first and pseudo-second order adsorption rate constants and calculated and experimental q_e values of different types of zeolite.

Adsorbent	**Pseudo-first order kinetic model**				**Pseudo-second order kinetic model**		
	q_e(exp) (mg/g)	**k_1 (1/min)**	**q_e(calc) (mg/g)**	**R^2**	**k_2 (g/mg min)**	**q_e(calc) (mg/g)**	**R^2**
Raw zeolite pH 6.5	0.65	$2.53x10^{-3}$	0.38	0.87	$2.40\ x10^{-2}$	0.67	0.99
Na zeolite pH 6.5	0.66	$2.53x10^{-3}$	0.44	0.94	$1.70\ x10^{-2}$	0.68	0.99
HDTMA-modified zeolite pH 6.5	0.55	$1.38x10^{-3}$	0.47	0.99	$6.44\ x10^{-3}$	0.59	0.95
HDTMA-modified zeolite pH 8	0.68	$8.06x10^{-3}$	0.41	0.88	$5.60\ x10^{-2}$	0.68	0.99

As can be seen in Table 4.2, the experimental q_e values did not agree with the calculated q_e values obtained by the pseudo-first order kinetic model for all types of zeolites. However, linear plots of t/q versus t show a better agreement of experimental data with the second order kinetic model for all zeolites and extremely high correlation coefficients were obtained (Table 4.2). This result revealed that chemisorption can be the rate limiting step for the adsorption of OTC.

The calculated initial sorption rates ($k_2q_e^2$) of raw, Na-zeolite, and HDTMA-modified zeolite at pH 6.5 were $1x10^{-2}$, $0.76x10^{-2}$, and $0.22x10^{-2}$ mg/g min, respectively. Among three adsorbents, HDTMA-modified zeolite has the fastest initial sorption rate at pH 8 and it was found as $2.5x10^{-2}$ mg/g min.

Intraparticle diffusion model of three types of zeolite presents in Figure 4.5.

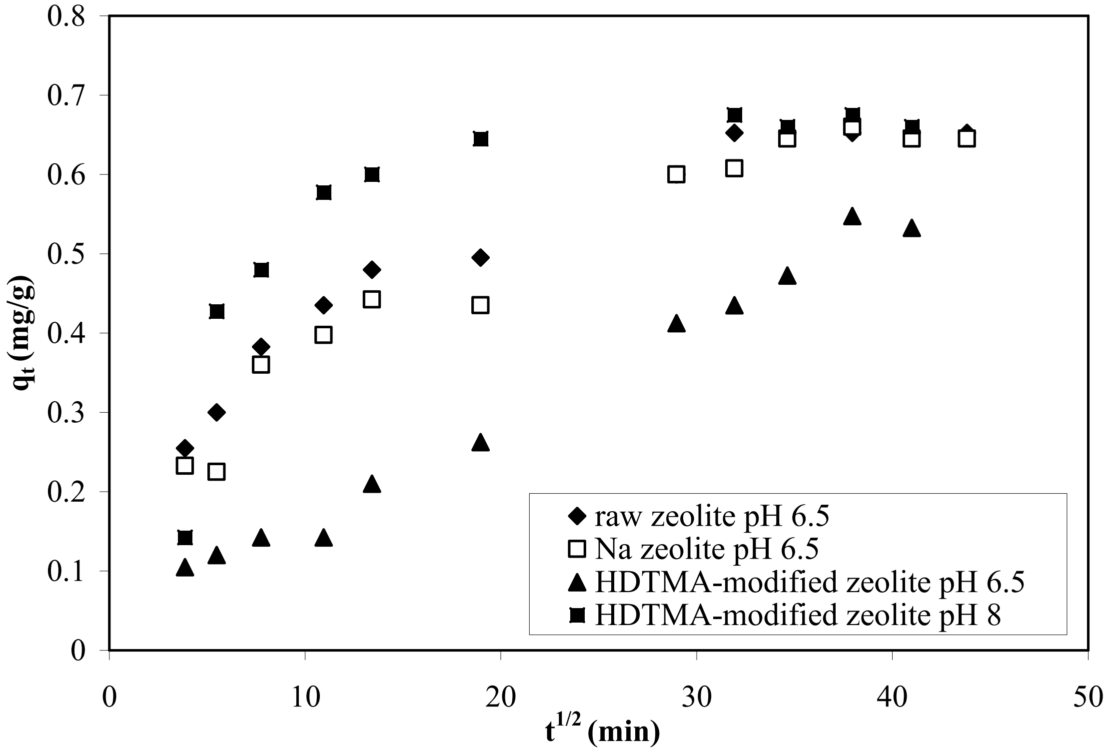

Figure 4.5. Intraparticle diffusion model plot of OTC adsorption on three types of zeolite.

As shown in Figure 4.5 the obtained data have multi-linearity character except obtained for HDTMA-modified zeolite at pH 6.5; two or more steps occurred in the adsorption process. At the beginning stage, OTC was adsorbed by the exterior surface of zeolite and the adsorption was fast when the exterior surface adsorption of zeolite reached saturation, the OTC further entered the pores of zeolite and was adsorbed by the interior surface. When OTC diffused in the pores of zeolite the diffusion resistance increased due to low OTC concentration and the adsorption rate decreased.

Intraparticle diffusion equation was fitted for the data obtained within 180 min contact time for raw, Na-zeolite at pH 6.5 and HDTMA-modified zeolite at pH 8. This period was the gradual adsorption stage where intraparticle diffusion started. However, the q_t versus $t^{0.5}$ plot of HDTMA-modified zeolite at pH 6.5 was straight line in the whole time interval studied. The intraparticle diffusion model constants were calculated using eq.4.6 and represented in Table 4.3.

Table 4.3. Intraparticle diffusion model parameters for three different types of zeolite.

Adsorbent	**C**	**k_p (mg. min$^{1/2}$/g)**	**R^2**
Raw zeolite pH 6.5*	0.17	2.3 x10^{-2}	0.97
Na-zeolite pH 6.5*	0.13	2.4 x10^{-2}	0.91
HDTMA-modified zeolite pH 6.5**	0.04	1.2 x10^{-2}	0.99
HDTMA-modified zeolite pH 8*	0.10	4.1 x10^{-2}	0.77

*from the obtained data within 180 min
**from the obtained data within 1680 min

As observed in Table 4.3, by application of intraparticle diffusion model the highest diffusion rate constant was obtained for HDTMA-modified zeolite at pH 8. However, the correlation coefficient is quite low at pH 8. In summary, the adsorption data was well described by both pseudo-second order kinetics and intraparticle diffusion models.

4.4. Effect of Zeolite Amount on Sorption

The adsorption of OTC on Na-zeolite was studied by changing the quantity of sorbent in the OTC solution whilst maintaining the initial concentration of OTC (0.06 mM), agitation speed (110 rpm), contact time (24 h), pH (pH=6.5), and temperature (25 ± 1^0C) constant. In order to investigate the effect of zeolite dosage on OTC sorption adsorption experiments were performed with solid/solution ratio of 1:50; 1:25; 1:5 and 1:1. These ratios were selected in accordance with OECD adsorption experiment procedure (OECD, 2000). Figure 4.6 represents sorbed OTC concentration q_e (mg/g) as a function of sorbent dosage.

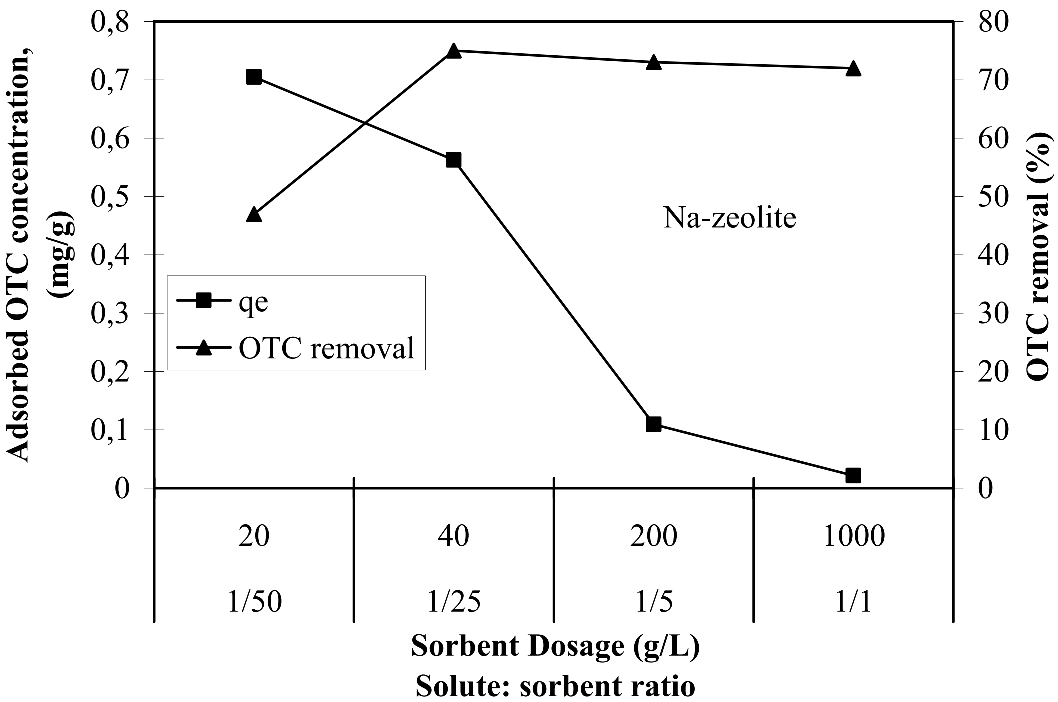

Figure 4.6. Adsorbed OTC concentration as a function of sorbent dosage ([OTC] =0.06 mM; pH 6.5; 25 ^{0}C).

It is evident from Figure 4.8 that as the amount of adsorbent dosage increases up to 40 g/L the maximum OTC removal percentage was attained with this amount due to the increase in the availability of surface active sites. However, if the adsorption capacity was expressed in mg adsorbed per gram of adsorbent, the capacity decreased with the increasing amount of sorbent. The increase in the extent of OTC removal is found to be almost constant above a dose of 40 g/L which were used as the optimum dose of adsorbent in further experiments.

4.5. Effect of pH on Sorption

For the adsorption of organic molecules on solid surfaces different mechanisms can be responsible (Hutzinger, 1982). Since pH influences both ionization forms of adsorbate and surface properties of adsorbent, it is one of the most important parameter for adsorption. As previously mentioned, OTC exists predominantly as a cation below pH 3.3 due to the protonation of dimethylammonium group, as a zwitterion between pH 3.3 and 7.3 resulting from the loss of proton from phenolic diketone moiety, and as an anion above pH 7.3 due to loss of protons from the tricarbonyl system and phenolic diketone moiety. Changes in the ionic form of OTC cause a shift in maximum absorbance wavelength. Before the adsorption experiments, the UV absorbance spectra of OTC at four different pH values were determined (Figure 4.7) in order to construct the calibration curves which are necessary to determine the sorbed amount of OTC.

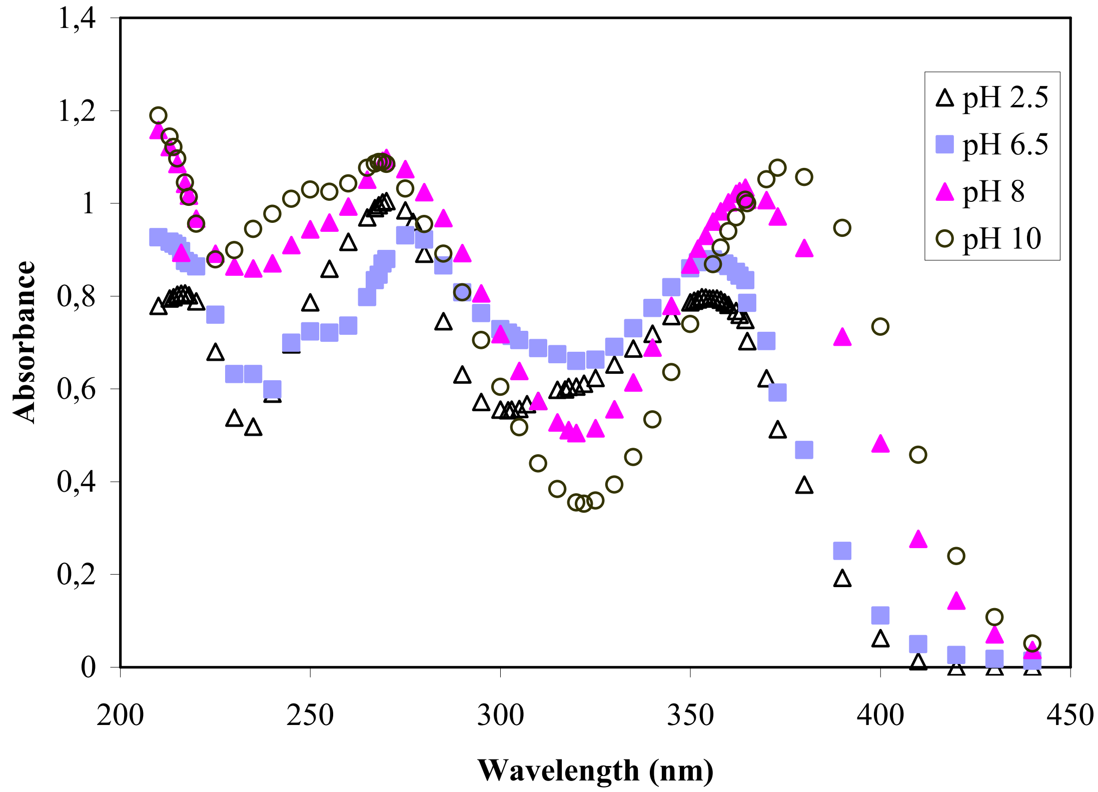

Figure 4.7. Absorption spectra of OTC (0.06 mM) at different pH values.

As observed from Figure 4.7, the absorption spectrum of 0.06 mM OTC displays three bands centered at 217, 270, and 353 nm wavelengths at pH 2.5. Deprotanation results in shift in these bands. As the pH increased from 2.5 to 10, the long wavelength absorption maxima bathochromically shifts to 373 nm wavelength and the short wavelength absorption maxima hypsochromically shifts from 217 to 210 nm as similar to previous studies (Buckley and Smyth, 1986; Linares and Brikgi, 2006). The shift was accompanied by variation of absorption intensity. Moreover, a second maximum placed at 270 nm wavelength first decreased at pH 6.5 and then increased as the pH rises. The band positioned at 217 nm wavelength disappears when the pH increased. Because of the variations both in absorption maxima and intensity at each pH value separate calibration curves had been prepared (Appendix A Figure A.1) and the results of adsorption experiments were evaluated according to these calibration curves.

In order to investigate the effect of pH on the adsorption of OTC, experiments were carried out with Na-zeolite and HDTMA-modified zeolites. By taking into account the pollution of both soil and sediment with antibiotics, experiments were performed over a wide pH range (2.5-10). For the evaluation of the adsorption data distribution coefficient (K_d) and OTC removal percentage values were used. Distribution coefficient and removal efficiency of OTC were calculated as follows,

$$K_d = \frac{q_e}{C_e} \qquad (4.7)$$

$$\text{OTC removal } (\%) = \frac{C_0 - C_e}{C_0} \times 100 \qquad (4.8)$$

K_d = distribution coefficient (L/g or L/kg),

q_e = adsorbed OTC concentration (mg/g or mmol/kg),

C_e = equilibrium OTC concentration (mg/L or mM),

C_0 = initial OTC concentration (mg/L or mM).

The effect of pH on OTC adsorption to Na-zeolite surface is shown in Figure 4.8.

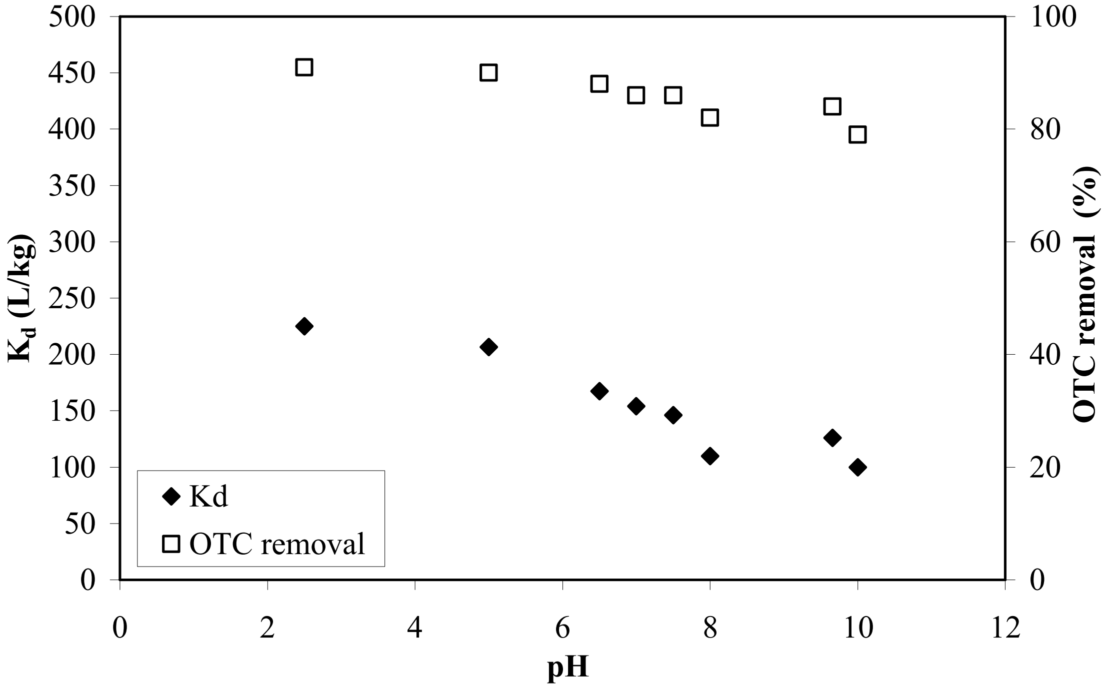

Figure 4.8. Sorption of OTC onto Na-zeolite as a function of pH ([OTC] =0.06 mM; [Na-zeolite] = 40 g/L).

Similar to the adsorption of OTC on clay surface (Sithole and Guy, 1987a, Kulstrestha et al., 2004; Figueroa et al., 2004), K_d values obtained by Na-zeolite exhibited a decreasing trend with increasing solution pH (Figure 4.8). Maximum OTC sorption onto Na-zeolite occurred at pH 2.5 was 90 per cent. It had been shown that zeolite exhibited negative zeta potential values in the pH range from 3-11 (Armağan et al., 2003). As the pH of OTC solution becomes lower, the association of OTC cations with negatively charged zeolite could take place. On the other hand, as the pH increased, sorption was decreased due to repulsion of OTC anions from the negatively charged zeolite surface. Although by increasing pH from 2.5 to 8 K_d decreased from 227 to 110 L/kg, OTC removal decreased from 91 to 82 per cent. This result obtained at alkaline pH suggests that sorption of OTC not only occurred by electrostatic attraction but also other mechanisms such as cation bridging.

In previous studies (Figueroa et al., 2004; Kulstrestha et al., 2004) sorption of OTC onto Ca–saturated montmorillonite at alkaline pH was explained by cation bridging between OTC anion and Ca^{2+}. However, K_d and K_f values of OTC determined in these studies were significantly higher than that obtained in the present study. From the results of previous studies (Figueroa et al., 2004; Kulstrestha et al., 2004) it can be concluded that higher CEC and higher organic carbon content of soil resulted in high sorption rate of OTC. Ionic strength, pH, and presence of complexing agents also affect the adsorption and desorption of OTC from clay and soil surfaces. In case of clay minerals, CEC and surface area are the predominant factors that affect adsorption.

For HDTMA-modified zeolite the effect of pH on OTC adsorption is presented in Figure 4.9.

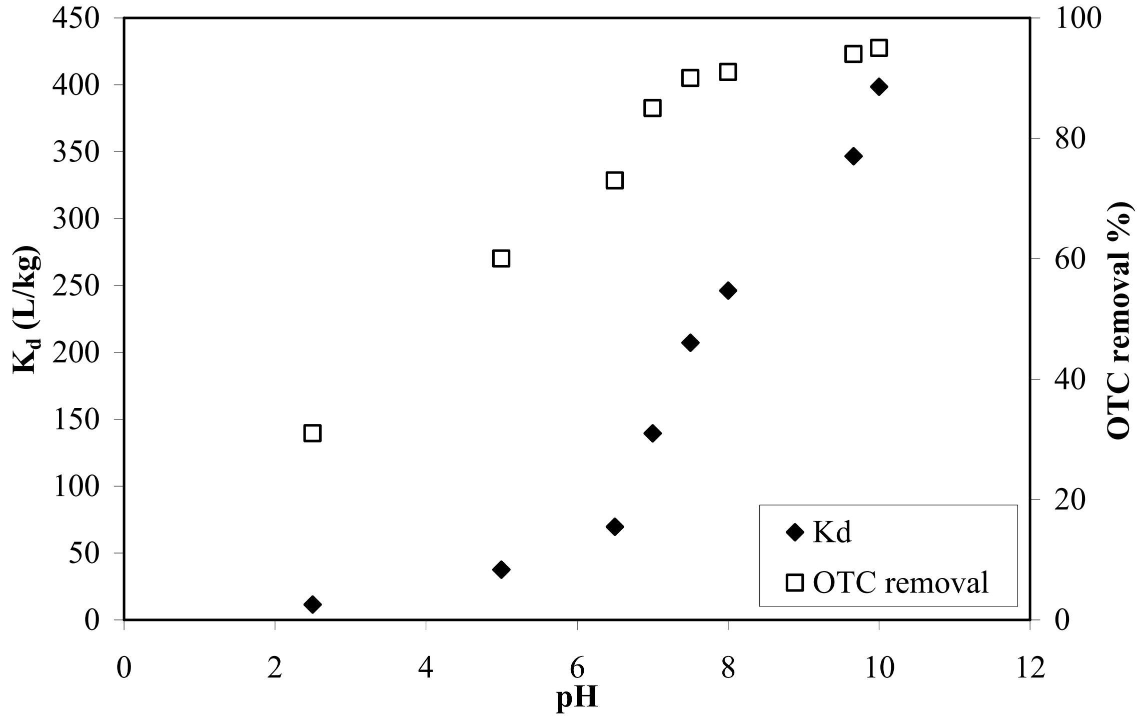

Figure 4.9. Sorption of OTC onto HDTMA-modified zeolite as a function of pH ([OTC] =0.06 mM; [HDTMA-modified zeolite] = 40 g/L).

In contrast to the results obtained by Na-zeolite, OTC adsorption onto HDTMA-modified zeolite increased with an increase in pH (Figure 4.9). This result is well expected since electrostatic interaction between positively charged zeolite surface and negatively charged OTC could be the main mechanism for the sorption on HDTMA-modified zeolite at alkaline pH. At pH 2.5 K_d value of OTC was comparably low (11.5 L/kg) As the pH increases, OTC became negatively charged and surface of HDTMA-modified zeolite favored the adsorption due to electrostatic attraction. Thus, 95 per cent OTC removal was obtained at pH 10 and K_d reached to 395 L/kg. The variation in K_d value by changing the pH of suspension is more pronounced for HDTMA-modified compare to that of Na-zeolite.

The pH of each OTC suspension solution was also measured at equilibrium. It was found that pH values of OTC solutions equilibrated with Na and HDTMA-modified zeolite were constant except for those performed at pH > 6.5. The pH decreased by ~ 0.5 unit in the experiments conducted at pH 6.5-7.5 and above pH > 7.5 equilibrium pH decreased by one unit. Therefore, additional experiments were performed in the presence of phosphate buffer (Figure 4.10 and 4.11) to maintain constant pH. The results were evaluated by using the calibration curve of OTC prepared in phosphate buffer (Appendix A Figure A.2).

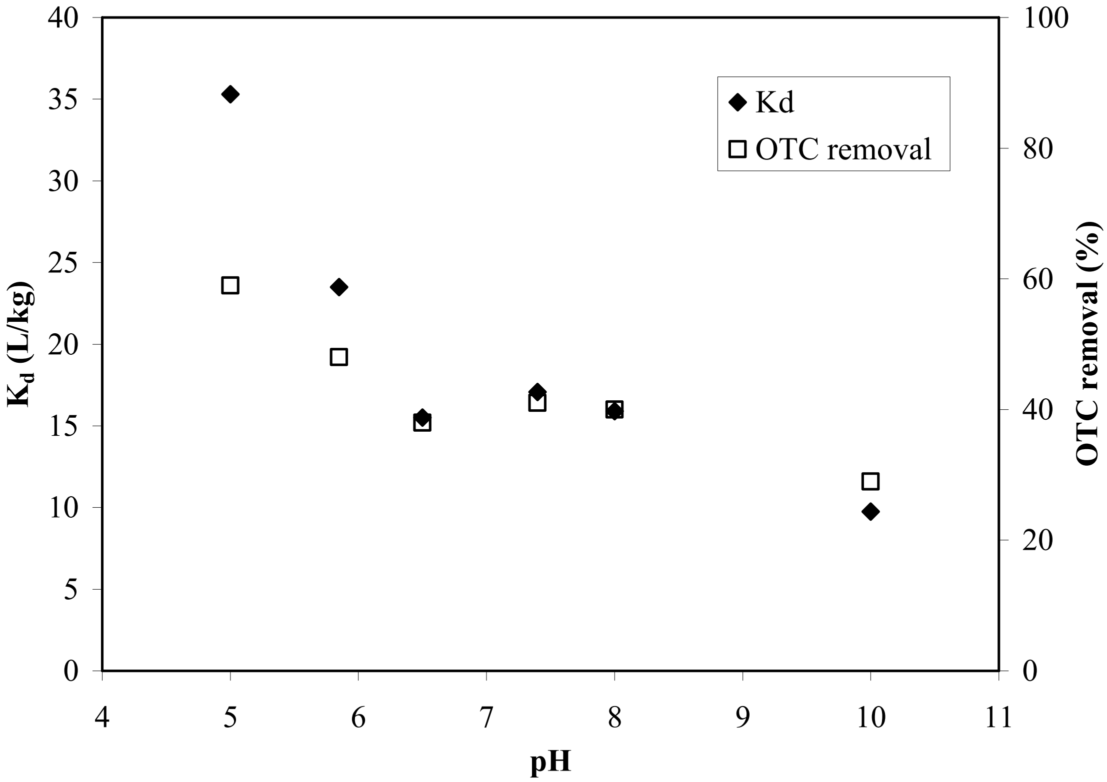

Figure 4.10. Sorption of OTC onto Na-zeolite as a function of pH in the presence of phosphate buffer ([OTC] =0.06 mM; [Na-zeolite] = 40 g/L).

Adsorption of OTC onto Na-zeolite decreased as the pH was increased similar to the results observed in Figure 4.8. However, the values of K_d and removal percentage of OTC were significantly different from those obtained in the absence of phosphate buffer. While K_d was 205 L/kg in the absence of phosphate buffer at pH 5, it was only 35 L/kg in the presence of phosphate buffer. This result could be explained by competitive sorption of phosphate buffer constituents and OTC on zeolite. It was reported that phosphate and citrate buffer cause the release of sorbed OTC and chlortetracycline from clay surface (Figueora et al., 2004). Moreover, it was known that phosphate at high concentration was used to extract the loosely bound OTC from the sediments (Simon, 2005).

The effect of pH on the adsorption of OTC in the presence of phosphate buffer for HDTMA-modified zeolite is presented in Figure 4.11.

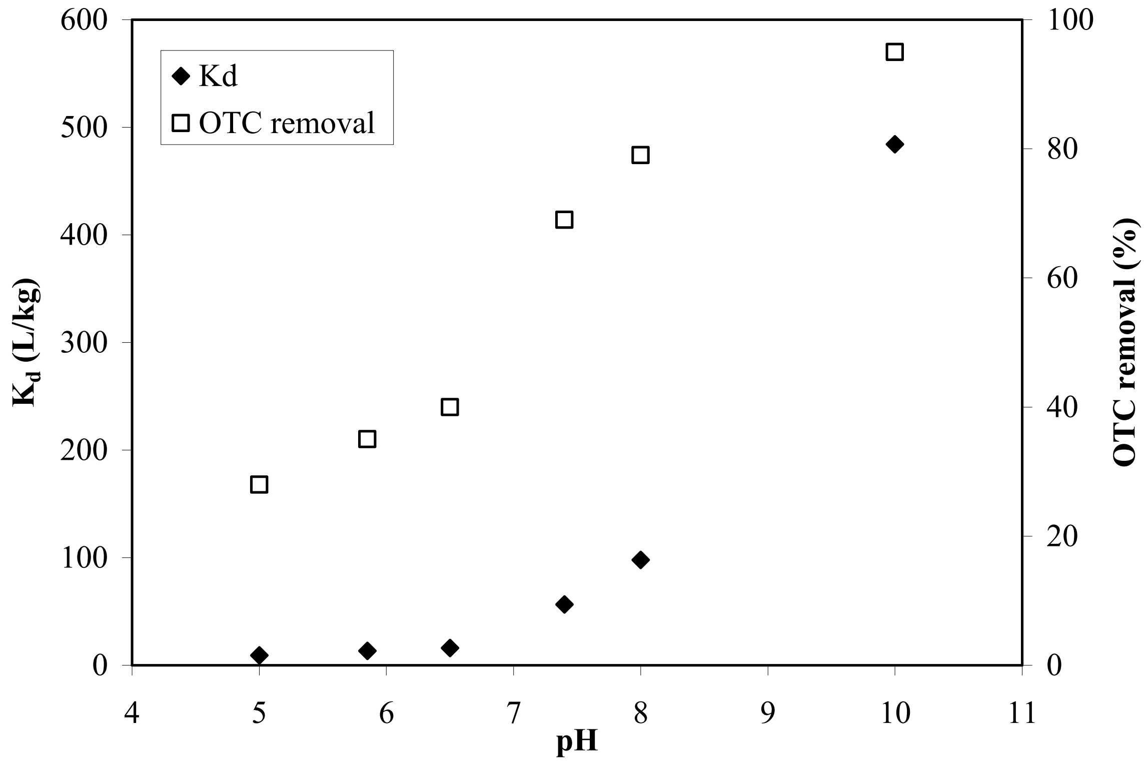

Figure 4.11. Sorption of OTC onto HDTMA-modified zeolite as a function of pH in the presence of phosphate buffer ([OTC] = 0.06 mM; [HDTMA-modified zeolite] = 40 g/L).

Similar to the results obtained in the absence of phosphate buffer, OTC sorption by HDTMA-modified zeolite increased with increasing pH in the presence of phosphate buffer. However, removal percentage and K_d values of OTC in the presence of phosphate buffer were smaller than those obtained in the absence of phosphate buffer. Only 30 per cent OTC removal was achieved in the presence of phosphate buffer at pH 5. On the other hand, OTC removal percentage was 60 per cent in the absence of buffer at the same pH (Figure 4.9).

In the control experiments carried out in the absence of zeolite, OTC concentration decreased 13 per cent with phosphate buffer at pH 10. However, OTC concentration did not change in the absence of phosphate buffer at the same pH.

In summary, the adsorption of OTC onto zeolite could be explained by a combination of electrostatic attraction and cation bridging between cations on zeolite and and OTC species (Sithole and Guy, 1987a; Figueora et al., 2004).

4.6. Adsorption Isotherms

The distribution of OTC between the adsorbent and solution when the system is at equilibrium is important to determine adsorption capacity of zeolite. Therefore, adsorption isotherm experiments were conducted at 25 °C by the using various concentrations of OTC ranged from 0.03 to 0.4 mg/mL. Although these concentrations are significantly greater than those detected in natural sources (Hirsch et al., 1999) the goal of the study was to compare the OTC sorption on Na-zeolite and HDTMA modified zeolite. However, higher concentrations of TCs may occur due to accumulation of them in the environment (Aga et al., 2003) since persistency of TCs in marine sediments had been reported (Samuelsen et al., 1992; Coyne et al., 1994; Hektoen et al., 1995). In the isotherm experiments, constant pH at 6.5 and 8 was maintained by using phosphate buffer. Additionally, in separate experiments, initial pH of suspension was adjusted by the addition of NaOH in order to prevent competitive sorption between buffer constituents and OTC.

A number of equations, which enable the equilibrium data to be correlated, exist and two most frequently used for dilute solutions are the Langmuir and Freundlich isotherms represented equations 4.9 and 4.10, respectively.

$$q_e = \frac{qK_L C_e}{1 + K_L C_e} \qquad (4.9)$$

$$q_e = K_f \times C_e^{\,n} \qquad (4.10)$$

where C_e (mg/L) is the equilibrium concentration of the adsorbate in the aqueous solution, q_e (mg/g) is the equilibrium adsorption capacity of adsorbent q and K_L are Langmuir constants related to maximum adsorption capacity and energy of adsorption, respectively. K_f (mg^{1-n} L^n/g) is the empirical Freundlich distribution parameter which describes adsorption density and n is an empirical exponent which indicates how dramatically the binding strength changes as the adsorption density changes. The linearized form of the Langmuir and Freundlich adsorption isotherm equations are given by equation 4.11 and 4.12, respectively.

$$\frac{C_e}{q_e} = \frac{C_e}{q} + \frac{1}{K_L q} \tag{4.11}$$

$$\log q_e = n \log C_e + \log K_f \tag{4.12}$$

The data obtained in this study were applied to both empirical Freundlich equation and theoretical Langmuir isotherm equation. In general, the Freundlich equation gives better correlation between theoretical and experimental data for the whole concentration range. Therefore only linearized Freundlich isotherms for both types of zeolite are depicted in Figures 4.12 and 4.13. Conformity of the data to the Freundlich equation usually suggests that heterogeneity in the surface and pores of adsorbent will play a role in adsorption (Kulstrestha et al., 2004). Adsorption isotherm of OTC and linearized Freundlich isotherms are presented in Figure 4.12, 4.13, and 4.14. The solid and dotted lines in these figures represent the fitted Freudlich and Langmuir equation, respectively.

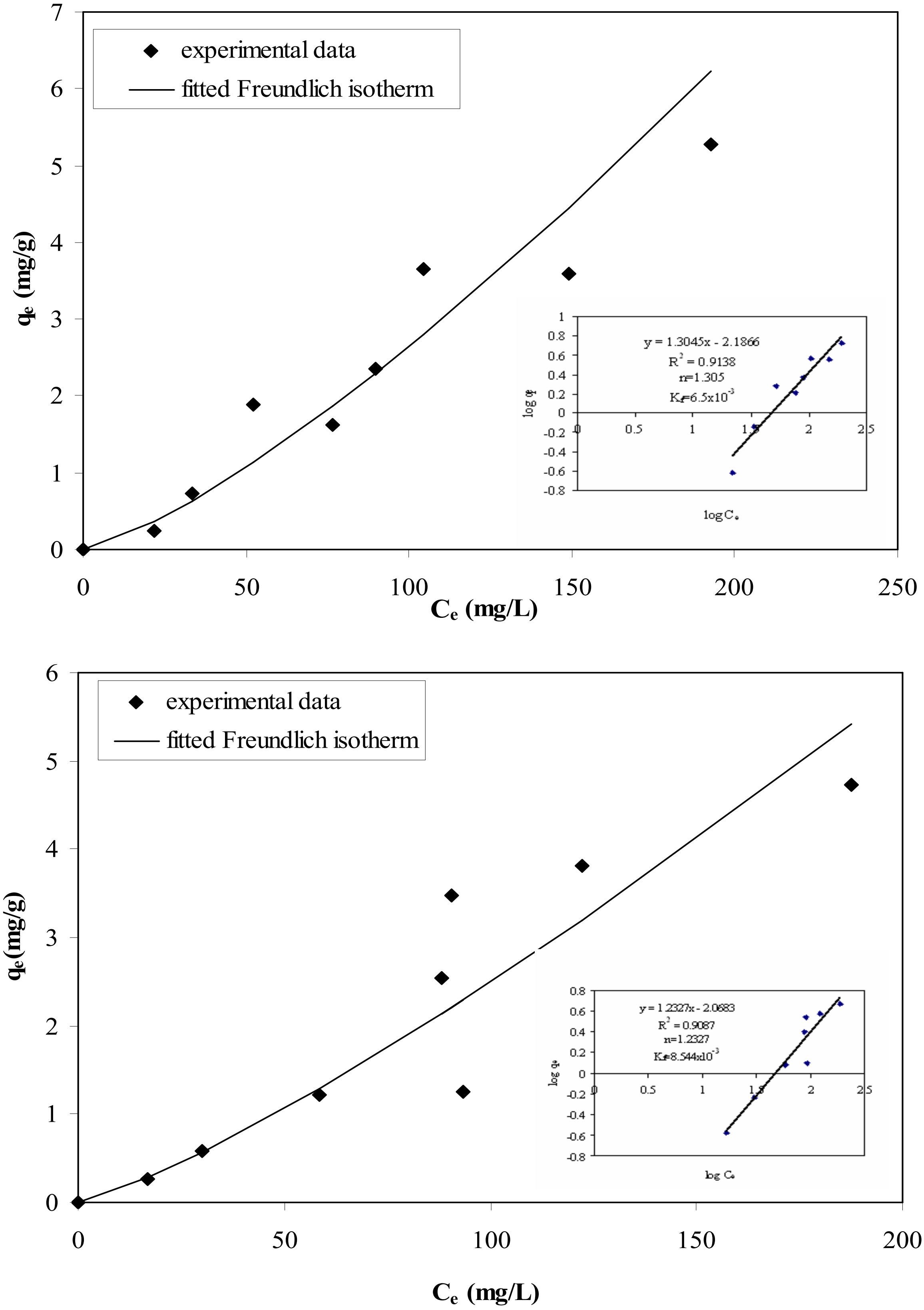

Figure 4.12. Adsorption isotherm of OTC by Na-zeolite at pH=6.5 (a) and pH=8 (b) in the presence of phosphate buffer. Inset: Linearized Freundlich isotherm.

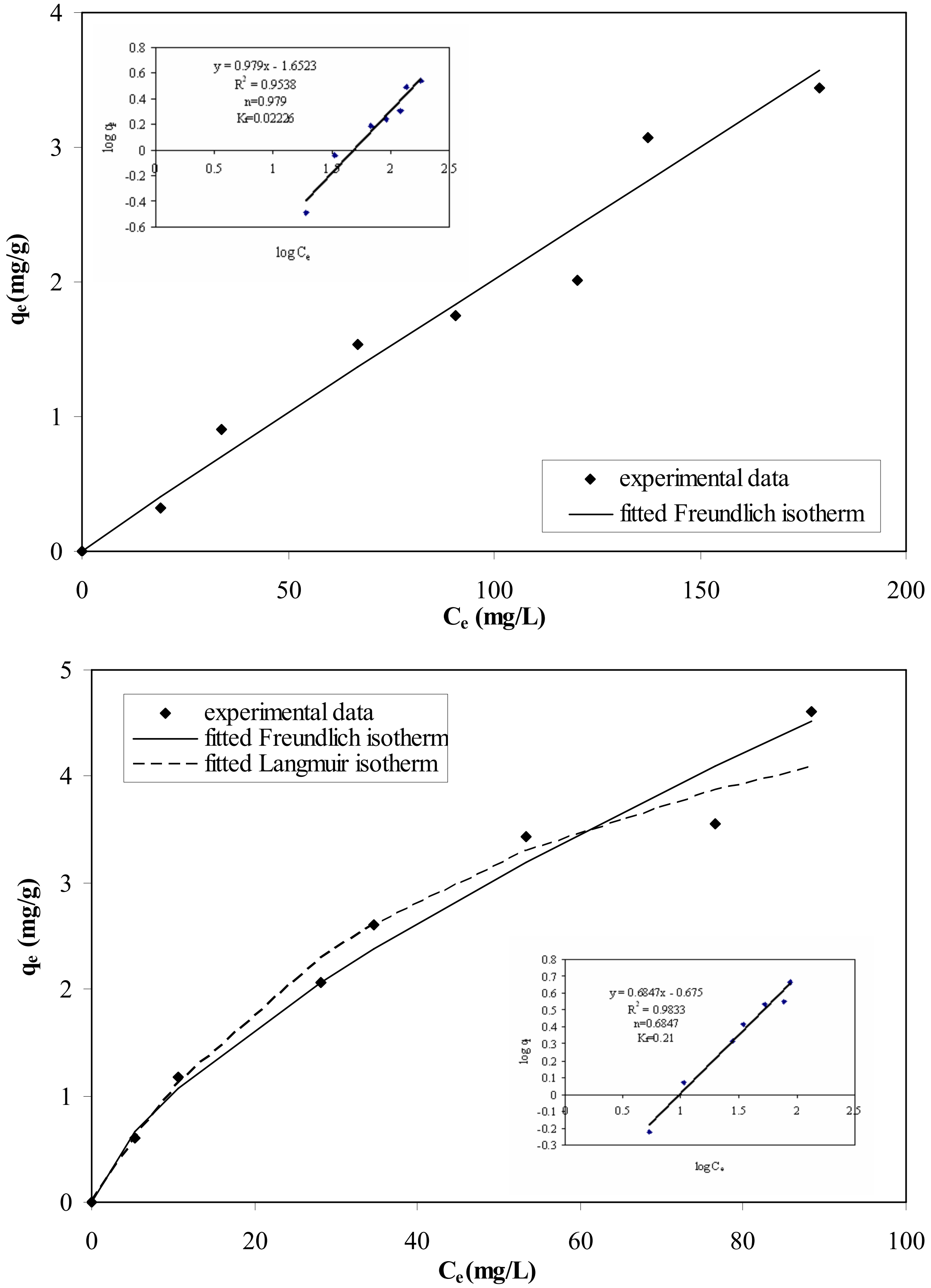

Figure 4.13. Adsorption isotherm of OTC by HDTMA-modified zeolite at pH=6.5 (a) and pH=8 (b) in the presence of phosphate buffer. Inset: Linearized Freundlich isotherm.

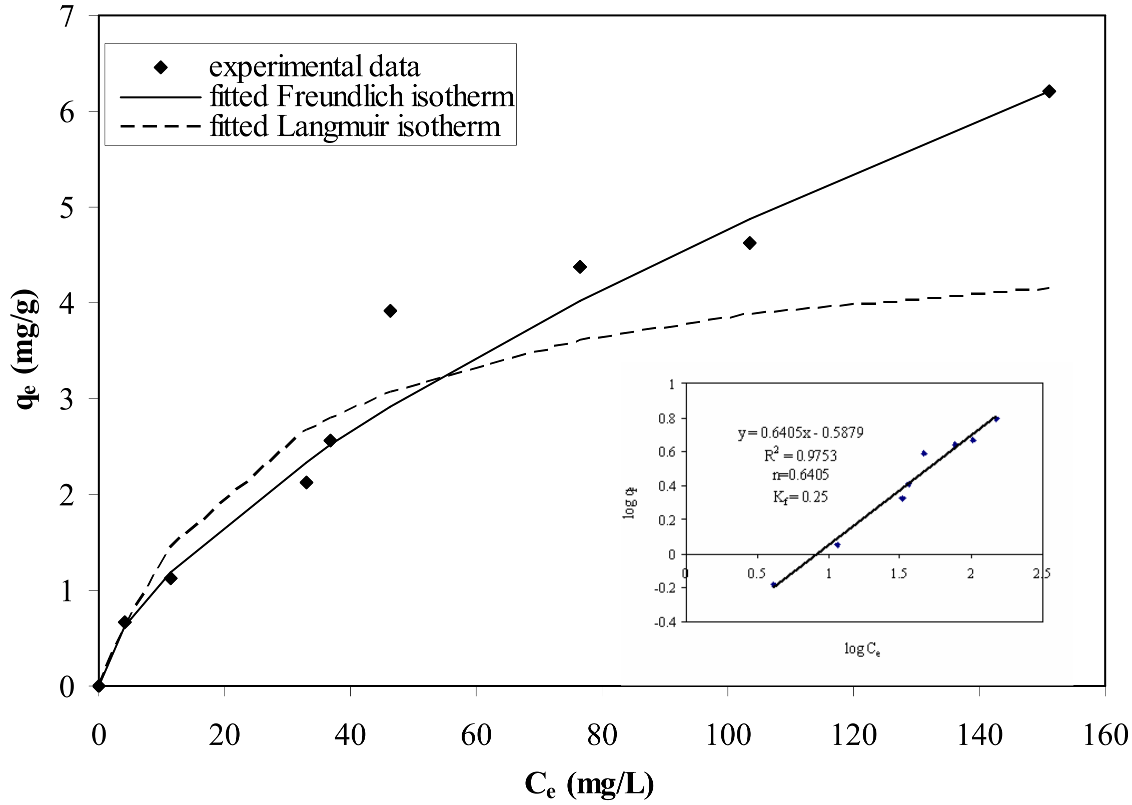

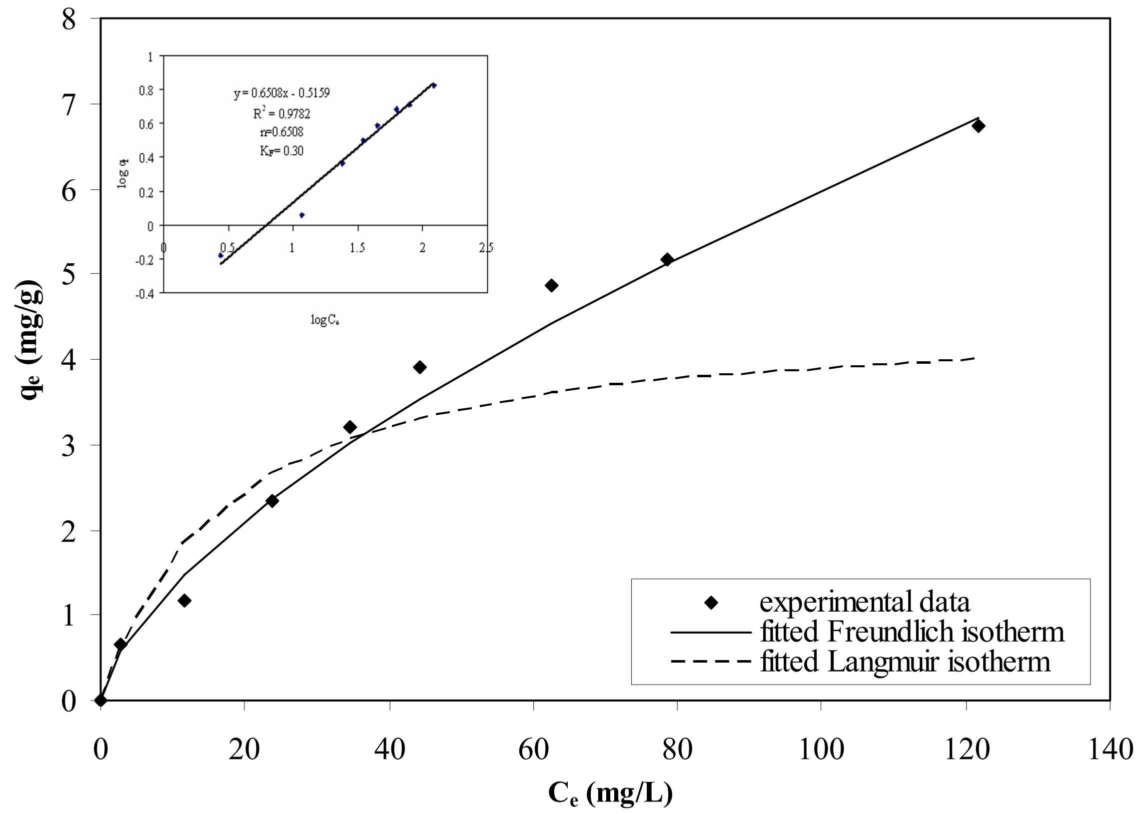

Figure 4.14. Adsorption isotherm of OTC by Na-zeolite at pH 6.5 (a) and HDTMA-modified zeolite at pH=8 (b). Inset: Linearized Freundlich isotherm.

As can be seen from figures the sorption capacity of Na and HDTMA-modified zeolite increased with increasing OTC concentration. The initial concentration provides an important driving force to overcome all mass transfer resistances. As shown in Figure 4.12, 4.13 and 4.14, no maximum adsorption capacity was observed in the isotherm experiment which could be due to the low concentrations of OTC. Another finding from the obtained data is that adsorption of OTC was reduced in the presence of phosphate buffer.

The Freundlich parameters, K_f and n and the Langmuir parameters K_L and q were determined from the intercept and slope of linearized Langmuir and Freundlich isotherms, respectively. The Freundlich and Langmuir parameters together with correlation coefficients are presented in Table 4.4.

Table 4.4. Comparison of the Freundlich and Langmuir isotherm parameters.

Freundlich isotherm	**n**	**K_f (mg^{1-n} L^n/g)**	**R^2**
Na-zeolite pH 6.5 *	1.30	0.65 x 10^{-2}	0.91
Na-zeolite pH 6.5 **	0.64	2.50 x 10^{-1}	0.97
Na-zeolite pH 8 *	1.23	0.85 x 10^{-2}	0.90
HDTMA-modified zeolite pH 6.5*	0.98	0.20 x 10^{-1}	0.95
HDTMA-modified zeolite pH 8 *	0.68	2.10 x 10^{-1}	0.98
HDTMA-modified zeolite pH 8 **	0.65	3.00 x 10^{-1}	0.97
Langmuir isotherm	**K_L (L/mg)**	**q (mg/g)**	**R^2**
Na-zeolite pH 6.5 *	-148.71	0.011	0.88
Na-zeolite pH 6.5 **	27.82	0.17	0.95
Na-zeolite pH 8 *	-261.95	0.015	0.97
HDTMA-modified zeolite pH 6.5*	-506.29	0.017	0.94
HDTMA-modified zeolite pH 8 *	51.17	0.12	0.99
HDTMA-modified zeolite pH 8 **	16.95	0.26	0.91

* pH adjusted with phosphate buffer solutions
** pH adjusted with NaOH solutions

Negative values for the Langmuir isotherm constant as given in Table 4.4 indicate the inadequacy of the isotherm model to explain the adsorption process.

Nonlinear sorption of OTC was detected on organic material (Sithole and Guy, 1987b); montmorillonite (Kulstrestha et al., 2004); pure clay (Figueroa et al., 2004); aluminum and iron hydrous oxides (Gu and Karthikeyan, 2005) and soils (Jones et al., 2005) in previous studies. Similar to these studies, in this study adsorption of OTC on Na and HDTMA-modified zeolite exhibited nonlinear trend except on HDTMA-modified zeolite at pH 6.5. For the OTC sorption on Na-zeolite in the presence of phosphate buffer n was greater than one and for all other cases n was lower than one.

It can be seen in Table 4.4, obtained K_f values varied widely depending upon presence of buffer, zeolite types, and pH. The presence of phosphate buffer significantly reduced the capacity of Na-zeolite at pH 6.5. While K_f value of Na-zeolite was 2.50 x 10^{-1}(mg^{1-n} L^n/g) in the absence of phosphate buffer, it decreased to a value of 0.65 x 10^{-2} in the presence of buffer. However, the effect of phosphate buffer on the K_f value of HDTMA-modified zeolite was not significant at pH 8. HDTMA-modified zeolite exhibited higher adsorption capacity for OTC at pH 8 than that of Na-zeolite at pH 6.5 both in the presence and absence of buffer. From these results it can be suggested that HDTMA-modified zeolite can be used as an effective adsorbent in aquaculture facilities.

K_f constants were found much higher for the different soils compare to zeolite used in the present study. Depending on the soil type and soil components, K_f varied from 92 to 269,000 ($mmol^{-1}L^n$/kg) (Kulshrestha et al., 2004, Jones et al., 2005; Sassman and Lee, 2005). It was found that physical factors of soil such as pore size, surface area, shrink and swell behavior, soil organic carbon, and chemical factors such as pH of solution influenced adsorbent capacity of soil. Low sorption behavior of zeolite can be explained by the absence of organic carbon content and shrink and swell behavior.

4.7. Effect of Ammonia on Sorption

Effect of ammonia on the sorption of OTC was investigated since ammonia has been found in wastewater originated from agricultural and animal farming activities (Liao and Mayo, 1972; Kruner and Rosenthal, 1983; Lin and Wu, 1996). In polluted water, ammonia concentration can be reached to a value of 800 mg/L (Peavy et al., 1985). In order to determine the effect of ammonia on the sorption of OTC, experiments were performed with 0.06 mM OTC and 40 g/L zeolite. Considering the adsorption capacity and practical use of zeolite as an adsorbent in animal farming activities, experiments with Na and HDTMA-modified zeolites were conducted at pH 6.5 and 8, respectively.

Effect of NH_4^+ in the concentration range from 25 to 200 mg/L was studied by the addition of NH_4Cl to the OTC suspension. The adsorption of OTC onto Na-zeolite is presented as a function of NH_4^+ concentration in Figure 4.15.

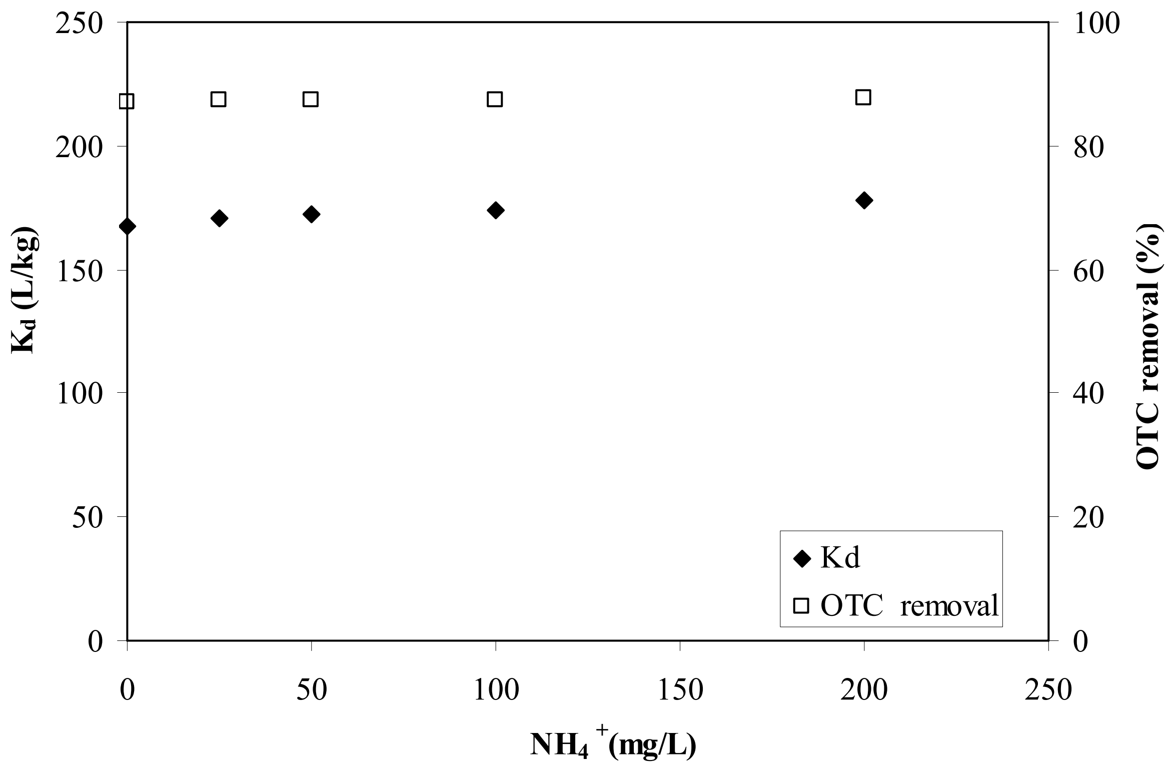

Figure 4.15. Sorption of OTC onto Na-zeolite as a function of NH_4^+ concentration ([OTC] =0.06 mM; [Na-zeolite] = 40 g/L; pH 6.5).

As observed in Figure 4.15, OTC adsorption was not significantly affected by the addition of NH_4^+ to the suspension in the concentration range of 25-200 mg/L. K_d values of OTC slightly increased from 167 to 171 L/kg by the addition of 25 mg/L NH_4^+ and remained almost constant by the increasing the NH_4^+ up to 200 mg/L. However, in a previous study the addition of ammonia increased adsorption of quinoline group antibiotic on natural zeolite (Ötker and Balcıoğlu, 2005).

Control experiments were also conducted in the absence of OTC to evaluate the competitive sorption of NH_4^+ on Na-zeolite. The differences between single and binary systems are shown in Figure 4.16.

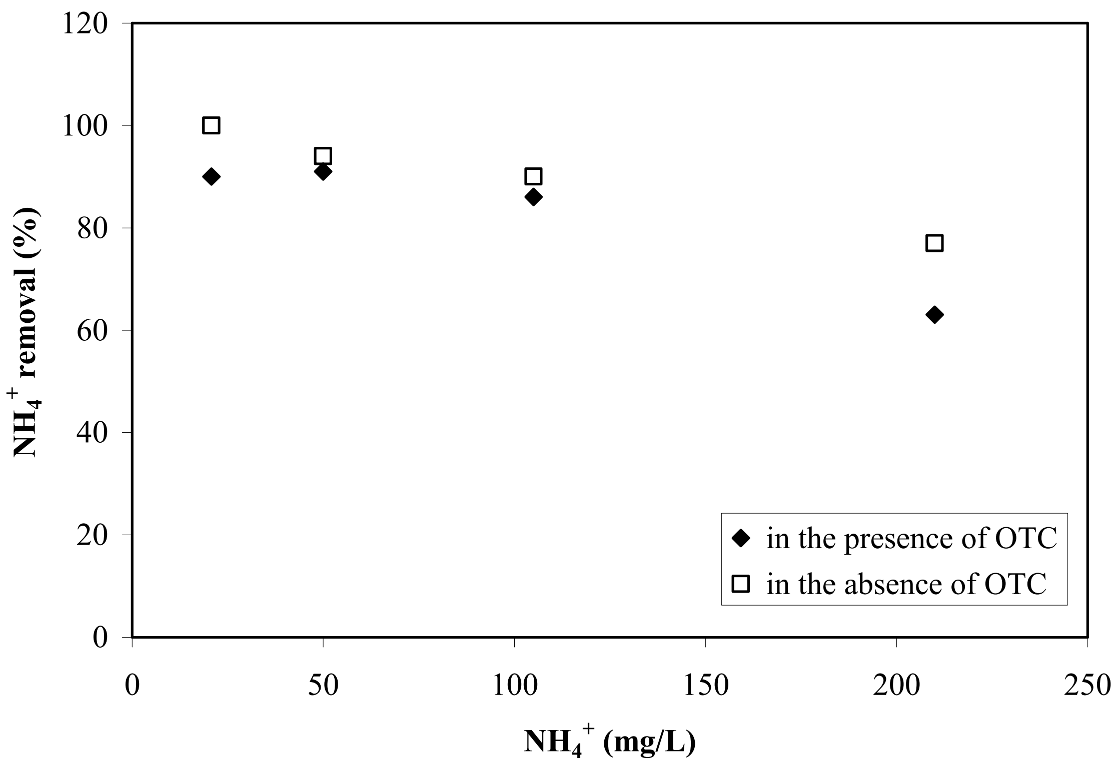

Figure 4.16. Removal percentage of NH_4^+ in the presence and absence of OTC ([OTC] = 0.06 mM; [Na-zeolite] = 40 g/L; pH 6.5).

Adsorption capacity of zeolite for ammonia was reduced by increasing the ammonia concentration from 25 to 200 mg/L (Figure 4.16). While at lower concentration (25 mg/L) ammonia was completely removed by Na-zeolite in the absence of OTC, NH_4^+ removal was 77 per cent at 200 mg/L ammonia concentration. However, sorbed ammonia concentration increased by the increasing ammonia concentration (data not shown). Higher initial concentration of NH_4^+ creates a driving force for the adsorption on the zeolite as in the case of previous studies (Wang et al., 2006; Karadağ et al., 2006**).** The presence of OTC slightly affected the NH_4^+ removal capacity of zeolite at low and high initial concentration of NH_4^+. By the addition of 200 mg/L NH_4^+ 63 per cent NH_4^+removal was achieved. However, in a previous study, presence of organic matter enhanced the uptake of ammonia by influencing surface tension of zeolite surface (Jorgensen and Weatherley, 2003).

4.8. Effect of Calcium and Magnesium on Sorption

It was known that, tetracyclines form reversible complexes with metal ions as well as with substances of low and high molecular weight (Martin, 1979; Wessels et al., 1998; Schmitt and Schneider, 2000). Metal chelates increase the solubility of tetracyclines in aqueous solution (Myers, 1983, Connors et al., 1986; Buckley and Smyth 1986; Tongaree et al., 1999a) and thus their adsorption properties can be modified. Moreover, complex formation changes the stability of the various tetracyclines (Tongaree et al., 1999b; Tongaree et al., 2000). Although, many studies have been performed to investigate the effect of Ca^{2+} and Mg^{2+} ions on the antibacterial action of tetracycline in organism (Martin, 1979; Buckley and Smyth, 1986; Lunestad and Goksayr, 1990; Wessels et al., 1998, Tongaree et al., 1999b) there are limited studies related with the effect of Ca^{2+} and Mg^{2+} ions on the adsorption of tetracyclines on solid surfaces (Sithole and Guy, 1987a; Ter laak et al., 2006).

Since Ca^{2+} and Mg^{2+} ions are abundant in natural water and soil, the complexation of OTC especially with these ions has special importance. To investigate the effect of Ca^{2+} and Mg^{2+} ions for the sorption of OTC on the zeolite, five different concentrations of $CaCl_2$ (11-3500 mg/L) and $MgCl_2$ (10-1016 mg/L) were added to 0.06 mM OTC suspension at pH 6.5. Since the complex formation with metal ions resulted in a change in the absorption spectrum of OTC, spectroscopic investigation of OTC with Ca^{2+} and Mg^{2+} ions were determined before the adsorption experiments.

4.8.1. Ultraviolet Spectra of OTC in the Presence and Absence of Calcium Ions

Figure 4.17 represents absorption spectra of 0.06 mM OTC in the absence and presence of Ca^{2+} (4-1264 mg/L) at pH 6.5. Chromophoric regions of OTC (Buckley and Smyth, 1986) are also indicated in Figure as inset.

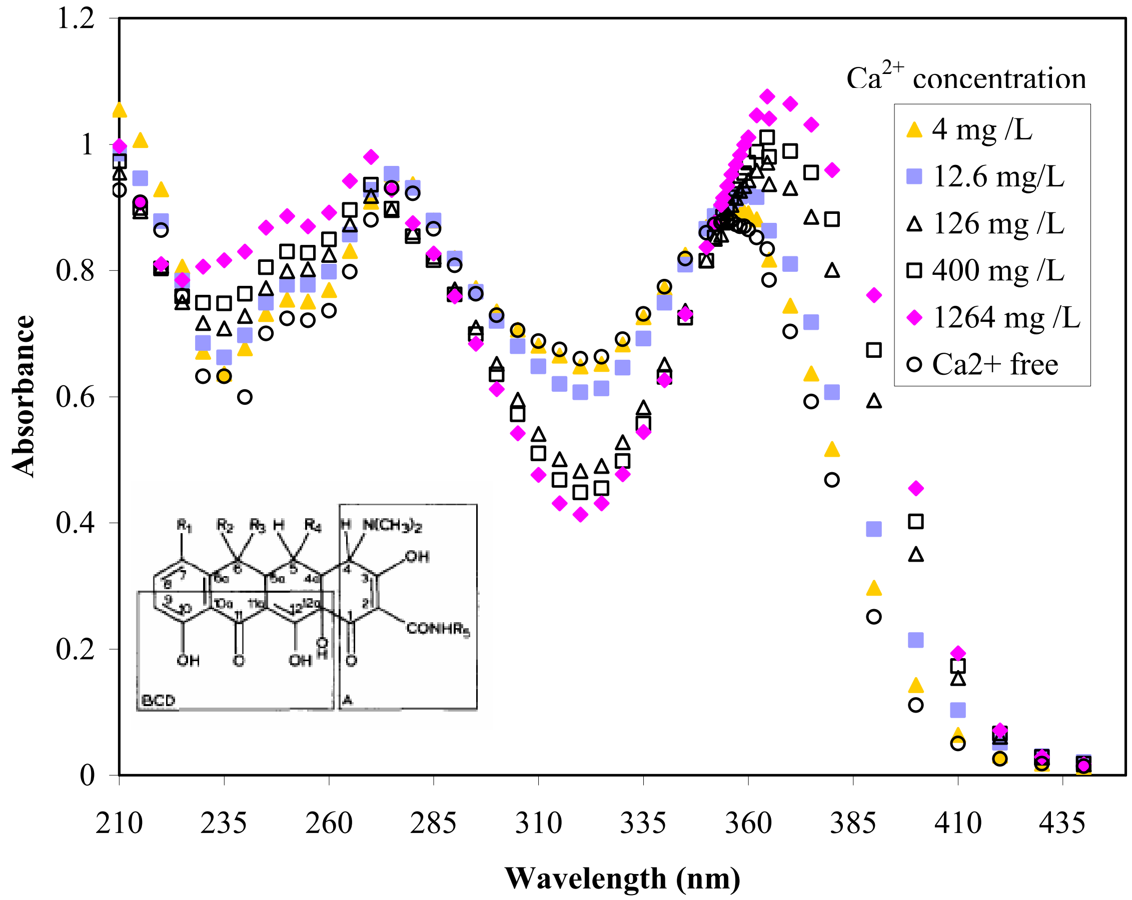

Figure 4.17. Absorption spectra of OTC in the presence and absence of Ca^{2+} ([OTC] =0.06 mM, pH =6.5). Inset: Binding sites of OTC with metal ions.

As can be seen from Figure 4.17 the absorption spectra of OTC exhibits two maxima at 275 and 354 nm wavelengths in the absence of Ca^{2+} ions. Previous studies indicated that the sites at which complex formation of metal ions take place both on the A ring and the BCD chromophore (Figure 4.17) of OTC (Buckley and Smyth, 1986; Schmitt and Schneider, 2000). BCD moiety alone is responsible for ultraviolet absorption at wavelengths > 330 nm. However, A chromophore is responsible for the ultraviolet absorption at wavelengths < 330 nm (Wessels et al., 1998). Upon the addition of 126 mg/L

Ca^{2+} (molar ratio OTC: Ca^{2+} 1:52.5), long wavelength absorption maxima shifted to 364.5 nm. However, further increase of the Ca^{2+}ion concentration did not cause shift for the maximum absorption of OTC. On the other hand, a hypsochromic shift occurred in short-wavelength absorption band from 275 to 270 nm by the addition of 126 mg/L Ca^{2+}. From this and previous studies (Buckley and Smyth, 1986; Schmitt and Schneider, 2000; Ter laak et al., 2006) it can be concluded that both the pH of the solution and the presence of divalent cations altered the spectra of OTC and this is important in quantitative determination of OTC.

The shifts at long and short wavelengths are accompanied by variation in the absorption intensity. Absorbances at 275 and 364.5 nm are presented as a function of Ca^{2+} /OTC molar ratio (Figure 4.18).

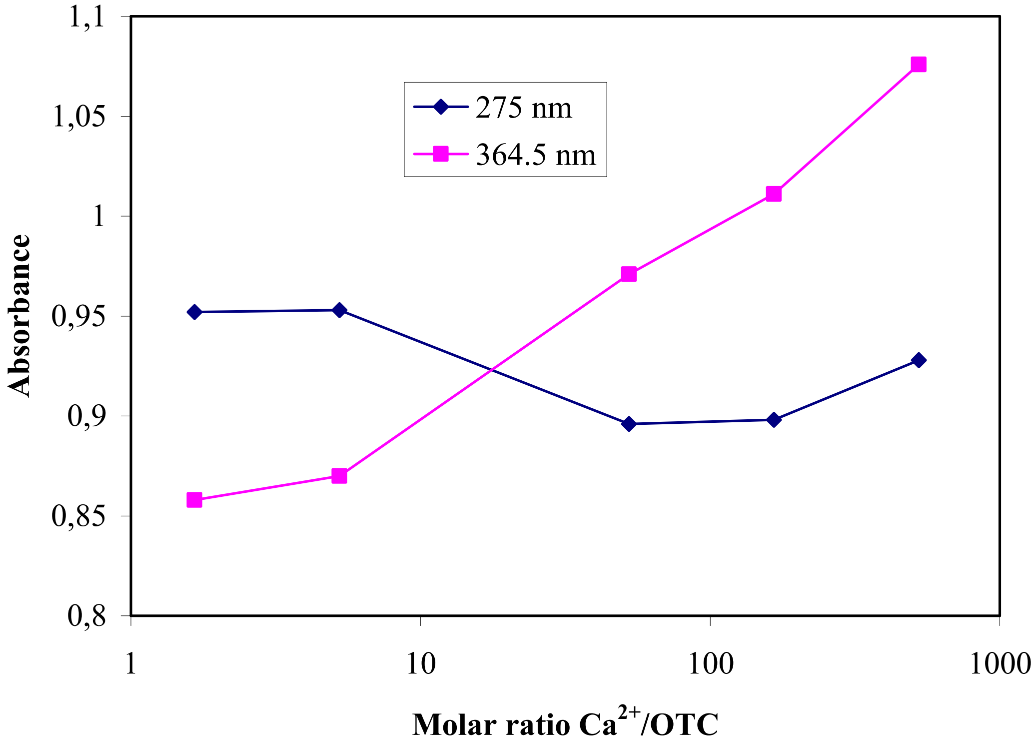

Figure 4.18. Optical density of OTC solution as a function of the Ca^{2+} / OTC molar ratio ([OTC] =0.06 mM; pH =6.5).

As can be seen from Figure 4.18 an inflection point was achieved at OTC: Ca^{2+} molar ratio of 1: 52.5.

4.8.2. Effect of Calcium on Sorption

Effect of Ca^{2+} on the sorption of OTC on Na-zeolite was investigated in the presence of 4-1,264 mg/L (0.1-31.6 mM) Ca^{2+}ions (hardness: 10-3,160 mg/L as $CaCO_3$) at pH 6.5. Since in polluted water hardness can reach to a value of 300-10,000 mg/L as $CaCO_3$ (Peavy et al., 1985) a wide range of Ca^{2+} concentration was selected in this study The obtained results, which were evaluated by using calibration curve prepared in the presence of Ca^{2+} (Appendix A Figure A.3), are presented in terms of K_d and OTC removal percentage in Figure 4.19.

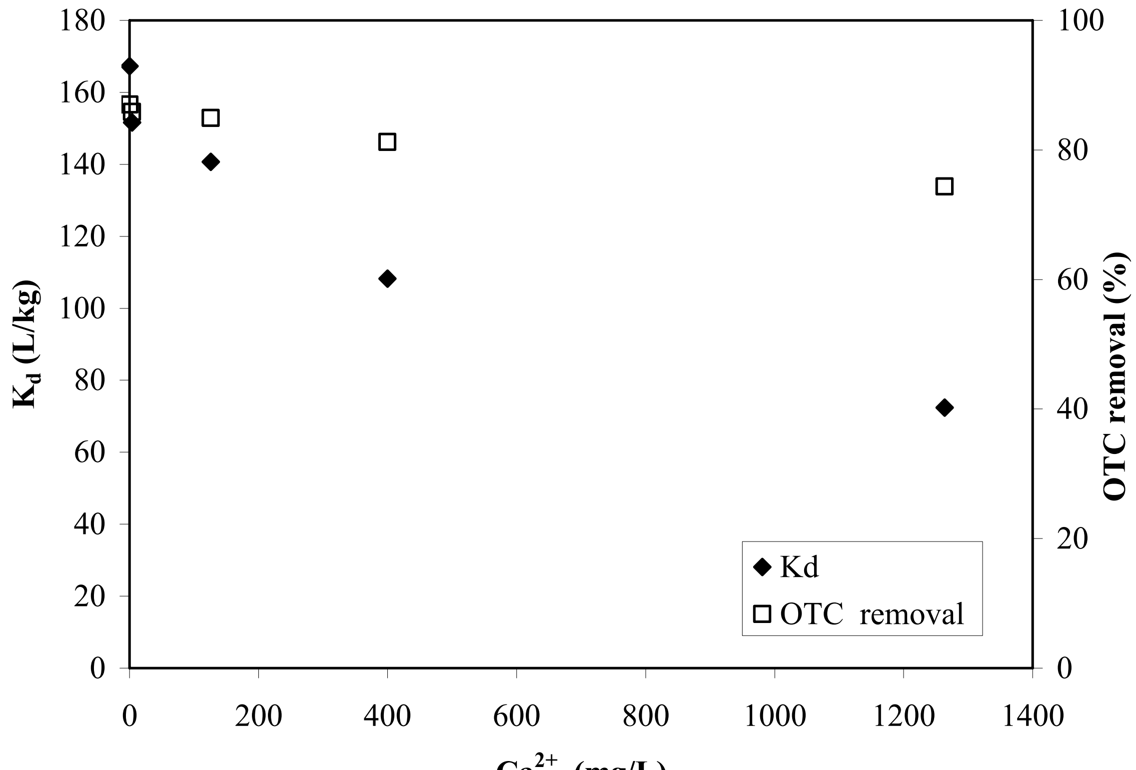

Figure 4.19. Sorption of OTC onto Na zeolite as a function of Ca^{2+} concentration ([OTC] =0.06 mM; pH =6.5; [Na –zeolite] = 40g/L).

K_d values of OTC significantly decreased with increasing Ca^{2+} concentration (Figure 4.19). It was known that (Sithole and Guy, 1987a) complexation with metal ions can either enhance or decrease the adsorption of tetracycline group antibiotics on different sorbents depending upon experimental conditions. The enhancement of tetracycline adsorption on clay and soil was explained by two mechanisms in the presence of Ca^{2+} ions:

dimethylammonium cation of TC can interact with the clay surface by cation exchange (Sithole and Guy 1987a; Sassman and Lee, 2005) and the phenolic diketone system could form chelates with the divalent cations on the clay structure. In other words, complexation with Ca^{2+}ions and OTC can serve as a bridge to the clay surface (Porubcan et al., 1978; Loke et al., 2002; Figuera et al., 2004). On the other hand adsorption can be decreased (Sithole and Guy, 1987a; Ter laak et al., 2006) by the formation of soluble complexes with Ca^{2+} ions as in the case of current study. Spectroscopic observations indicated the OTC-Ca^{2+}complex formation and soluble OTC-Ca^{2+} complex led to a decrease of K_d value from 167.3 to 72.4 L/kg by the addition of 1264 mg/L Ca^{2+} (ionic strength 0.094 M). Similar effect was observed in a previous study (Ter laak et al., 2006) in which K_d values of OTC in soil decreased from 1000 to 316 L/kg by the increasing ionic strength of solution 1000 fold.

Before and after the equilibration of OTC with Na-zeolite, the cations (K^+, Na^+, Mg^{2+}, Ca^{2+}) found in the aqueous medium were determined. The control experiments were also performed in the absence of OTC. The release of cations within 24 hours from the zeolite surface as a function of added Ca^{2+} is presented in the presence and absence of OTC in Figure 4.20.

The release of cations depended upon the presence of OTC and addition of Ca^{2+} ions (Figure 4.20). By increasing the OTC concentration 100 fold, about 10 fold increase was observed for released Mg^{2+} and Ca^{2+} ion concentration (data not shown). Although an immediate release was detected, the amount of cations exhibited a slight increase in 24 h equilibration time.

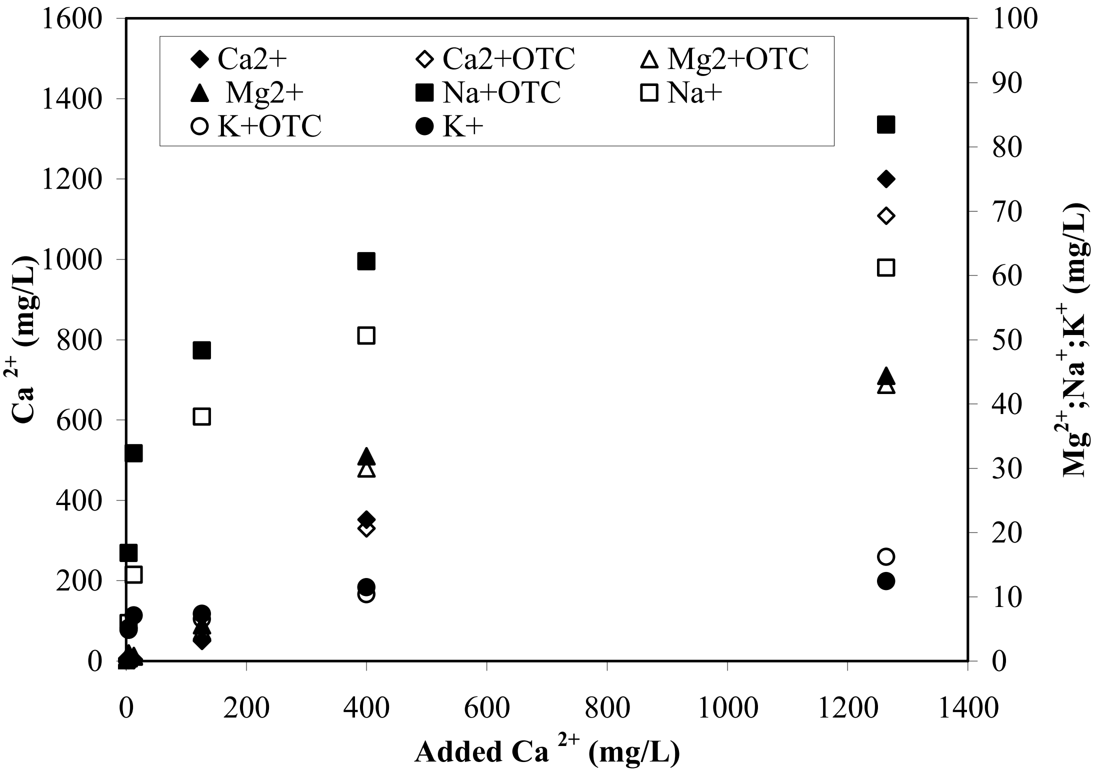

Figure 4.20. Release of cations (Mg^{2+}, Ca^{2+}, Na^{+}, K^{+}) from zeolite surface as a function of added Ca^{2+} in the presence and absence of OTC ([OTC] = 0.06 mM; [Na-zeolite] = 40 g/L; pH =6.5).

The results indicated that addition of Ca^{2+} resulted in ion exchange on the surface of zeolite and the release of Mg^{2+}, Na^{+}, K^{+} into solution. Even at the highest concentration Ca^{2+} retained on the surface of zeolite and this result is consistent with cation exchange capacity of Na-zeolite (Table 4.1). Although the adsorbed Ca^{2+} ion was found higher amount on the surface of the zeolite in the presence of OTC than in the absence of OTC, the obtained results indicated that OTC has higher tendency to form soluble complexes with Ca^{2+} ions in solution causing lower adsorption.

4.8.3. Ultraviolet Spectra of OTC in the Presence and Absence of Magnesium Ions

Figure 4.21 indicates absorption spectra of 0.06 mM OTC in the presence of five different Mg^{2+}concentrations (1.215-121.5 mg/L) and in the absence of Mg^{2+} at pH 6.5.

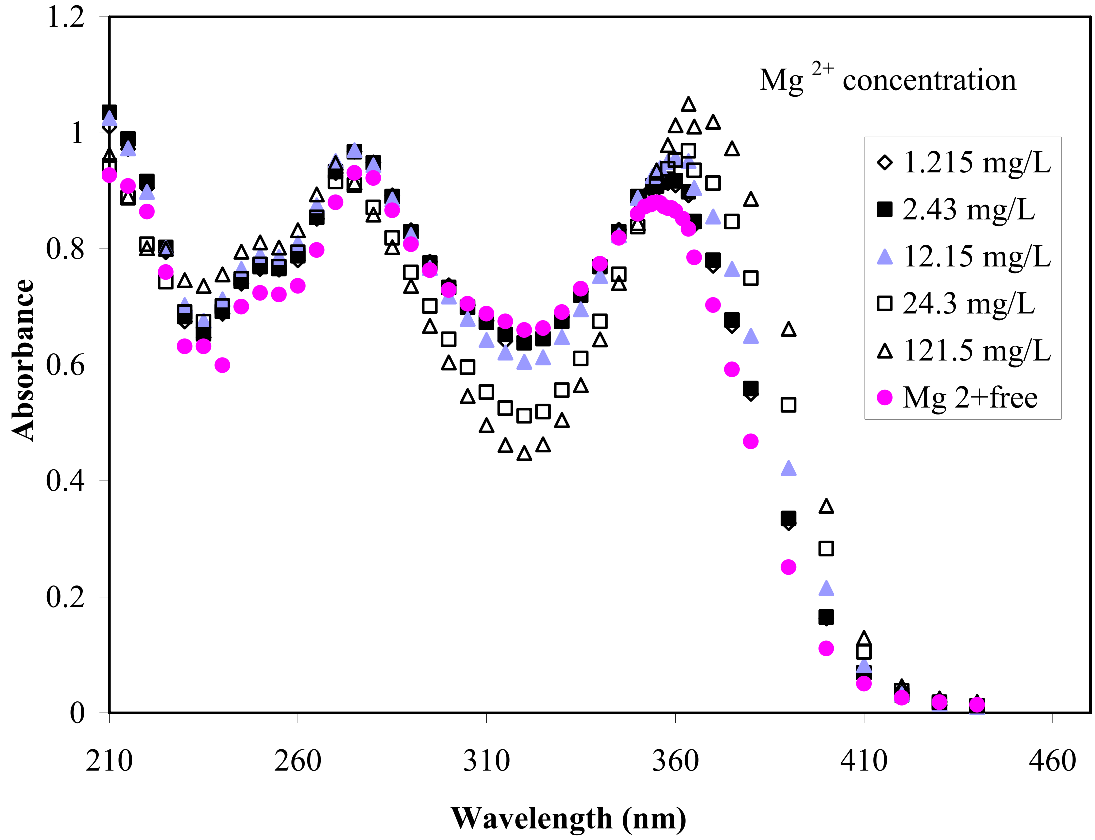

Figure 4.21. Absorption spectra of OTC in the presence and absence of Mg^{2+} ([OTC] =0.06 mM; pH =6.5).

By the addition of 24.3 mg/L Mg^{2+} long wavelength absorption maxima band shifts to 363.5 nm and a hypsochromic shift occurred in short-wavelength absorption band from 275 to 270 nm similar to the addition of Ca^{2+} (Figure 4.21). The bathochromic and hypsochromic shifts were accompained by variation of absorption intensity. Absorbances evaluated 275 and 363.5 nm showed one inflection point at molar ratio OTC: Mg^{2+} 1: 16.66 (Figure 4.22).

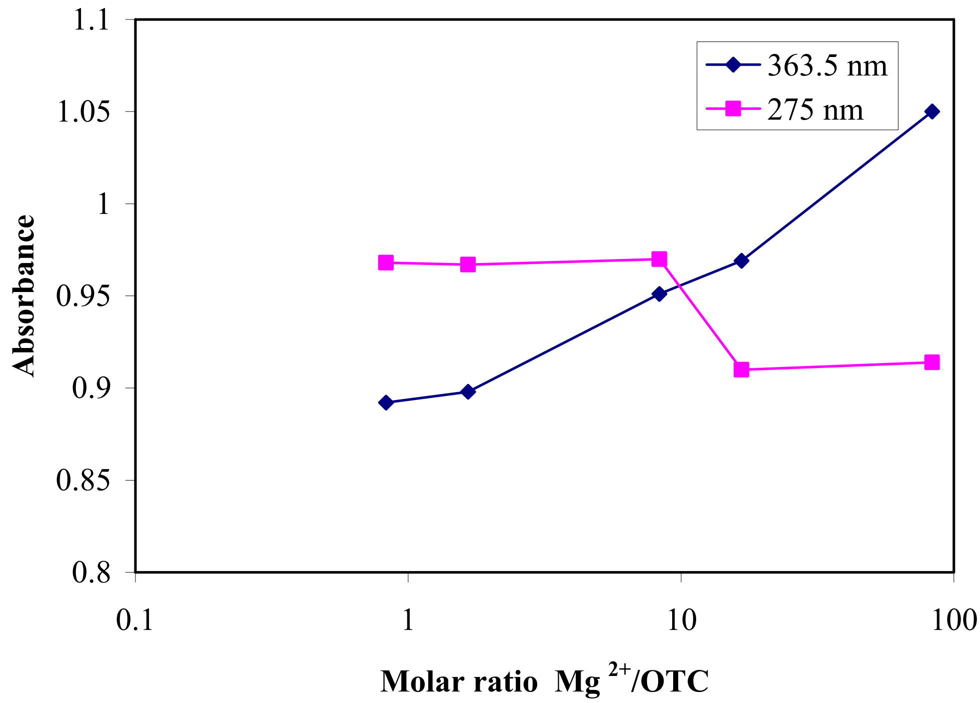

Figure 4.22. Optical density of OTC: Mg^{2+} solutions as a function of Mg^{2+}/ OTC molar ratio ([OTC] =0.06 mM; pH =6.5).

4.8.4. Effect of Magnesium on Sorption

Effect of Mg^{2+} ion on the adsorption of OTC on Na-zeolite was investigated in the presence of 1.21-121.5 mg/L (0.05-5 mM) Mg^{2+} concentration (hardness: 4.95-498 mg/L as $CaCO_3$) at pH 6.5. The results, which were assessed by using calibration curve (Appendix A Figure A.4) prepared in the presence of Mg^2, are represented in terms of K_d and OTC removal percentage in Figure 4.23.

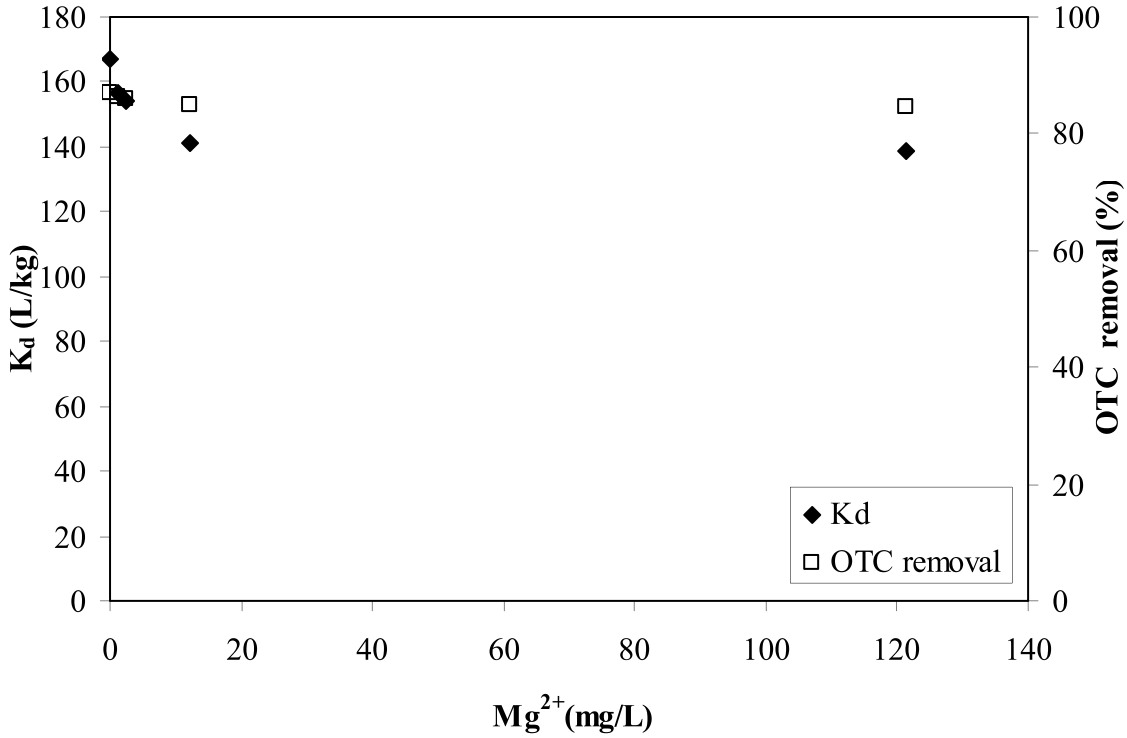

Figure 4.23. Sorption of OTC onto Na-zeolite as a function of Mg^{2+}ions ([OTC] =0.06 mM; pH =6.5; [Na zeolite] = 40 g/L).

As observed in Figure 4.23 K_d values of OTC slightly decreased with increasing Mg^{2+}concentrations and reached to a value of 138.5 L/kg upon addition of 121.5 mg/L Mg^{2+} (ionic strength 0.015 M).

Exchangeable cations (K^+, Na^+, Mg^{2+}, Ca^{2+}) released from Na-zeolite were determined before and after equilibration with OTC. The control experiments were also conducted in the absence of OTC and the obtained results are depicted in Figure 4.24.

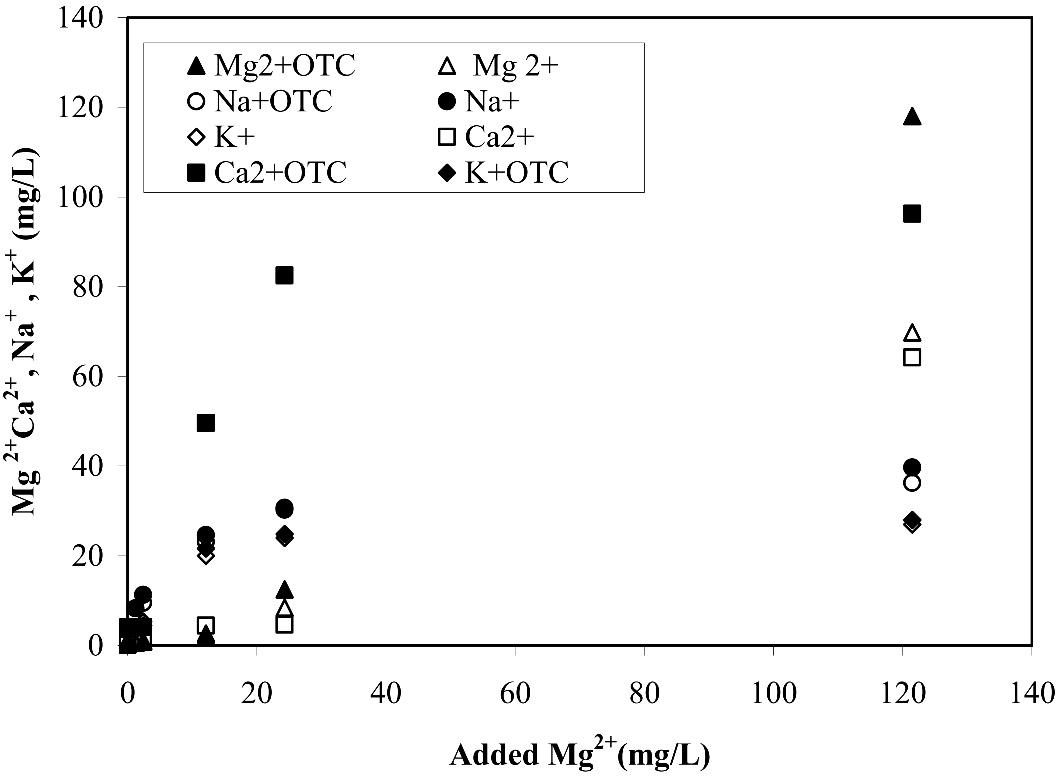

Figure 4.24. Release of cations (Mg^{2+}, Ca^{2+}, Na^{+}, K^{+}) from zeolite surface as a function of added Mg^{2+}in the presence and absence of OTC ([OTC] = 0.06mM ;[Na-zeolite] = 40 g/L; pH =6.5).

It was observed that the release of cations depended upon the concentration of OTC and added Mg^{2+} ions. As the added Mg^{2+} concentration increased, Mg^{+2} ion increased in the solution after equilibration in the absence and presence of OTC. Mg^{2+} adsorption on the surface of the zeolite was found higher especially at higher concentration of Mg^{2+} in the absence of OTC. However, in the presence of OTC, sorbed Mg^{2+} concentration was decreased. Other cations such as Na^{+} and Ca^{2+} were found higher amount in the presence of OTC in suspension. Among other cations K^{+} was found smallest amount in the absence and presence of OTC. The results indicated that, OTC has preferred to form soluble complexes with Mg^{2+} ion in solution.

4.9. Effect of Chloride on Sorption

Effect of chloride ion on OTC sorption was investigated by the addition of 35 to 500 mM NaCl. K_d values and removal percentages of OTC on Na-zeolite are presented as a function of chloride ion concentration in Figure 4.25.

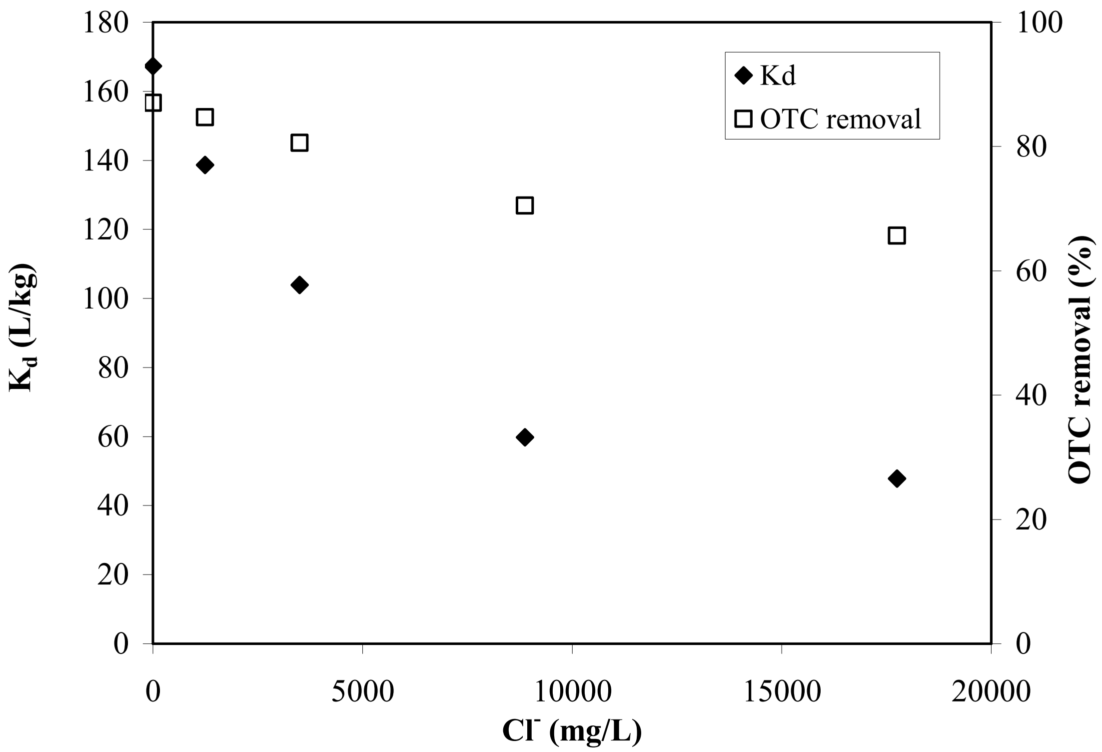

Figure 4.25. Sorption of OTC onto Na-zeolite as a function of Cl^- concentration ([OTC] =0.06 mM; [Na zeolite] = 40 g/L; pH 6.5).

The maximum adsorption of OTC was obtained when suspension was not contained Cl^- as shown in Figure 4.25. Higher Cl^- concentration resulted in a higher decline in adsorption capacity. By increasing chloride ion concentration up to 250 mM, K_d value of OTC decreased from 167 L/kg to 60 L/kg. However, further increase in chloride ion concentration from 250 mM to 500 mM K_d value slightly decreased. In previous studies, negative effects of chloride ion have been observed for the adsorption of tetracycline on bentonite (Sithole and Guy, 1987a), montmorillonite (Figueroa et al., 2004), aluminum and iron hydrous oxides (Gu and Karthikeyan, 2005), and soil surface (Ter laak et al., 2006). K_d values and removal percentages of OTC are also presented for HDTMA-modified zeolite as a function of chloride ion in Figure 4.26.

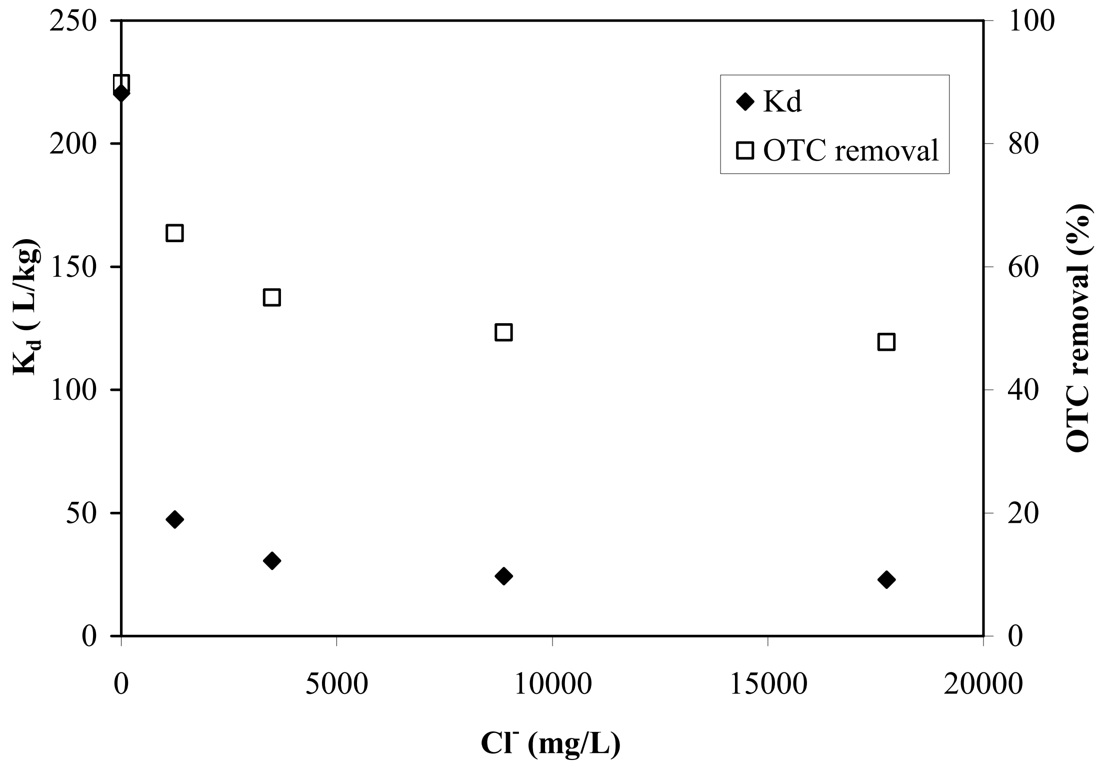

Figure 4.26. Sorption of OTC onto HDTMA-modifed zeolite as a function of Cl^- concentration ([OTC] =0.06 mM; [HDTMA-modifed zeolite] = 40 g/L; pH 8).

At pH 8 surface of HDTMA-modified zeolite was favorable for the adsorption of negatively charged OTC due to electrostatic attraction. However, in the presence of chloride ion, sorption of OTC on HDTMA-modified zeolite was decreased significantly. In contrast to Na-zeolite, a sharp decrease in the adsorption of OTC on HDTMA-modified zeolite was observed by the addition of 35 mM chloride ion (Figure 4.26). Further increase in NaCl concentration to 500 mM inhibited OTC sorption almost completely. Increase in Cl^- level due to the addition of NaCl may cause a competition to occupy the active sites on zeolite and this competition can be the reason of the observed decrease in OTC removal efficiency.

4.10. Effect of Phosphate on Sorption

Phosphate can enter water from sewage or from agricultural run-off containing fertilizers and animal waste. The presence of phosphate ion in water sources plays a central role in the aquatic ecosystem and water quality. In polluted water, phosphate concentration may reach to a value of 234 mg/L (Ghosh et al., 2006). In the present study, considering the presence of phosphate ion in polluted water, the influence of phosphate ion on the adsorption of OTC was investigated by the addition of 0.2-100 mg/L phosphate using Na_2HPO_4 into the 0.06 mM OTC suspension. K_d values and removal percentages of OTC on Na-zeolite and HDTMA-modifed zeolite are presented as a function of phosphate concentration in Figures 4.27 and 4.28, respectively.

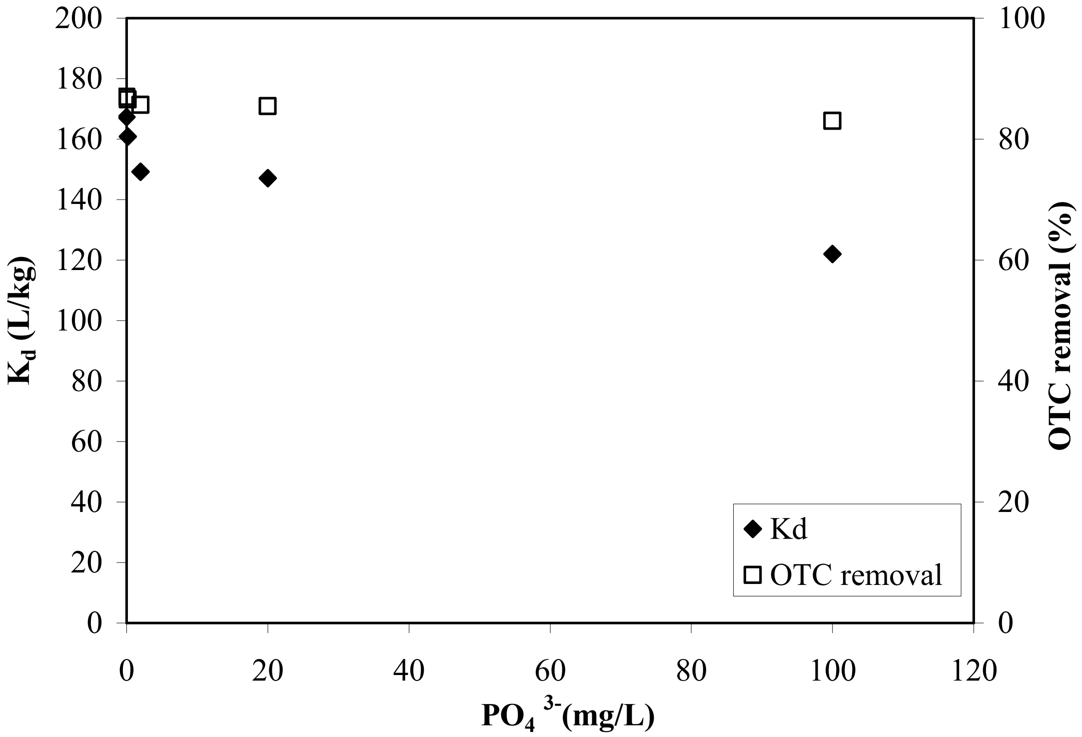

Figure 4.27. Sorption of OTC onto Na-zeolite as a function of PO_4^{3-} concentration ([OTC] =0.06 mM; [Na-zeolite] = 40 g/L; pH 6.5).

The presence of phosphate ion led to decrease in K_d value of OTC. It was decreased from 167 to 122 L/kg by the addition of 100 mg/L PO_4^{3-}. On the other hand, removal percentage did not change significantly, 82 per cent OTC was efficiently removed from water in the presence of 100 mg/L PO_4^{3-}. Decrease in K_d value can be explained by the competition between OTC^+ and PO_4^{3-} anion for the available adsorption sites on Na-zeolite. Similarly, competition has been proposed for the adsorption of organic compounds on mineral surfaces with the phosphate (Gu et al., 1994; Geelhoed et al., 1998). Moreover, it was known that phosphate ions caused desorption of OTC from soil surface (Jones et al., 2005).

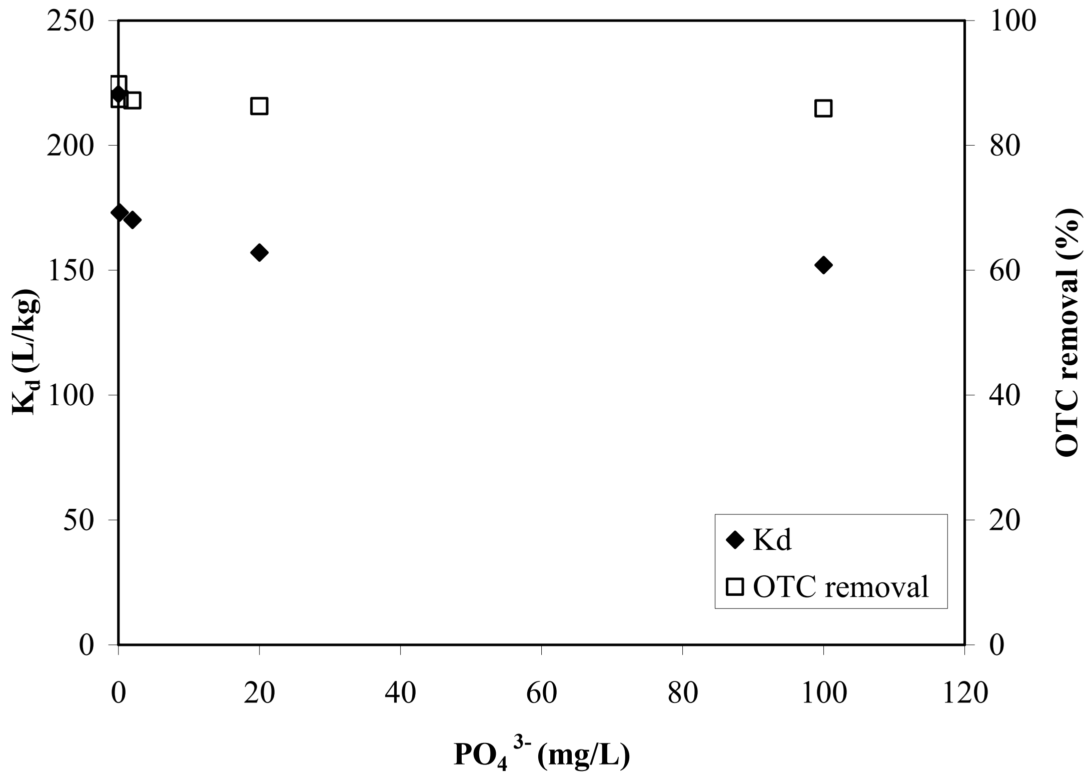

Figure 4.28. Sorption of OTC onto HDTMA-modified zeolite as a function of PO_4^{3-} concentration ([OTC] =0.06 mM; [HDTMA-modified zeolite] = 40 g/L; pH 8).

Phosphate ion has more pronounced effect on the adsorption of OTC onto HDTMA-modified zeolite (Figure 4.28). K_d values decreased from 220 to 173 L/ kg by the addition of 0.2 mg/L phosphate ion and K_d value declined to 150 L/kg by further increase in phosphate concentration to 100 mg/L.

Control experiments were also conducted in the absence of OTC to elucidate competitive adsorption of phosphate on Na-zeolite and HDTMA-modified zeolite. The amount of adsorbed phosphate was calculated from the difference between initial phosphate concentration and the concentration of phosphate remained in the solution. Adsorbed phosphate amount onto Na and HDTMA-modified zeolite is presented as a function of initial phosphate ion concentration in the absence and presence of OTC, respectively (Figure 4.29, 4.30).

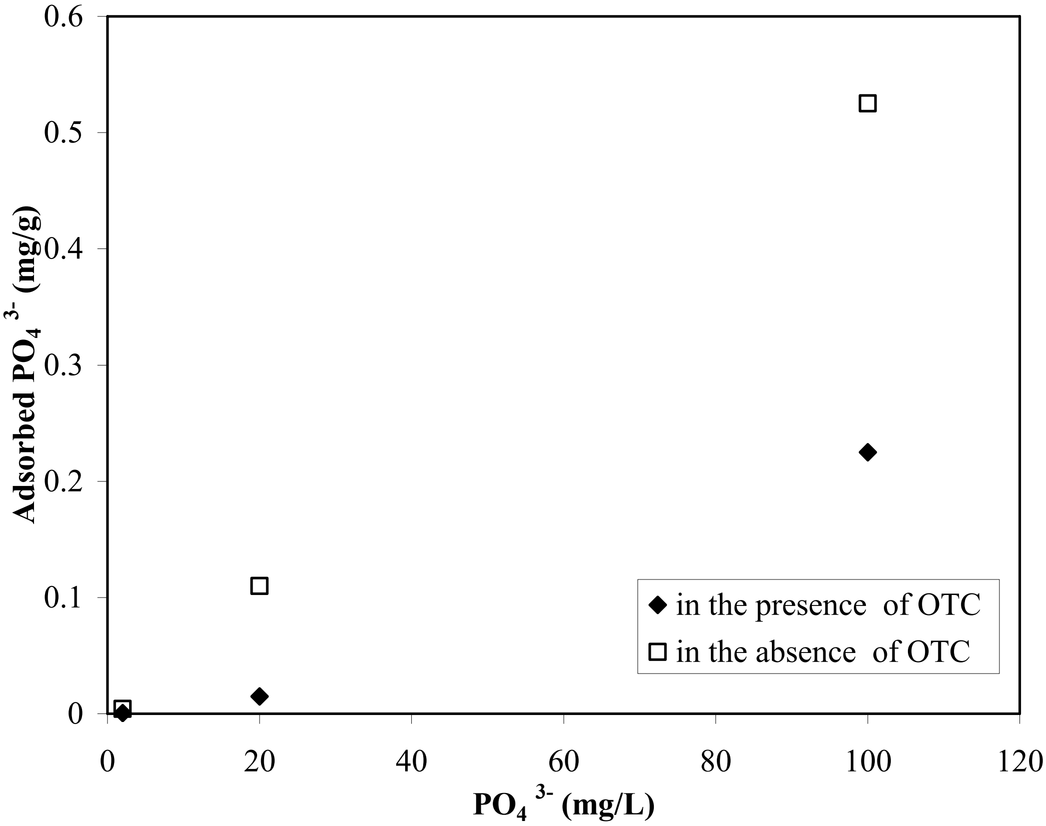

Figure 4.29. Adsorbed PO_4^{3-} amount onto Na-zeolite in the presence and absence of OTC ([OTC] =0.06 mM; [Na zeolite] = 40 g/L; pH 6.5).

Figure 4.29 indicated that an increase in phosphate concentration decreased phosphate adsorption in the presence of OTC at pH 6.5. Similarly, phosphate adsorption on mineral surfaces decreased in the presence of organics below pH 7 (Geelhoed et al., 1998).

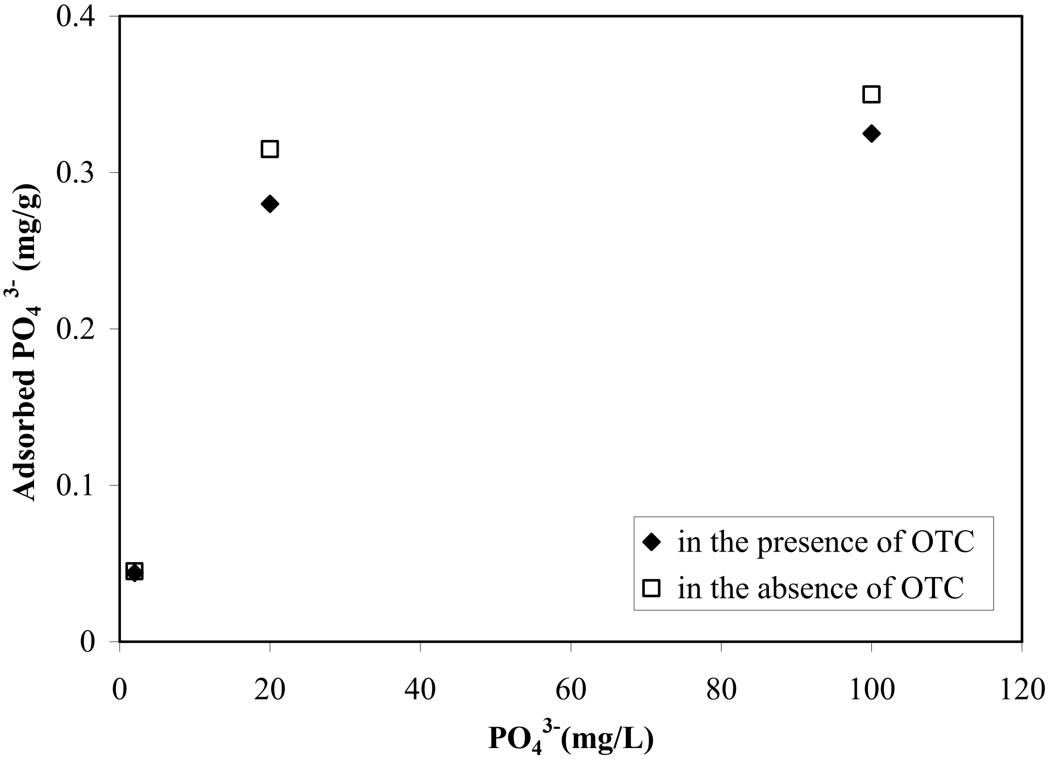

Figure 4.30. Adsorbed PO_4^{3-} amount onto HDTMA modified zeolite in the presence and absence of OTC ([OTC] =0.06 mM; [HDTMA- modified zeolite] = 40 g/L; pH 8).

In the case of HDTMA-modified zeolite, phosphate adsorption was not significantly influenced in the presence of OTC at pH 8. By the addition of 100 mg/L phosphate ion, 0.325 and 0.350 mg/g phosphate was adsorbed in the presence and absence of OTC, respectively (Figure 4.30). Similar results have been reported for the adsorption of phosphate ion on mineral surfaces at pH over 6 in the presence of organics (Violente and Gainfreda, 1993; Geelhoed et al., 1998).

4.11. Effect of Sulfate on Sorption

Sulfate is the most common anion in natural water system. In polluted natural water sources, sulfate concentration may reach to a value of 5,000 mg/L (Ghosh et al., 2006). Presence of sulfate ion may modify the adsorption of organic molecules on solid surfaces in natural environmental systems. To investigate the effect of sulfate ion on the sorption of OTC, adsorption experiments were conducted in the sulfate ion concentration range of 50-2,500 mg/L by the addition of Na_2SO_4. K_d values and removal percentage of OTC on Na and HDTMA-modified zeolite are presented as a function of sulfate concentration in Figure 4.31 and 4.32, respectively.

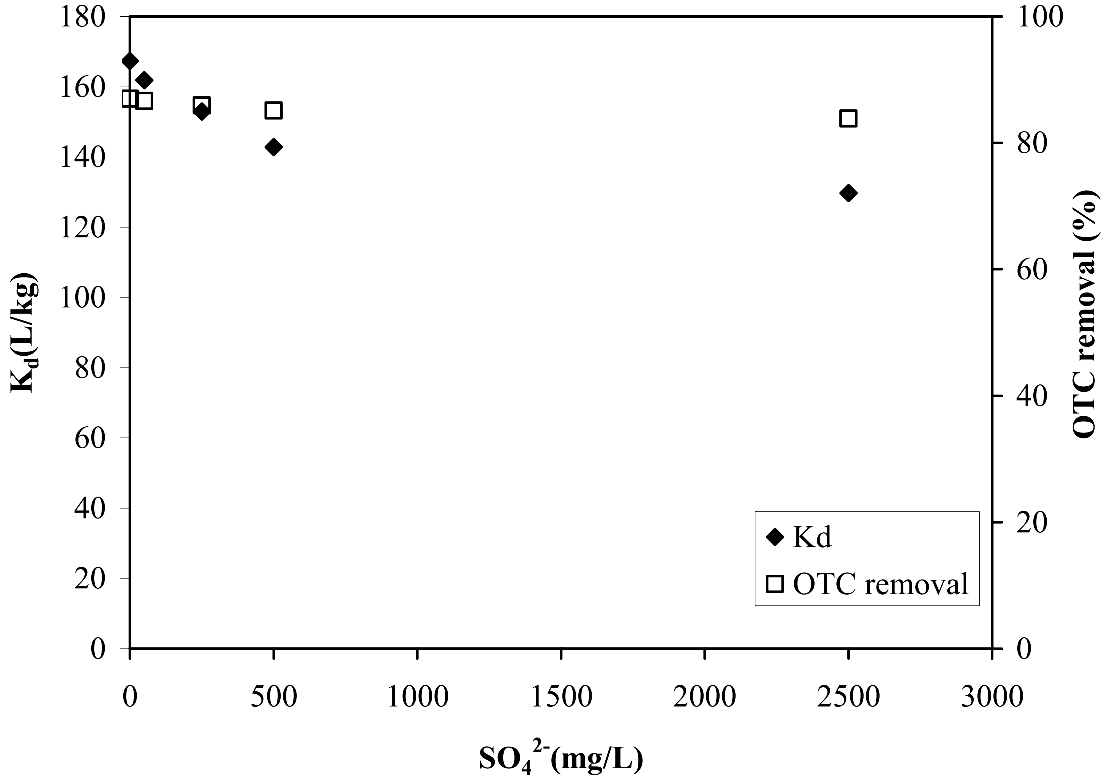

Figure 4.31. Sorption of OTC onto Na-zeolite as a function of SO_4^{2-} concentration ([OTC] = 0.06 mM; [Na -zeolite] = 40 g/L; pH 6.5).

As observed in Figure 4.31 K_d values of OTC decreased from 167 to 129 L/kg when the sulfate ion concentration was increased from 0 to 2,500 mg/L. Competition between sulfate anion and anionic OTC species on Na -zeolite may be the reason for decreasing sorption of OTC. Several studies on soil indicated direct competition between organic anions and sulfate is of considerable importance (Gobran and Nilsson, 1988; Karltun, 1998; Kooner et al., 1995).

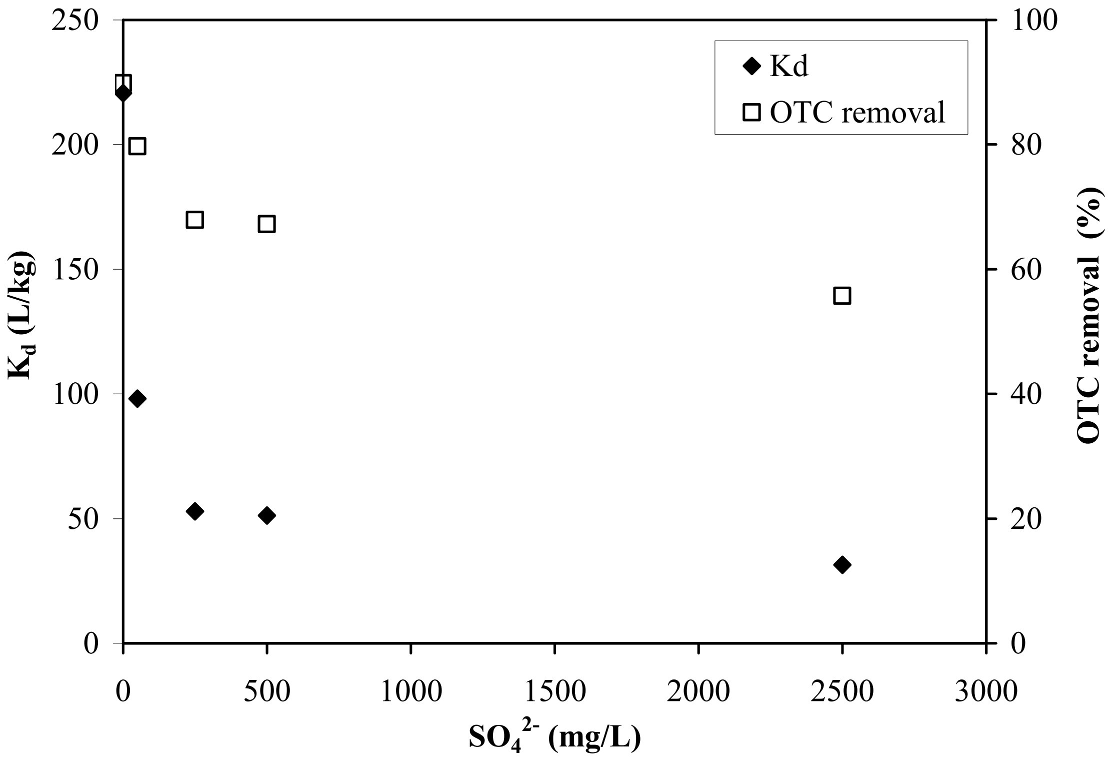

Figure 4.32. Sorption of OTC onto HDTMA-modified zeolite as a function of SO_4^{2-} concentration ([OTC] = 0.06 mM; [HDTMA- modified zeolite] = 40 g/L; pH 8).

The presence of sulfate ion significantly influenced the removal of OTC by HDTMA-modified zeolite as demonstrated in Figure 4.32. The removal capacity of HDTMA- modified zeolite decreased from 90 to 56 per cent when the solution contained 2,500 mg/L SO_4^{2-} OTC has negatively charged at pH 8 and it may compete for available binding sites for sulfate ion. Therefore significant reduction of sorbed OTC was observed on HDTMA-modified zeolite surface.

4.12. Effect of Bicarbonate on Sorption

Alkalinity is an important parameter for adsorption since it is natural component of ground and surface water. In the polluted water sources, alkalinity may reach to a value of 12,336 mg/L as $CaCO_3$ (Ghosh et al., 2006). The presence of dissolved carbonate may influence the adsorption of OTC by competing for sites on zeolite surface or forming complexes on zeolite that can either enhance or suppress adsorption. By considering these facts, in order to understand effect bicarbonate ion for the sorption of 0.06 mM OTC, adsorption experiments were conducted with the HCO_3^- ion in the concentration range of 60-2400 mg/L (49.1-1967 mg/L as $CaCO_3$ alkalinity) by the addition of $NaHCO_3$. K_d values and removal percentages of OTC on Na and HDTMA-modified zeolite are presented as a function of bicarbonate concentration in Figure 4.33 and 4.34, respectively.

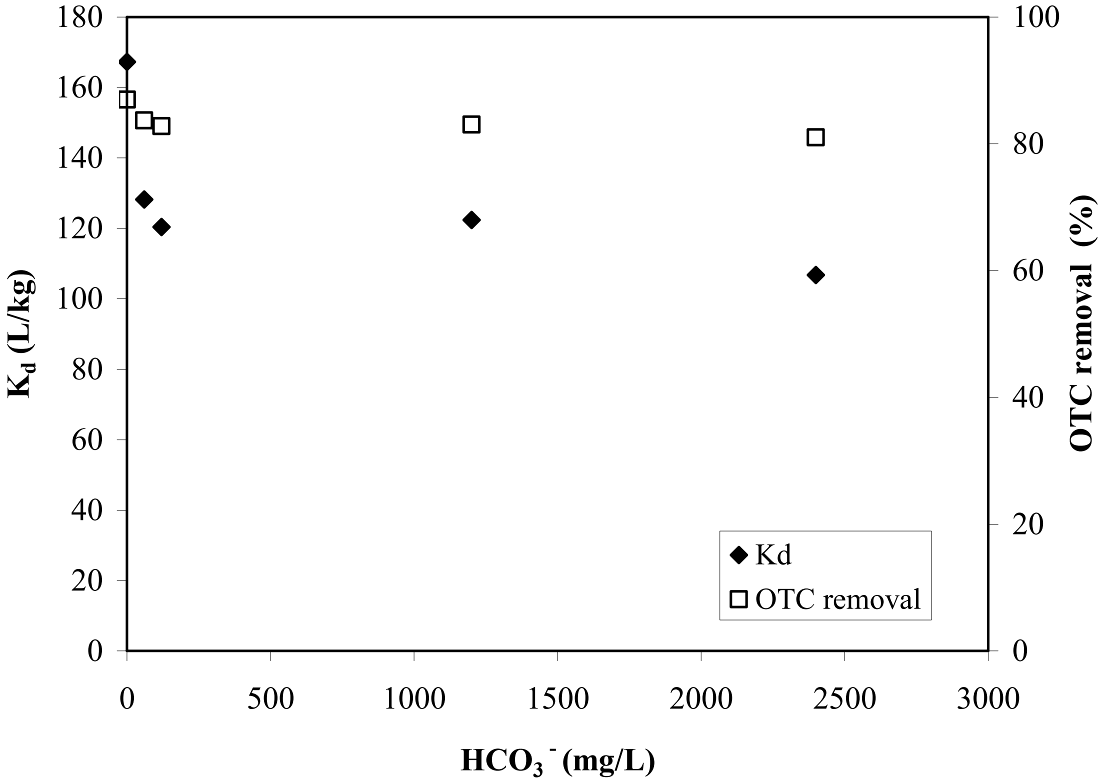

Figure 4.33. Sorption of OTC onto Na-zeolite as a function of HCO_3^- concentration ([OTC] =0.06 mM; [Na-zeolite] = 40 g/L; pH 6.5).

Similar to the chloride, sulfate, and phosphate ions, the presence of bicarbonate diminished the removal of OTC on Na-zeolite surface. K_d value of OTC was found as 106 L/kg by the addition of 2,400 mg/L bicarbonate ion. Competition between HCO_3^- and OTC anion on Na-zeolite surface could be the main reason for decreasing sorption.

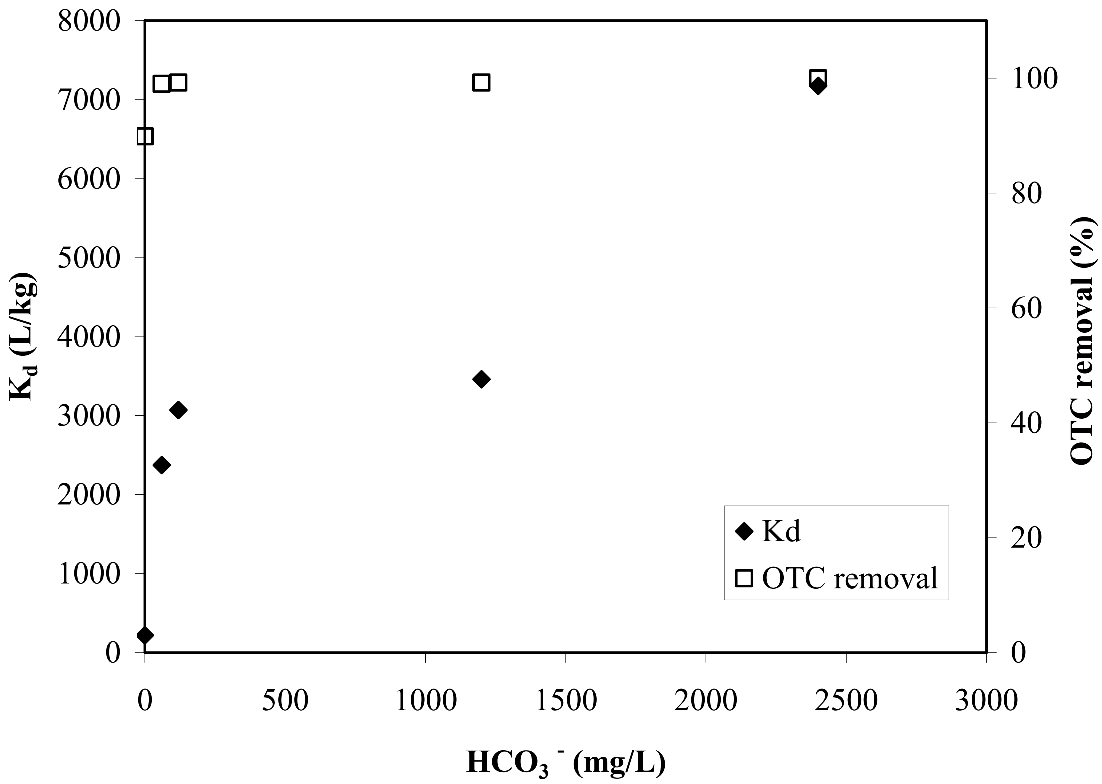

Figure 4.34. Sorption of OTC onto HDTMA-modified zeolite as a function of HCO_3^- concentration ([OTC] =0.06 mM; [HDTMA-modified zeolite] = 40 g/L; pH 8).

As mentioned previously the surface of HDTMA-modified zeolite is positively charged and OTC is found as anionic form at pH 8. Based on these, a competitive effect of HCO_3^- on OTC would be expected. However, the experimental data shows a promotive effect. The promotive HCO_3^- for the OTC sorption onto effect of HDTMA-modified zeolite contrasts with the competitive effect of HCO_3^- onto Na-zeolite. By the addition of 2,400 mg/L HCO_3^- ion to OTC suspension, adsorption increased from 90 to 99.6 per cent. The adsorption experiment was also repeated by using 0.6 mM OTC. Similarly, addition of 2,400 mg/L bicarbonate increased the adsorption of OTC from 75 to 88 per cent. The promoter anion may cause an alteration of surface protonation or surface charge that favors the adsorption of coadsorbing OTC anion.

4.13. SEM Image and EDAX Analysis

SEM image and EDAX analysis of zeolite were performed by scanning electron microscopy in order to get detailed knowledge of the physical and chemical composition of the zeolite surface on a sub-micrometer scale. These analyses provide important information for the adsorption of OTC on Na and HDTMA-modified zeolite surface. SEM and EDAX analysis of Na and HDTMA-modified zeolites were conducted before and after adsorption experiments.

4.13.1. SEM Image and EDAX Analysis of Na-Zeolite

Figures 4.35 and 4.36 represent SEM images and EDAX analysis of the two different areas of the Na-zeolite mineral surface.

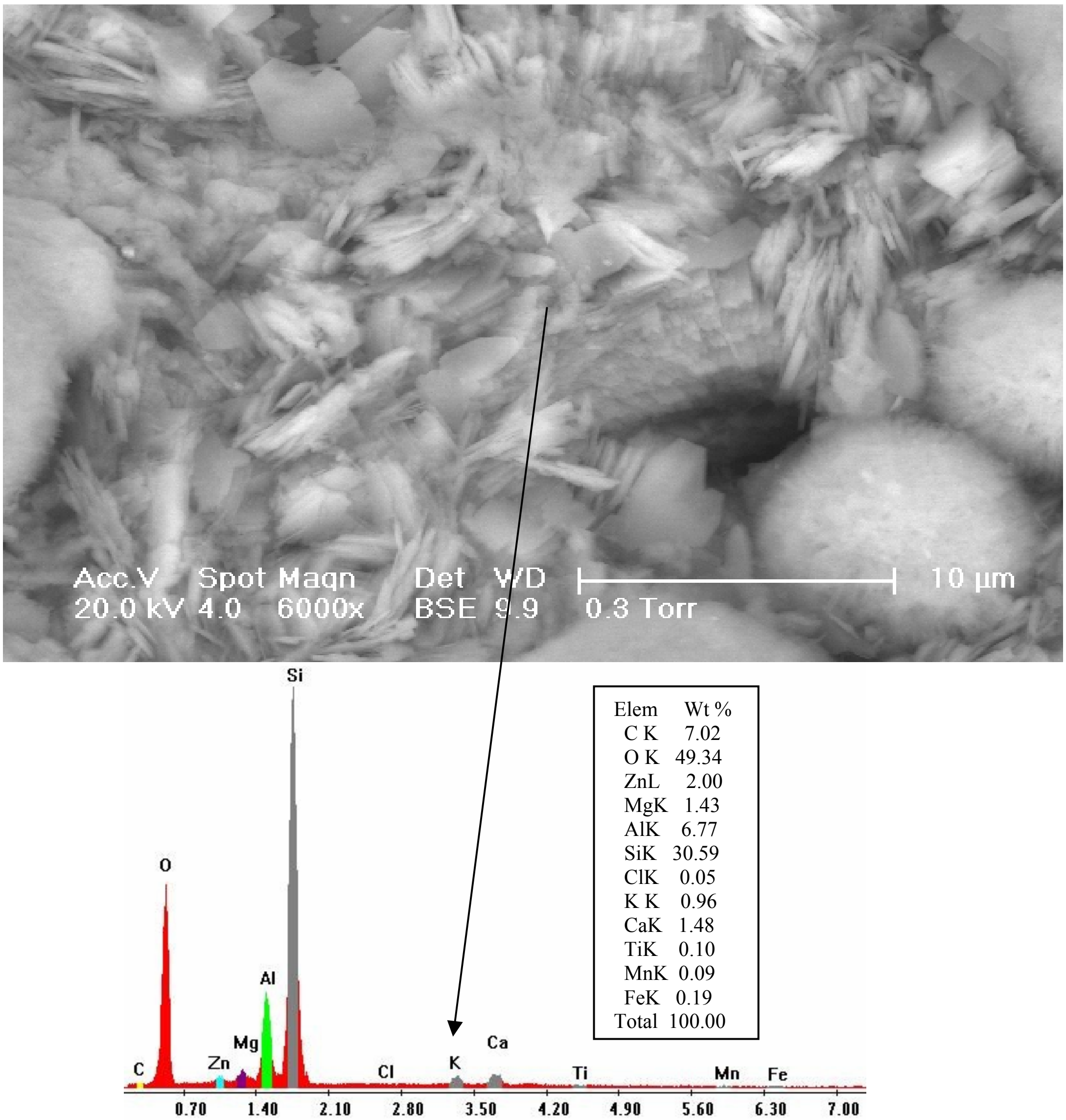

Figure 4.35. SEM image I and EDAX spectra of Na-zeolite.

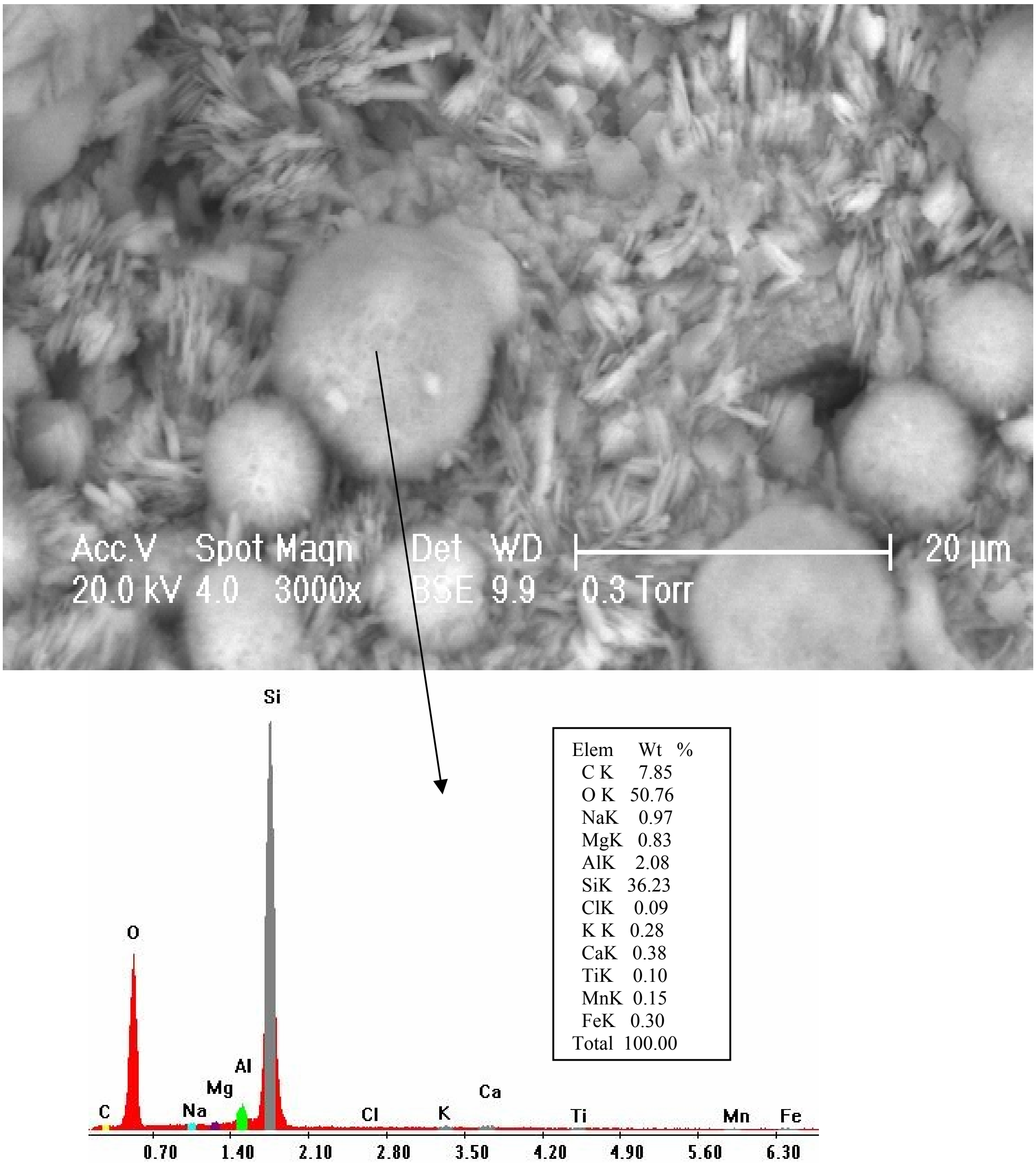

Elem	Wt %
C K	7.85
O K	50.76
NaK	0.97
MgK	0.83
AlK	2.08
SiK	36.23
ClK	0.09
K K	0.28
CaK	0.38
TiK	0.10
MnK	0.15
FeK	0.30
Total	100.00

Figure 4.36. SEM image II and EDAX spectra of Na zeolite.

Figure 4.35 and 4.36 indicate the presence of crystal particles on the Na-zeolite. While figure 4.35 displays bright, flat, well defined shaped crystals, figure 4.36 represents irregularly dispersed white spherical crystals on Na zeolite structure. Typical Si:Al ratio (Inglezakis et al., 2003) for zeolite minerals is 4-5.5:1. This ratio exhibited variations in different sites of Na zeolite. Si:Al ratio were detected as 4.5:1 and 17.4:1 in figure 4.35 and 4.36, respectively. These figures and EDAX spectra of the elemental figures and EDAX spectra of the elemental analysis revealed that surface of zeolite was heterogeneous in accordance to isotherm study.

4.13.2. SEM Image and EDAX Analysis of Na-Zeolite Equilibrated with OTC

In order to obtain clear image for the adsorption of OTC on Na-zeolite 0.6 mM OTC was used in experiment performed at pH 6.5. Figure 4.37 and 4.38 indicate SEM image and EDAX spectra of Na-zeolite equilibrated with OTC.

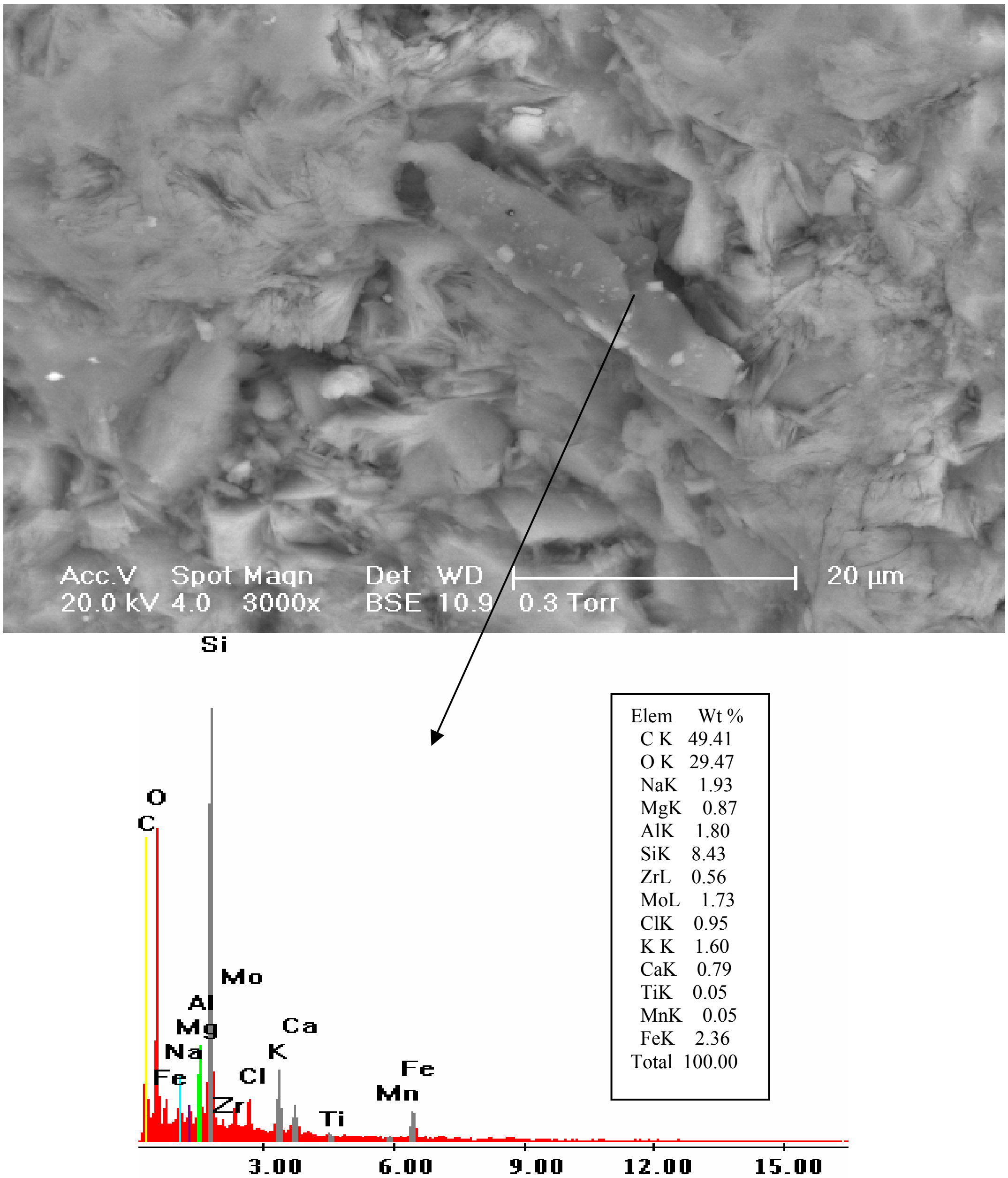

Figure 4.37. SEM image I and EDAX spectra of Na-zeolite equilibrated with OTC.

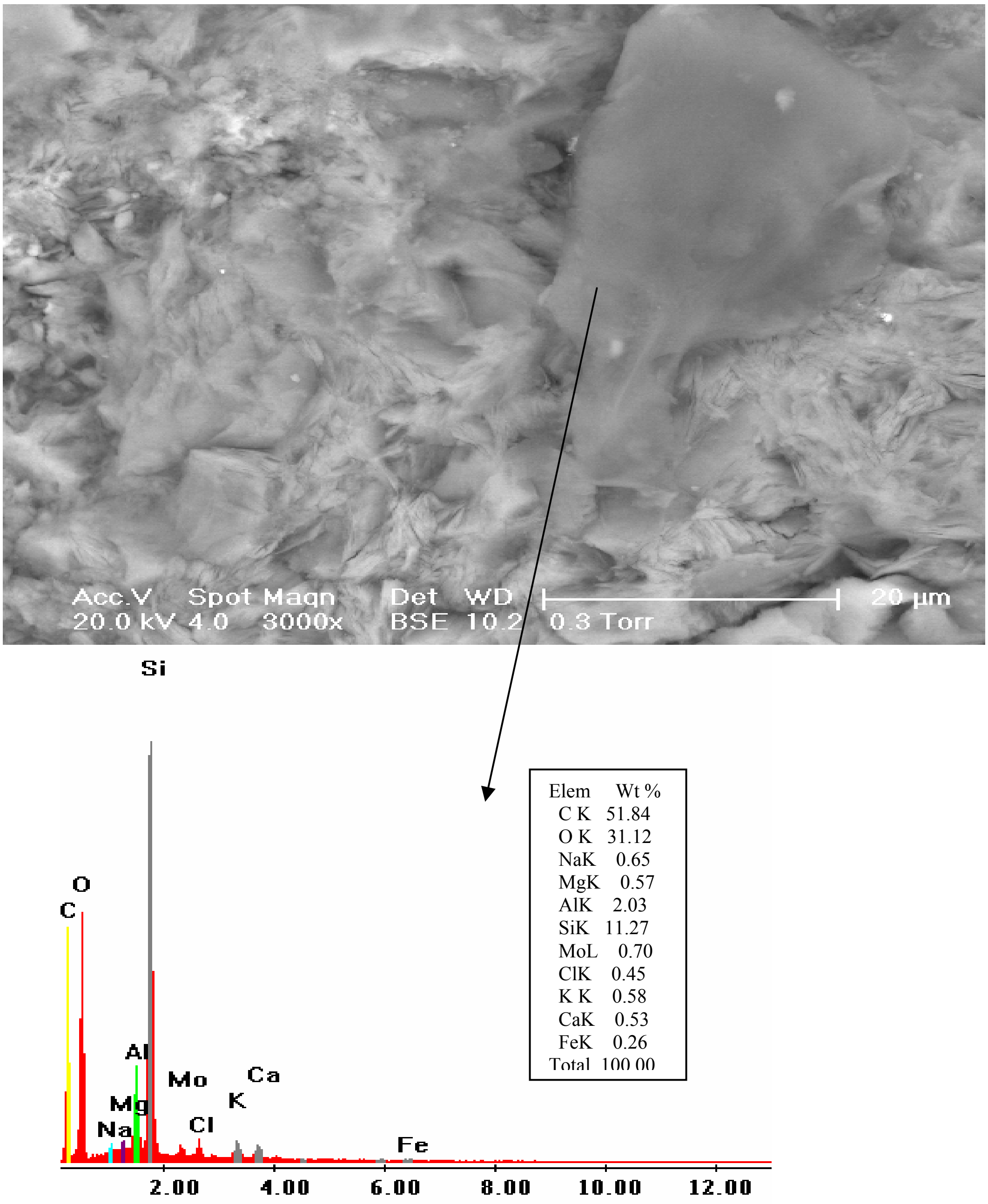

Figure 4.38. SEM image II and EDAX spectra of Na-zeolite equilibrated with OTC.

Surface morphologies of the Na-zeolite reveals that thin, flat (Figure 4.37), and large tabular shaped OTC crystals (Figure 4.38) are differentiated easily. EDAX analysis of these OTC crystals implies that carbon content reached to value of 50 per cent in contrast to virgin Na-zeolite. Moreover, chloride ion was also detected at the carbon abundant areas (Figures 4.37, 4.38). Presence of these elements indicated the adsorption of

OTC on the Na-zeolite surface. Figure 4.39 indicates SEM image and EDAX spectra of Na-zeolite on a site near to OTC crystal.

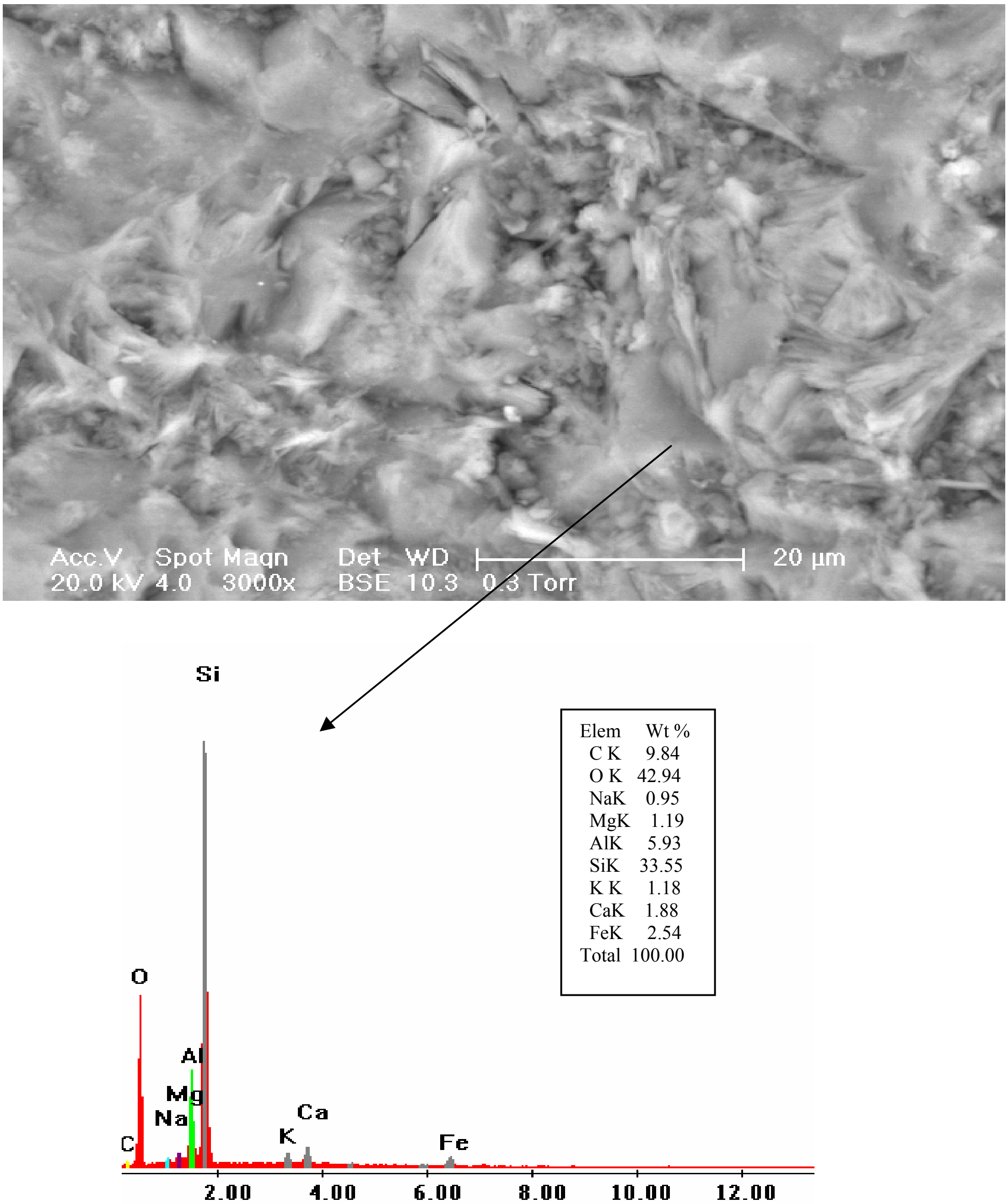

Figure 4.39. SEM image III EDAX spectra of Na-zeolite equilibrated with OTC.

Figure 4.39 indicated that iron content of Na-zeolite at the carbon abundant site was higher (2.54 per cent) than the other sites.

4.13.3. SEM Image and EDAX Analysis of Na-Zeolite Equilibrated with OTC in the Presence of Calcium Ions

To explain the decrease OTC sorption on Na-zeolite in the presence of Ca^{2+} ions at pH 6.5, SEM and EDAX analysis were performed and Figure 4.40 represents the results.

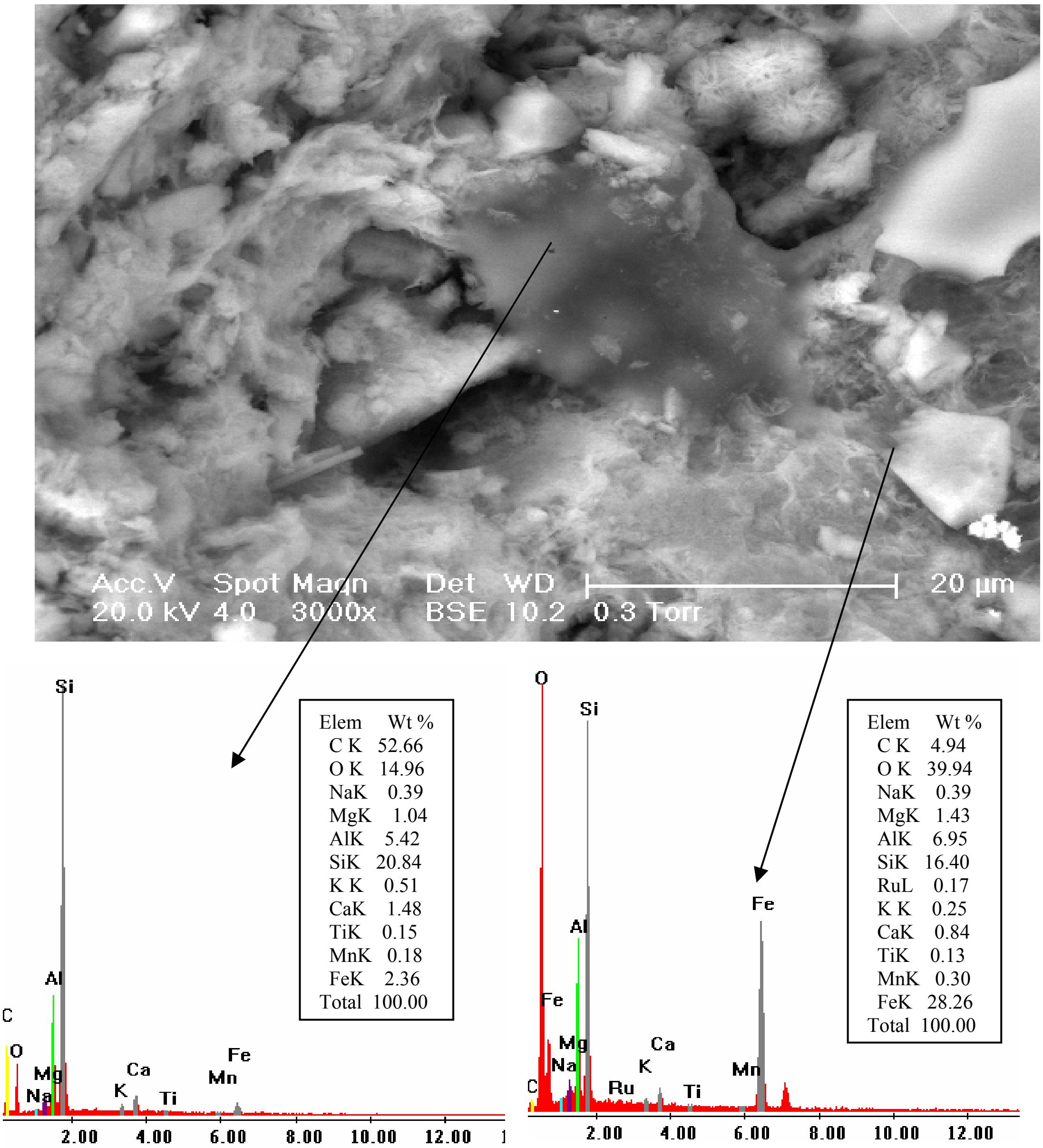

Figure 4.40. SEM image and EDAX spectra I, II of Na-zeolite equilibrated with OTC in the presence of Ca^{2+} ions.

According to Figure 4.40, large, flat, and wide shaped OTC crystal was discerned on Na-zeolite surface. EDAX (Figure 4.40) analysis of OTC revealed that carbon percentage reached to a value of 52.66 per cent similar to other OTC crystal analysis (Figure 4.38). According to EDAX (Figure 4.40), iron percentage was found to a value of 28 per cent a site near OTC crystal. Increasing iron per cent near OTC area may indicate metal-OTC complex formation on the zeolite surface. EDAX analysis also indicated that Ca^{2+} did not exhibit any increase on zeolite surface.

4.13.4. SEM Image of HDTMA-modified Zeolite

SEM image of HDTMA-modified zeolite was investigated to get knowledge about organo modified zeolite surface (Figure 4.41).

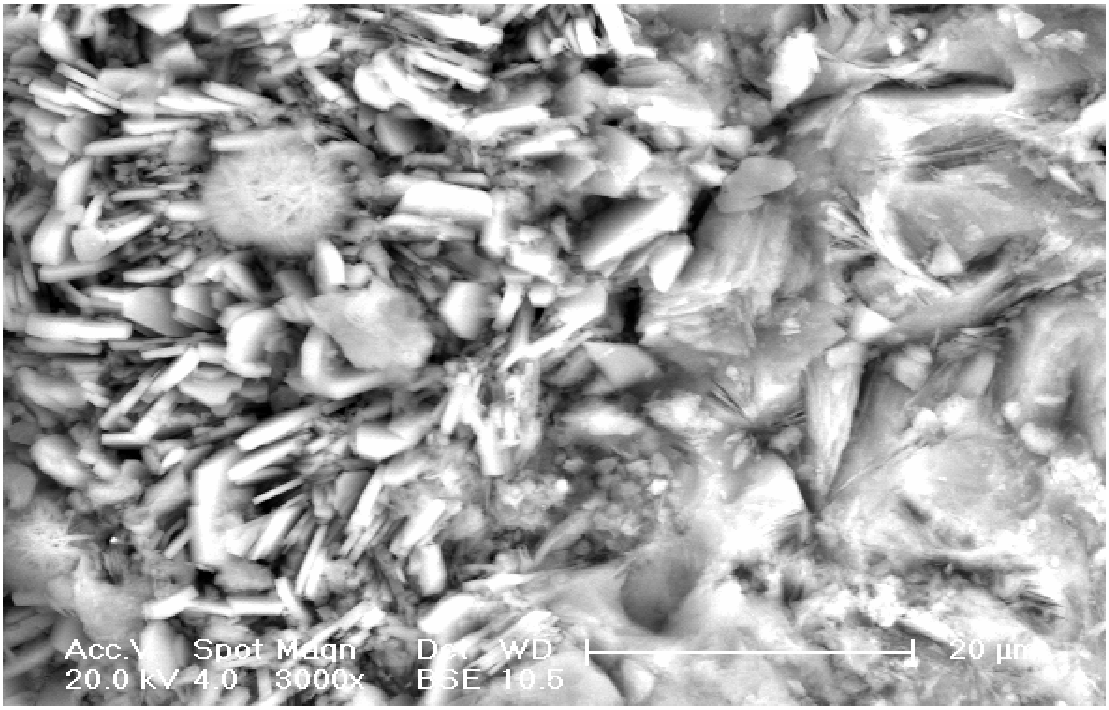

Figure 4.41. SEM image of HDTMA-modified zeolite.

As can be seen from the Figure 4.41, as the surface covered by surfactant, smaller, more agglomerated crystals were observed in the SEM image of HDTMA-modified zeolite.

4.13.5. SEM Image and EDAX Analysis of HDTMA-modified Zeolite Equilibrated with OTC

To identify the adsorption of OTC (0.6 mM) on HDTMA-modified zeolite at pH 8, SEM and EDAX analysis were performed. Figures 4.42 and 4.43 represent the obtained results.

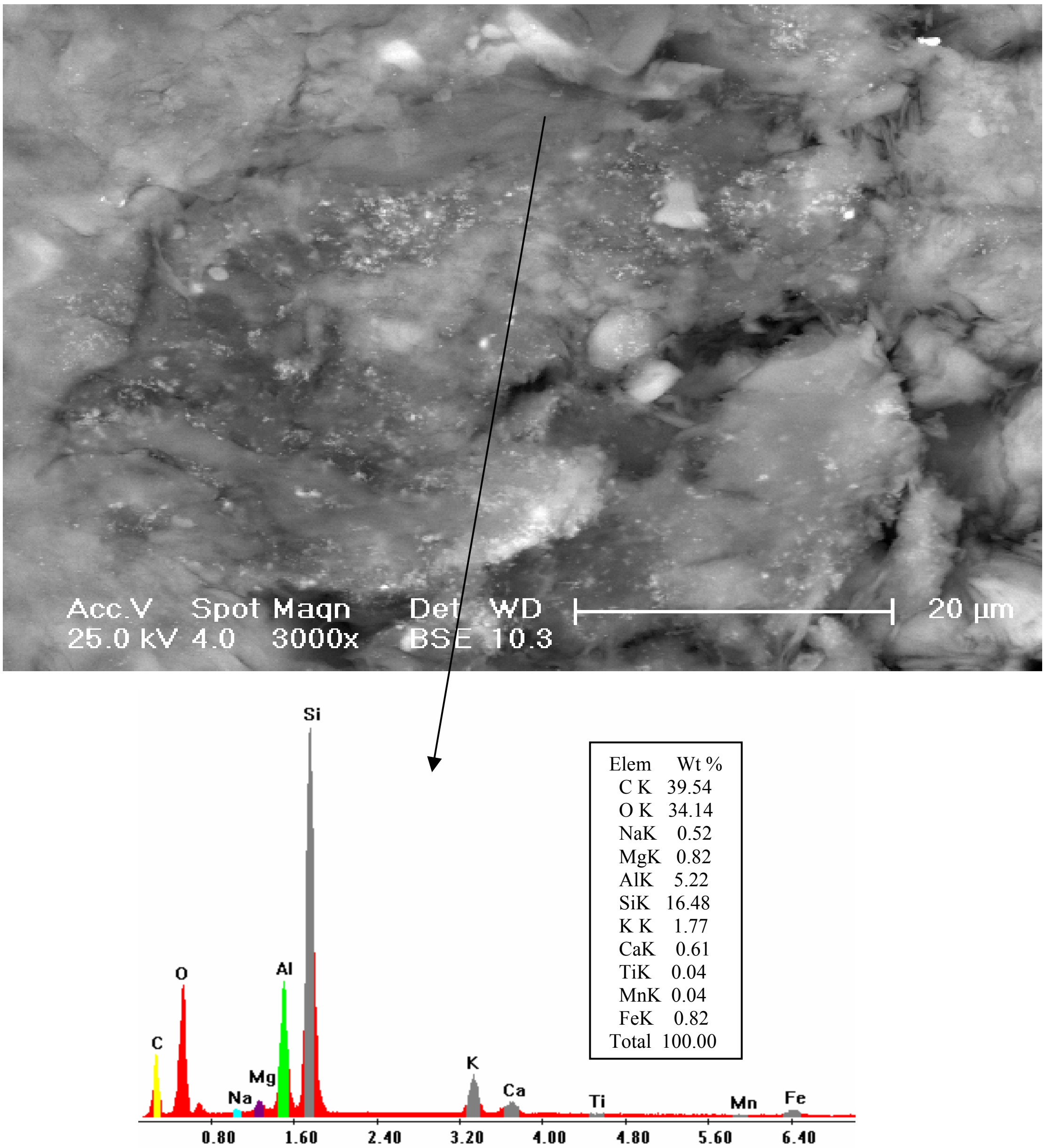

Figure 4.42. SEM image I and EDAX spectra of HDTMA-modified zeolite equilibrated with OTC.

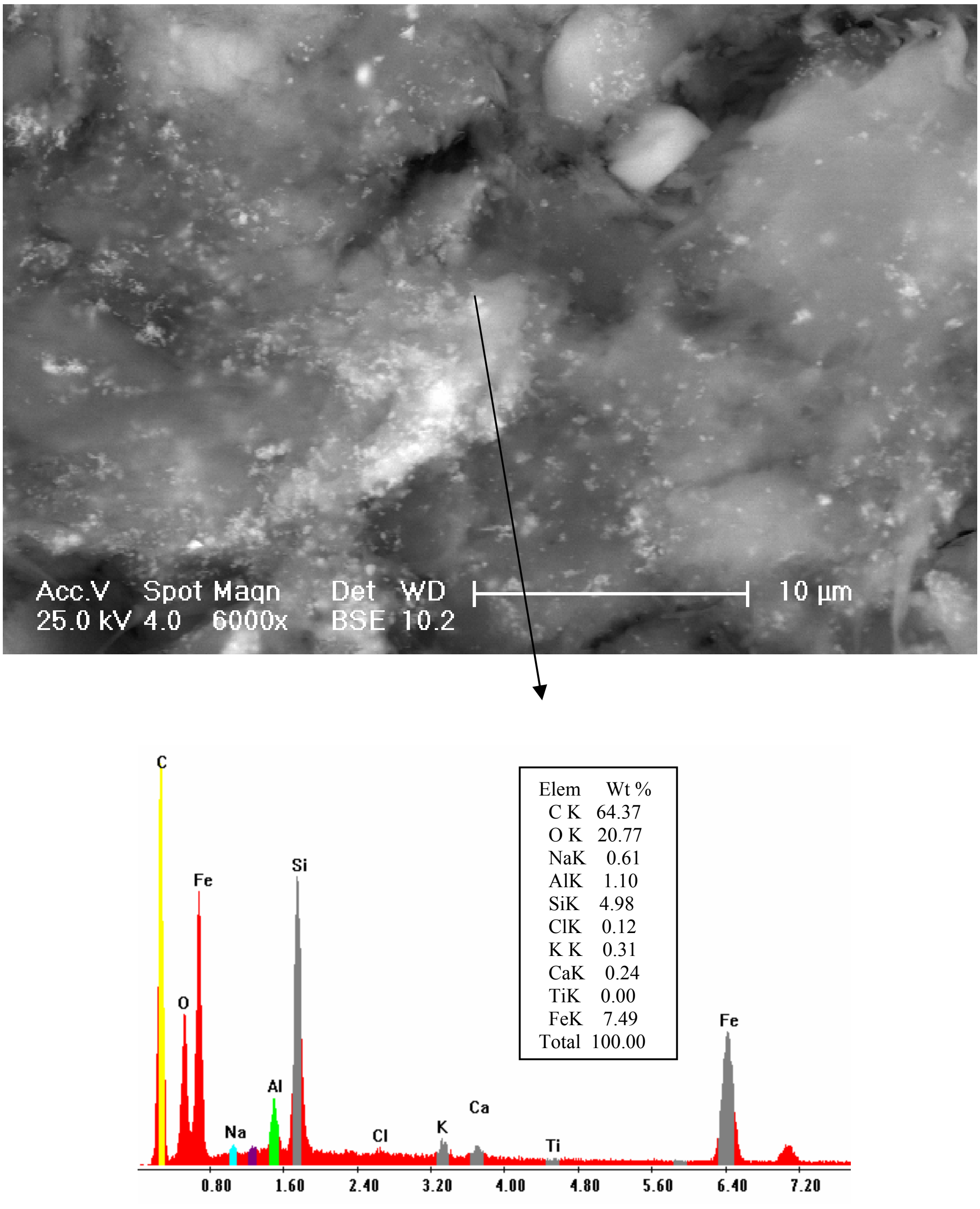

Figure 4.43. SEM image II and EDAX spectra of HDTMA-modified zeolite equilibrated with OTC.

Figures 4.42 and 4.43 indicate that poorly defined crystal edges are observed on HDTMA-modified zeolite surface equilibrated with OTC. Although SEM analysis was also performed at x 6000 magnification (Figure 4.43), it can not be distinguished OTC crystals on the surface. EDAX analyses indicate that carbon content reached to a value of 40 and 65 per cent in Figure 4.42 and Figure 4.43 respectively. Additionally, iron content is 7.5 per cent at this site.

The results of the SEM analysis confirmed that the surfaces of Na and HDTMA-modified zeolite were heterogeneous. Although OTC was clearly identified on Na-zeolite, it could not be differentiated on HDTMA-modified zeolite surface. Adsorption of OTC preferred to site on which iron content of zeolite high.

4.14. FTIR Analysis

FTIR analysis was performed to investigate the spectral shifts in characteristic functional groups of zeolite and OTC by the adsorption. In this respect, FTIR analyses of zeolites were employed before and after adsorption experiments. In addition to this, FTIR spectrum of OTC was also given. Figure 4.44 represents FTIR spectra of OTC, Na, and HDTMA-modified zeolites, respectively.

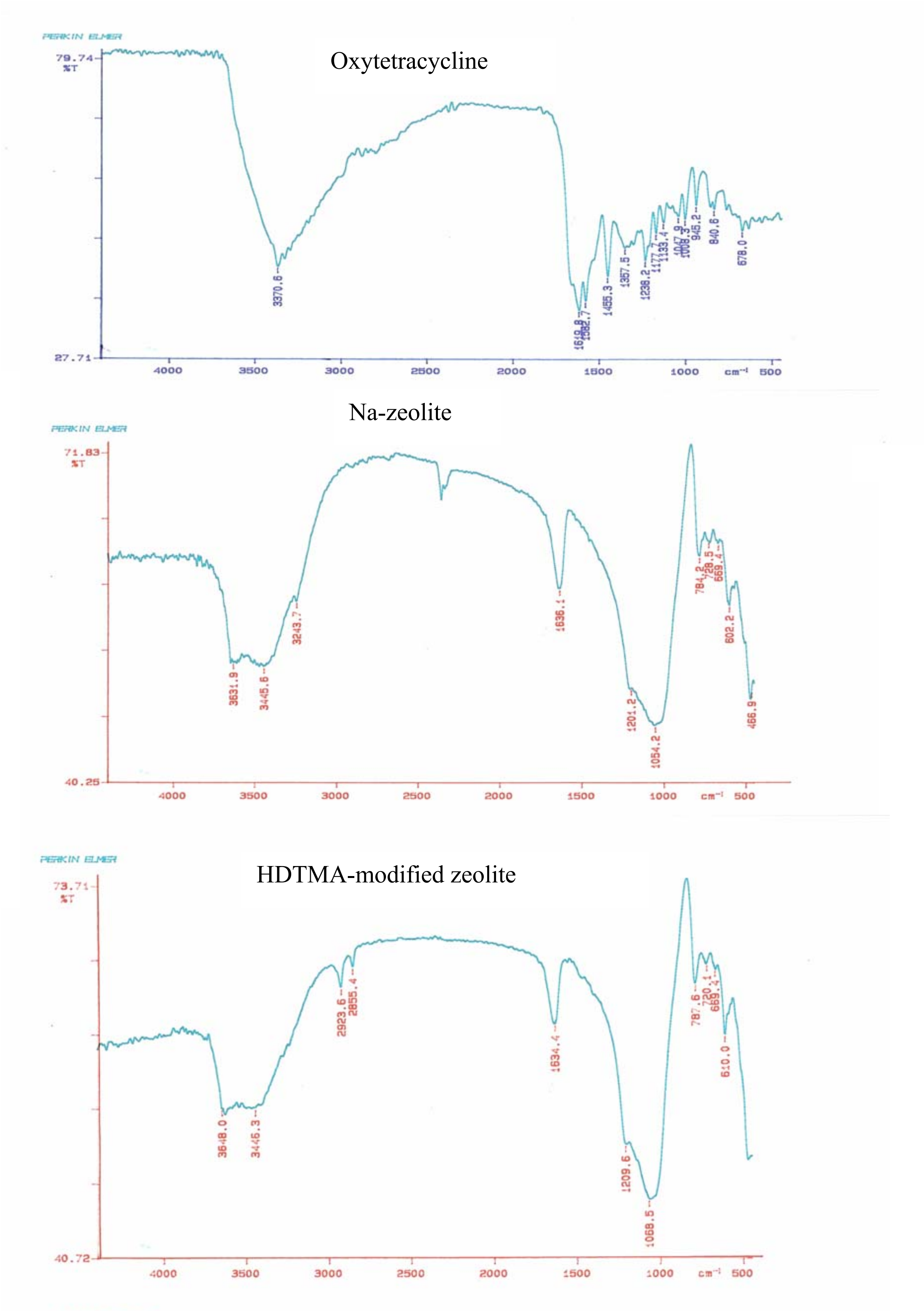

Figure 4.44. FTIR spectra of OTC, Na and HDTMA-modifed zeolite.

FTIR analysis of OTC showed that (Figure 4.44) a series of characteristic bands can be identified between 1200 and 1700 cm^{-1}. Characteristic bands of OTC at 1619 and 1582 cm^{-1}correspond to aromatic alkane and 1582 for amide II band, respectively. A band at 1458 cm^{-1} is attributed to CH_3 bending in OTC (Kulstrestha et al., 2004; Gu and Karthikeyan, 2005). Additionally, the band observed at 3370 cm^{-1} corresponds to O-H stretching vibration (Conley, 1972).

In FTIR spectra of the Na-zeolite (Figure 4.44), the bands occurred between 500-1200 $cm^{-1}$and from 1600 to 3700 cm^{-1}. A wide band placed between 3650 and 3440 cm^{-1} corresponds to OH^- groups from water molecules entrapped inside the framework of zeolite. The band at 1636 cm^{-1} corresponds to water molecules. The band between 1200-900 cm^{-1} have been assigned to Al-O-Si asymetric strech vibrations of framework (Linares and Brikgi, 2006).

The spectra of the HDTMA-modified zeolite indicated that zeolite remained unaltered after the modification and two new additional bands appeared (Figure 4.44). It was known that these bands correspond to the carbon hydrogen stretching vibrations of the hydrocarbon chain (2923 and 2855 cm^{-1}) (Kulstrestha et al., 2004; Rivera and Farias, 2005).

To determine a possible chemical interaction of OTC on the surface of zeolite FTIR analysis was performed for zeolite equilibrated with 0.6 mM OTC at pH 1.5 (Figure 4.45).

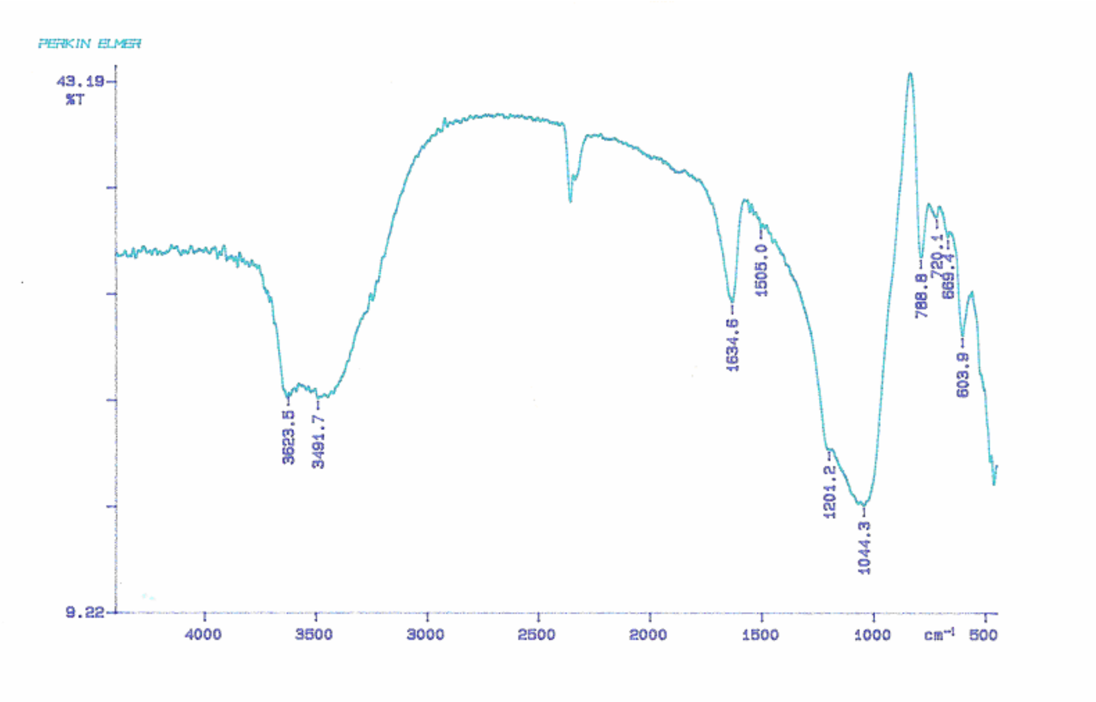

Figure 4.45. FTIR spectra of Na-zeolite equilibrated with OTC.

As can be seen from Figure 4.45, it was not possible to detect presence of OTC on zeolite since the most important band of the OTC molecule (1619 cm^{-1}) overlapped with the main water band of the zeolite (1630 cm^{-1}). Similar result was observed for the adsorption of sulfanomide group antibiotics on natural zeolite (Rivera and Farias, 2005).

The results of the FTIR analyses revealed the characteristics functional group of zeolites and OTC. However, it was not possible to identify OTC onto Na-zeolite after equilibration due to overlapping with the main band of OTC and zeolite.

4.15. X-ray diffraction analysis of Na-zeolite equilibrated with OTC

Adsorption may lead to changes in crystalline structures of the adsorbent and resulting changes thereof would provide valuable information regarding adsorption reaction. Hence, XRD patterns of adsorbent before and after equilibration with OTC have been studied. To determine possible changes crystalline structures of zeolite XRD analysis was performed for Na-zeolite equilibrated with 0.6 mM OTC at pH 1.5 and pH 10 (Figure 4.46).

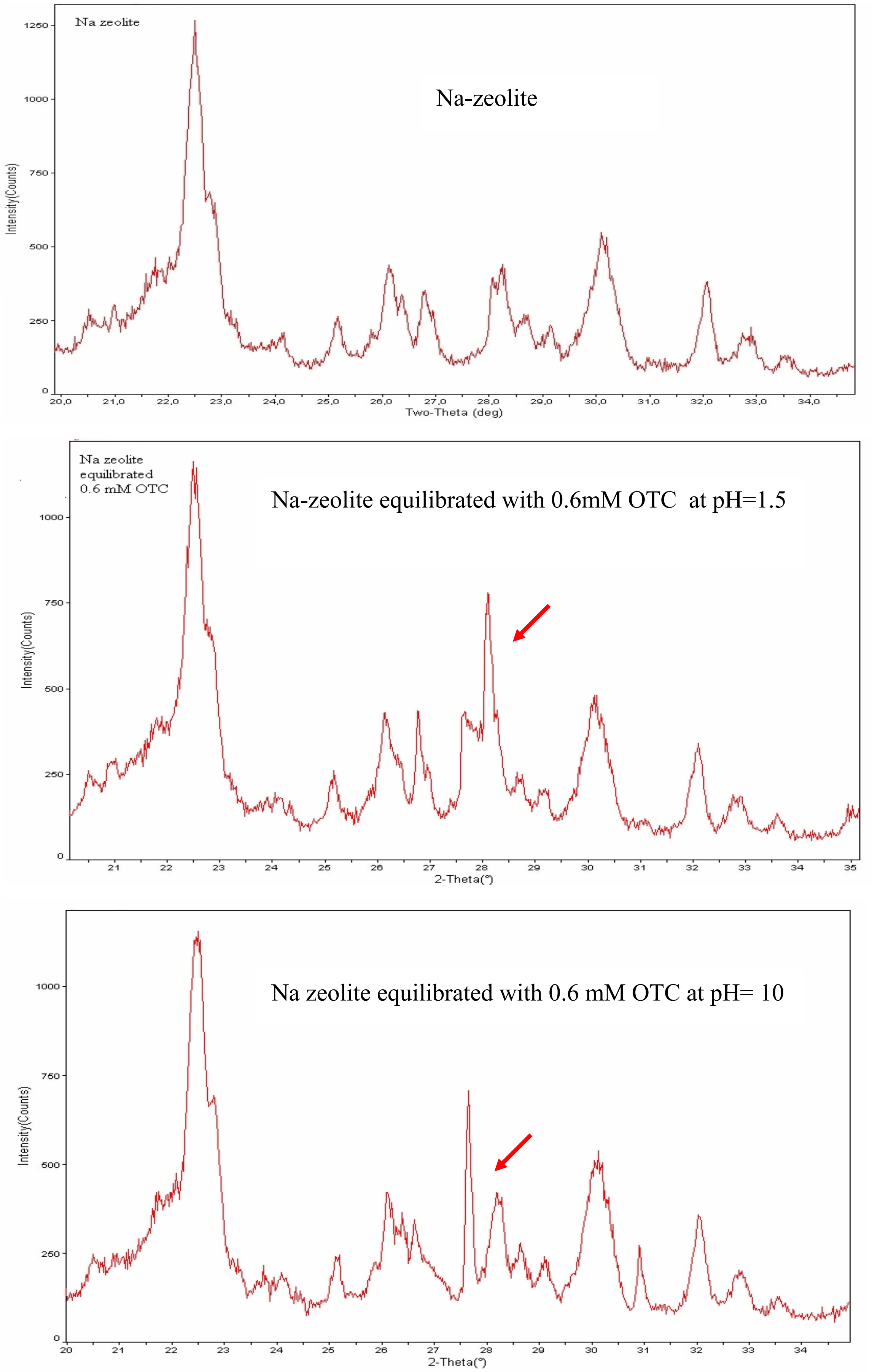

Figure 4.46. X-ray analysis of Na-zeolite before and after adsorption of OTC.

X-ray diffraction of zeolite equilibrated with 0.6 mM OTC did not lead to significant structural changes. However new peaks were observed between $2\theta = 28\text{-}28.5$ at pH 1.5 and $2\theta = 27.5\text{-}28$ at pH 10. Interlayer spacings and peak intensities are tabulated in Appendix B Table B.4 and B.5.

5. CONCLUSION

In the present study, adsorption of OTC by raw, Na, and HDTMA-modified zeolite was investigated. Based on the results of this study following conclusions can be drawn.

- The XRD diffraction pattern indicated that clinoptilolite–Ca (KNa_2Ca_2 (Si_{29} Al_{17}) O_{72} 24 .H_2O) was the principal component present in the zeolitic sample.

- In contrast to Na-zeolite, modification of zeolite surface with HDTMA decreased total cation exchange capacity of zeolite. Modification of zeolite both Na^+ and HDTMA resulted in enhancement of external cation exchange capacity.

- In the kinetic experiments, pseudo second order and intraparticle diffusion models were well described adsorption data of OTC on Na and HDTMA-modified zeolite. HDTMA-modified zeolite had the fastest initial sorption and diffusion rates.

- Adsorption isotherm of OTC on Na and HDTMA-modified zeolite were best described by the Freundlich model considering the better correlation between theoretical and experimental data. The Freundlich model constant K_f varied from 0.65 x 10^{-2} to 3.00 x 10^{-1} mg^{1-n} L^n/g depending upon pH and modification of surface. Depending upon the K_f values HDTMA-modified zeolite had the highest adsorbent capacity at pH 8.

- The effect of pH on the adsorption of OTC revealed that OTC adsorption on Na-zeolite decreased by increasing pH. K_d decreased from 167 to 111 L/kg on Na-zeolite as pH increased from 6.5 to 8. On the other hand, HDTMA-modified zeolite exhibited higher sorption capacity for OTC sorption by increasing pH. K_d increased from 67 to 220 L/kg as pH increased from 6.5 to 8.

- In general, presence of some cations (Ca^{2+}, Mg^{2+}, and NH_4^+) and anions (Cl^-, SO_4^{2-}, $PO_4^{3-}$and HCO_3^-) had a negative impact on the adsorption of OTC on zeolite except NH_4^+ and HCO_3^-.

- Na-zeolite was effective for the simultaneous removal of NH_4^+ and OTC at pH=6.5. The presence of OTC did not significantly decreased ammonia removal capacity of zeolite.

- By the addition of 120 mg/L Ca^{2+} and Mg^{2+} K_d value of OTC on Na-zeolite slightly decreased from 167 to 140 L/kg. Soluble OTC-Ca^{2+} and OTC-Mg^{2+} complex formation were responsible for decreasing the sorption of OTC.

- The effects of chloride and sulfate ions for OTC sorption on HDTMA-modified zeolite were more pronounced than those on Na-zeolite. K_d of OTC decreased 10 fold by the addition of 500 mM chloride and decreased 7 fold by the addition of 26 mM sulfate ion.

- Due to the competition between OTC and PO_4^{3-} anion for the available adsorption sites on Na-zeolite, phosphate ion decreased considerably OTC sorption. K_d of OTC decreased 11 fold by the addition of 100 mM phosphate. However, phosphate or OTC adsorption on HDTMA-modified zeolite was not significantly influenced by the presence of OTC or phosphate.

- Unlike other anions, bicarbonate improved OTC sorption on HDTMA-modified zeolite. K_d of OTC increased 10 fold by the addition of 120 mg/L bicarbonate ions.

Based on all results, Na-zeolite can be suggested as bedding material or barrier for confined animal feeding operations. Considering the high sorption capacity of HDTMA-zeolite at pH=8 it can be suggested as an adsorbent in aquaculture facilities.

REFERENCES

Accinelli, C., Koskinen, W. C., Becker, J., Sadowsky, M. J., 2007. Environmental fate of two sulfonamide antimicrobial agents. Journal Agricultural Food Chemistry, 55, 2677-2682.

Aga, D., Goldish, R., Kulshtrestha, P., 2003. Application of ELISA in determining the fate of tetracyclines. Analyst, 128, 658–662.

Aksu, Z., Tezer, S., 2000. Equilibrium and kinetic modelling of biosorption of Remazol Black B by *Rhizopus arrhizus* in a batch system: effect of temperature. Process Biochemistry, 36, 431-439.

Armağan, B., Özdemir, O., Turan, M., Çelik., M.S., 2003. The removal of reactive azo dyes by natural and modified zeolites. Journal of Chemical Technology and Biotechnology, 78, 725-732.

Barreiro, C.G., Lores, M., 2003. Simultaneous determination of neutral and acidic pharmaceuticals in wastewater by high performance liquid chromatography-post-column photochemically induced fluorimetry. Journal Chromotography A, 993, 29-37.

Batchelder, A.R., 1981. Chlortetracycline and oxytetracycline effects on plant growth and development in liquid cultures. Journal of Environmental Quality, 10, 515–518.

Batt, A. L., Bruce, I. B., Aga, D. S., 2006. Evaluating the vulnerability of surface waters to antibiotic contamination from varying wastewater treatment plant discharges. Environmental Pollution, 142, 295-302.

Bjorklund, H.V., Bondestam, J., Bylund, G., 1990. Residues of oxytetracycline in wild fish and sediments from fish farms. Aquaculture, 86, 359-367.

Bjorklund, H.V., Bylund, G., 1991. Comparitive pharmakokinetics and bioavailability of oxolonic acid and oxytetracycline in rainbow trout. Xenobiotica, 21, 1511-1520.

Bjorklund, H.V., Ragergh, C.M.I., Bylund, G., 1991. Residues of oxolinic acid and oxytetracycline in fish and sediments from fish farms. Aquaculture, 97, 85-96.

Booker, N.A., Cooney, E.L., Priestly, A.J., 1996. Ammonia removal from sewage using natural Australian zeolite. Water Science Technology, 34, 17-24.

Bowman, R.S., 2003. Applications of surfactant-modified zeolites to environmental remediation. Microporous and Mesoporous Materials, 61, 43-56.

Boxall, A.B.A., Blackwell, P., Cavallo, R., Kay, P., Tolls, J., 2002. The sorption and transport of a sulfonamide antibiotic in soil systems. Toxicology Letters, 131, 19-28.

Boxall, A.B.A., Fogg, L.A. Blackwell, P.A., Kay, P., Pemberton, E.J., Croxford, A., 2004. Veterinary medicines in the environment. Review Environmental Contamination Toxicology, 180, 1-91.

Buckley, D.L., Smyth, M.R., 1986. An ultraviolet spectral and polarographic investigation of the acid-base and complexation behaviour of oxytetracycline hydrochloride. Journal Electroanalytical Chemistry, 214, 199-212.

Cahill, J.D., Furlong, E.T., Burkhardt, M.R., Kolpin, D., Anderson, L.G., 2004. Determination of pharmaceutical compounds in surface and groundwater samples by solid-phase extraction and high-performance liquid chromatography-electronspray ionization mass spectrometry. Journal Chromatograhy A, 1041, 171-180.

Capone, D.G., Weston, D.P., Miller, W., Shoemaker, C., 1996. Antibacterial residues in marine sediments and invertebrates following chemotherapy in aquaculture. Aquaculture, 145, 55-75.

Chee-Sanford, J.C., Amino, R.I., Kropac, I.J., Garrigues, N., Mackie, R.I., 2001. Occurrence of diversity of tetracycline genes in lagoons and groundwater underlying to swine production facilities. Applied Environmental Microbiology, 65, 1494-1502.

Chiou, M.S., Li, H.Y., 2002. Equilibrium and kinetic modeling of adsorption of reactive dye on cross-linked chitosan beads. Journal of Hazardous Materials B 93, 233-248.

Chui, S.H.L., Green, M.L., Baylis, F.P., Eline, D., Rosegay, A., Meriwether, H., Jacob, T.A., 1990. Absorption, tissue distribution, and excretion of tritium-labelled ivermectin in cattle, sheep and rat. Journal Agricultural Food Chemistry, 38, 2072-2076.

Cincotti, A., Lai, N., Orru, R., Cao, G., 2001. Sardinian natural clinoptilolites for heavy metals and ammonium removal: Experimental and modeling. Chemical Engineering Journal, 84, 275-282.

Conley, R.T., 1972. Infrared Spectroscopy, Second Ed., Allyn and Bacon Inc., Boston, 186.

Connors, K. A., Amidon, G. L. Stella, V. L., (Eds) 1986. Chemical Stability of Pharmaceuticals; A Handbook for Pharmacists, Second Ed., John-Wiley and Sons Inc., New York.

Coyne, R., Hiney, M., O'Connor, B., Kerry, J., Cazabon, D., Smith, P., 1994. Concentration and persistence of oxytetracycline in sediment under a marine salmon farm. Aquaculture, 123, 31-42.

Dakoviç, A., Tomasoviç-Canoviç, M., Dondur, V., Rottingehaous, G.E., Medakoviç, V., Zaric, S., 2005. Adsorption of mycotoxins by organozeolites. Colloids and Surfaces B: Biointerfaces, 46, 20-25.

Delepee, R., Pouliquen, H., Le Bris, H., 2004. The bryophyte *Fontinalis antipyretica* bioaccumulates oxytetracycline, flumequine and oxolinic acid in the freshwater environment. The Science of the Total Environment, 322, 243-253.

Diaz-Cruz, M.S., Lopez de Alda, M.J., Barcelo, D., 2003. Environmental behaviour and analysis of veterinary and human drugs in soils, sediments and sludge. Trends in Analytical Chemistry, 22, 340-351.

Diaz-Nava, C., Olguin, M.T., Solache-Rios, M., 2002. Water defluoridation by Mexican heulandite-clinoptilolite. Separation Science and Technology, 37, 3109-3128.

Ersoy, B., Çelik, M.S., 2004. Uptake of aniline and nitrobenzene from aqueous solution by organo-zeolite. Environmental Technology, 25, 341-348.

Ervik, A., Thorsen, B., Eriksen, V., Lunestad, B.T., Samuelsen, O.B., 1994. Impact of administrating antibacterial agents on wild fish and blue mussels in the vicinty of fish farms. Diseases of Aquatic Organisms, 18, 45-51.

Farre, M.L., Ferrer, I., Ginebreda, A., Figueras, M., Olivella, L., Tirapu, L., Vilanova, M., Barcelo, D., 2001. Determination of drugs in surface water and wastewater by liquid chromatography-mass spectrometry; methods and preliminary results including toxicity studies with *Vibrio fischeri*. Journal of Chromatography, A, 938, 187-197.

Figueroa, R.A., Leonard, A., Mackay, A.A., 2004. Modeling tetracycline antibiotics sorption to clays. Environmental Science and Technology, 38, 476-483.

Figueroa, R.A., Mackay, A.A., 2005. Sorption of oxytetracycline to iron oxides and iron oxide-rich soils. Environmental Science and Technology, 39, 6664-6671.

Gavalchin, J., Katz, S.E., 1994. The persistence of fecal-borne antibiotics in soil. Journal AOAC International, 177, 481-485.

Geelhoed, J.S., Hiemstra, T., Van Riemsdıjk, W.H., 1998. Competitive interaction between phosphate and citrate on goethite. Environmental Science and Technology, 32, 2119-2123.

Ghosh, A., Saez, A. E., Ela, W., 2006. Effect of pH, competitive anions and NOM on the leaching of arsenic from solid residuals. Science of the Total Environment, 363, 46-59.

Glassmeyer, S.T., Furlong, E.T., Kolpin, D.W., Cahill, J.D., Zaugg, S.D., Wener, S.L. Myer, M.T., Kryak, D.D., 2005. Transport of chemicals and microbial compounds from known wastewater discharges: Potential use as indicators of human fecal contamination. Environmental Science and Technology. 39, 5157-5169.

Gobel, A., McArdell C.S., Suter, M.J.F., Giger W., 2004. Trace determination of macrolide and sulfonamide antimicrobials, a human sulfonamide metabolite, and trimethoprim in wastewater using liquid chromatography coupled to electrospray tandem mass spectrometry. Analytical Chemistry, 76, 4756-4764.

Gobran, G.R., Nilsson, S.I., 1988. Effects of forest floor leachate on sulfate retention in a spodosol soil. Journal of Environmental Quality, 17, 235-239.

Golet, E.M., Alder, A.C., Giger, W., 2002. Environmental exposure and risk assessment of fluoroquinolone antibacterial agents in wastewater and river water of Glatt valley watershed, Switzerland. Environmental Science and Technology, 36, 3645-3651.

Gross, B., Montgomery-Brown, J., Naumann, A., Reinhard, M., 2004. Occurrence and fate of pharmaceuticals and alkylphenol ethoxylate metabolites in an effluent-dominated river and wetland. Environmental Toxicology and Chemistry, 23, 2074-2083.

Gu, B., Schmitt, J., Chen, Z., Liang, L., McCcharty, J.F., 1994. Adsorption and desorption of natural organic matter on iron oxide mechanisms and models. Environmental Science and Technology, 28, 38-46.

Gu, C., Karthikeyan, K.G., 2005. Interaction of tetracycline with aluminum and iron hydrous oxides. Environmental Science and Technology, 39, 2660-2667.

Haggerty, G.M., Bowman, R.S., 1994. Sorption of chromate and other inorganic anions by organo-zeolite. Environmental Science and Technology, 28, 452-458.

Haidouti, C., 1997. Inactivation of mercury in contaminated soils using natural zeolites. The Science of the Total Environment, 208, 105-109.

Halling Sorensen, B. Nielsen, S.N., Sengelov, G., Tjornelund, J., 2002. Toxicity of teracyclines and tetracycline degradation products to environmentally relevant bacteria, including selected tetracycline-resistant bacteria. Achieved Environmental Contamination Toxicology, 44, 7-16.

Hamscher, G., Sczesny, S., Hooper, N. H., 2002. Determination of persistent tetracycline residues in soil fertilised with liquid manure by high-performance liquid chromatography with electrospray ionization tandem mass spectrometry. Analytical Chemistry, 74, 1509-1518.

Heberer, T. 2002. Occurrence, fate, and removal of pharmaceutical residues in the aquatic environment: a review of recent research data. Toxicology Letters, 131, 5-17.

Hektoen, H., Berge, J. A., Hormazabal, V., Yndestad, M., 1995. Persistence of antibacterial agents in marine sediments. Aquaculture, 133, 175-184.

Hirsch, R., Ternes, T., Haberer, K., Kratz, K.L., 1999. Occurence of antibiotics in the aquatic environment. Science of the Total Environment, 225, 109-118.

Ho, Y.S., McKay, G., 1999. Pseudo-second order model for sorption processes. Process Biochemistry, 34, 451-465.

Ho, Y.S., Chiang, C.C., 2001. Sorption studies of acid dye by mixed sorbents. Adsorption, 7, 139-147.

Hustvedt, S.O., Salte, R., Kvendseth, O., Vassik, V., 1991. Bioavailibility of oxolinic acid in Atlantic salmon from medicated feed. Aquaculture, 97, 305-310.

Hutzinger, O., 1982. The Handbook of Environmental Chemistry, Reactions and Procesesses, Volume 2 Part B, Springer-Verlag, New York.

Ingerslev, F., Halling Sorensen, B., 2001. Biodegredability of metronidazole, olaquandix, tylosin and formation of tylosin degredation products in aerobic soil/manure slurries. Chemosphere, 48, 311-320.

Inglezakis, V J., Zorpas, A., Loizidou, M D, Grigoropoulou, H P., 2003. Simultaneous removal of metals Cu^{2+}, Fe^{3+} and Cr^{3+} with anions SO_4^{2-} and HPO_4^{2-} using clinoptilolite. Microporous and Mesoporous Materials, 61, 167-171.

Iznaga, I., Gomez, A., Rodriguez- Fuentes, G., Aguilar, A. B., Ballan, J.S., 2002. Natural clinoptilolite as an exchanger of Ni^{2+} and NH_4^+ ions under hydrothermal conditions and high ammonia concentration. Microporous and Mesoporous Materials, 53, 71-80.

Jacobsen, P., Berglind, L., 1988. Persistence of oxytetracycline in sediments from fish farms. Aquaculture, 70, 365-370.

Jones, A.D., Bruland, G.L., Agrawal, G., Vasudevan, D., 2005. Factors influencing the sorption of oxytetracycline to soils. Environmental Toxicology and Chemistry, 24, 761-770.

Jorgensen, T.C., Weatherley, L.R., 2003. Ammonia removal from wastewater by ion exchange in the presence of organic contaminants. Water Research, 37, 1723-1728.

Karadağ, D., Koç, Y., Turan., M., Armağan, B., 2006. Removal of ammonium ion from aqueous solution using Turkish clinoptilolite. Journal of Hazardous Materials B, 136, 604-609.

Karltun, E., 1998. Modelling SO_4^{2-}surface complexation on variable charge minerals. II. Competition between SO_4^{2-}, oxalate and fulvate. European Journal of Soil Science, 49, 113-120.

Kay, P., Blackwell, P.A., Boxall, B.A., 2004. Fate of veterinary antibiotics in a macroporous tile drained clay soil. Environmental Toxicology and Chemistry, 23, 1136-1144.

Khraisheh, M A. M., Al-Dogs, Y.S., Allen, S.J., Ahmad, M.N., 2002. Elucidation of controlling steps of reactive dye adsorption on activated carbon. Industrial and Engineering Chemistry Research, 41, 1651-1657.

Kolpin, D.W., Furlong, E.T., Meyer, M.T., Thurman, E.M., Zaugg, S.D., Barber, L.B., Buxton, H.T., 2002. Pharmaceuticals, hormones and other organic wastewater contaminants in US streams. Environmental Science and Technology, 36, 1202-1211.

Kolpin, D.W., Skopec, M., Meyer, M.T., Furlong, E.T., Zaugg, S.D., 2004. Urban contribution of pharmaceuticals and other organic wastewater contaminants to streams during differing flow conditions, Science of the Total Environment, 328, 119-130.

Kooner, Z.S., Jardine, P.M., Feldman, S., 1995. Competitive surface complexation reactions of sulfate and natural organic carbon on soil. Journal of Environmental Quality, 24, 656-662.

Kruner, G., Rosenthal., H., 1983. Efficiency of nitrification in trickling filter using different substrates. Aquaculture Engineering, 2, 49-56.

Kulshreshtha, P., Giese, R., Aga, D. S., 2004. Investigating the molecular interactions of oxytetracycline in clay and organic matter: Insights on factors affecting its mobility in soil. Environmental Science andTechnology, 38, 4097- 4105.

Kumar, K., Gupta, S. C., Chander, Y., Singh, A. K., 2005. Antibiotic use in agriculture and its impact on the terrestrial environment. Advances in Agronomy, 87, 1-54.

Kurama, H., Zimmer, A., Reschetilowski, W., 2002. Chemical modification effect on the sorption capacities of natural clinoptilolite. Chemical Engineering Technology, 25, 301-305.

Kühne, M., Ihnen, D., Moller, G., Agthe, O., 2000. Stability of tetracycline in water and liquid manure. Journal Veterinary Medicine Series, A47, 379–384.

Kümmerer K., 2001. Pharmaceuticals in the Environment, Springer-Verlag Berlin.

Lalumera, G. M., Calamari, D., Galli, P., Castiglioni, S., Crosa, G., Fanelli, R., 2004. Preliminary investigation on the environmental occurrence and effects of antibiotics used in aquaculture in Italy. Chemosphere, 54, 661-668.

Le Bris, H., Pouliquen, H., 2004. Experimental study on the bioaccumulation of oxytetracycline and oxolinic acid by the blue mussel (*Mytilus edulis*) an evaluation of its ability to biomonitor antibiotics in the marine environment. Marine Pollution Bulletin, 48, 434-440.

Li, Z., Bowman, R., 1997. Counterion effects on the sorption of cationic surfactant and chromate on natural clinoptilolite. Environmental Science and Technology, 31, 2407-2412.

Li, Z., Bowman, R., 1998. Sorption of perchloroethylene by surfactant-modified zeolite as controlled by surfactant loading. Environmental Science and Technology, 32, 2278-2282.

Li, Z., Jones, H.K., Bowman, R., Helferich, R., 1999. Enhanced reduction of chromate and PCE by pelletized surfactant-modified zeolites/zerovalent iron. Environmental Science and Technology, 33, 4326-4330.

Li, Z., Burt, T., Bowman, R., 2000. Sorption of ionizable organic solutes by surfactant-modified zeolite. Environmental Science and Technology, 34, 3756-3760.

Li, Z., 2004. Influence of solution pH and ionic strength on chromate uptake by surfactant-modified zeolite. Journal of Environmental Engineering, 130, 205-208.

Liao, P.B., Mayo, R.D., 1972. Intensified fish culture combining water reconditioning with pollution abatement. Aquaculture, 3, 61-85.

Lin, S.H., Wu, C.L., 1996. Ammonia removal from aqueous solution by ion exchange. Industrial Engineering Chemical Residues, 35, 553-558.

Linares, C.F., Brikgi, M., 2006. Interaction between antimicrobial drugs and antacid based on cancrinite type of zeolite. Microporous and Mesoporous Materials, 96,141-148.

Lindsey, M. E., Meyer, M., Thurman, E. M., 2001. Analysis of trace levels of sulfonamide and tetracycline antimicrobials in groundwater and surface water using solid phase extraction and liquid chromatography/mass spectrometry. Analytical Chemistry, 73, 4640–4646.

Loke, M.L., Tjornelund, J. Halling- Sorensen, B., 2002. Determination of the distribution coefficient (log K_d) of oxytetracycline, tylosin A, olaquidox and metronidazole in manure. Chemosphere, 48, 351-361.

Lunestad, B.J., Goksoyr, J., 1990. Reduction in the antibacterial effect of oxytetracycline in sea water by complex formation with magnesium and calcium. Diseases of Aquatic organisms, 9, 67-72.

Machado, F C., Demicheli, C., Garnier-Suillerot, A., Beraldo, H., 1995. Metal complexes of anhydrotetracycline, absorption and circular dichroism study of Mg(II), AMID, and Fe(III) complexes. Possible influence of the Mg (II) complex on the toxic side effects of tetracycline. Journal of Inorganic Biochemistry, 60, 163-173.

Magnussen, J.D., Dalidowicz, J.E., Thomson, T.D., Donoho, A.L., 1991. Tissue residues and metabolism of avilamycin in swine and rats. Journal Agricultural Food Chemistry, 39, 306-310.

Martin, S.R., 1979. Equilibrium and kinetic studies on the interaction of tetracyclines with calcium and magnesium. Biophysical Chemistry, 10, 319-326.

Martinez-Carbollo, E., Gonzalez, C., Scharf, S., Gans., O., 2007. Environmental monitoring study of selected veterinary antibiotics in animal manure and soils in Austria. Environmental Pollution, 148, 570-579.

McArdell, C.S., Molnar, E. Suter, M.J.F., Giger, W., 2003. Occurrence and fate of macrolide antibiotics in wastewater treatment plants and in the Glatt valley watershed, Switzerland. Environmental Science and Technology, 37, 5479-5486.

Meyer, M.T., Bumgarner, J.E., Varns, J.L., Daughtritge J.V., Thurman, E.M., Hostetler, K.A., 2000. Use of radioimmunoassay as a screen for antibiotics in confined animal feeding operations and confirmation by liquid chromatography/mass spectrophotometry. Science of the Total Environment, 248, 181-187.

Miao, X.S., Koenig, B.G., 2002. Analysis of acidic drugs in the effluents of sewage treatment plants using liquid chromatography-electrospray ionization mass spectrometry. Journal Chromatography A, 952, 139-147.

Migliore, L , Cozzolino, S., Fiori, M., 2003. Phytotoxicity to and uptake of enrofloxacin in crop plants. Chemosphere, 52, 1233-1244.

Ming, D.W., Dixon, J.B., 1987. Quantitative determination of clinoptilolite in soils by a cation-exchange capacity method. Clays and Clay Minerals, 35, 463-468.

Mitscher, L.A., 1978. The Chemistry of the Tetracycline Antibiotics, Volume 9, Marcel Decker Inc., New York, 330.

Myers, H.M., Tochon-Danguy, H.J., Baud, C.A., 1983. IR absorption spectrophotometric analysis of the complex formed by tetracycline and synthetic hydroxyapatite. Calcified Tissue International, 35, 745-749.

Newman, E.C., Frank, C.W., 1976. Circular dichroism spectra of tetracycline complexes with Mg^{2+} and Ca^{2+}. Journal of Pharmaceutical Sciences, 65, 1728-1732.

Nowara, A., Burhenne, J., Spiteller, M., 1997. Binding of floroquinoline carboxylic acid derivatives to clay minerals. Journal Agricultural Food Chemistry, 45, 1459-1463.

Oka, H., Ikai, Y., Kawamura, N., Yamada, M., Harada, K., Ito, S., Suzuki, M., 1989. Photodegradation products of tetracycline in aqueous solution. Journal Agricultural Food Chemistry, 37, 226–231.

OECD, 2000. Adsorption-Desorption Using a Batch Equilibrium Method; Technical Guideline 106. Organization for Economic Cooperation and Development.

Ötker H.M., Balcıoğlu, I., 2005. Adsorption and degradation of enrofloxacin, a veterinary antibiotic on natural zeolite. Journal of Hazardous Materials, 122, 251-258.

Paesen, J., Cypers, W., Busson, R., Roets, E., Hoogmartens, J., 1995. Isolation of decomposition products of tylosin using liquid chromatography. Journal Chromatography A, 699, 99-106.

Pathak, S. P., Gopal, K., 2005. Occurrence of antibiotic and metal resistance in bacteria from organs of river fish. Environmental Research, 98, 100-103.

Peavy, H.S., Rowe, D.R., Tchobanoglous, G., 1985. Environmental Engineering, Mc Graw Hill, Newyork, 633.

Perraki, T., Kakali, G., Kontori, E., 2005. Characterization and pozzolonic activity of thermally treated zeolite. Journal of Thermal Analysis and Calorimetry, 82, 109-113.

Porubcan, L.S., Serna, C.J., White, J.L., Hem, S.L., 1978. Mechanism of adsorption of clindamycin and tetracycline by montmorillonite. Journal of Pharmaceutical Sciences, 67, 1081-1087.

Pouliquen, H., Le Bris, H., 1996. Sorption of oxolinic acid and oxytetracycline to marine sediments, Chemosphere, 33, 801- 815.

Rabolle M., Spliid, N.H., 2000. Sorption and mobility of metranidazole, olaquandix, oxytetracycline and tylosin in soil. Chemosphere, 40, 715-722.

Riviera, A., Farias, T., 2005. Clinoptilolite-surfactant composites as drug support: A new potential application. Microporous and Mesoporous Materials, 80, 337-346.

Ru, J., Liu, H., Qu, J., Wang, A., Dai, R., 2007. Removal of dieldrin from aqueous solution by a novel triolein- embedded composite adsorbent. Journal of Hazardous Materials, 141, 61- 69.

Samuelsen, O.B., 1989. Degredation of oxytetracycline in seawater at two different temperatures and light intensities and the persistence of oxytetracycline in the sediment from a fish farm. Aquaculture, 83, 7-16.

Samuelsen, O.B., Torsvik, V., Ervik, A., 1992. Long-range changes in oxytetracycline concentrations and bacterial resistance towards oxytetracycline in a fish farm sediment after medication. Science of the Total Environment, 114, 25-36.

Sarmah, A.K., Meyer, M.R., Boxall, A.B.A., 2006. A global perspective on the use, sales, exposure pathways, occurrence, fate and effects of veterinary antibiotics (VAs) in the environment. Chemosphere, 65, 725-759.

Sarter, S., Nguyen, H.N.K., Hung, L., Lazard, J., Montet, D., 2007. Antibiotic resistance in Gram-negative bacteria isolated from farmed Cat-fish. Food Control, 18, 1391-1396.

Sassman, S.A., Lee, L.S., 2005. Sorption of three tetracyclines by several soils: Assessing the role of pH and cation exchange. Environmental Science and Technology, 39, 7452-7459.

Schmitt, M.O., Schneider, S., 2000. Spectroscopic investigation of complexation between various tetracyclines and Mg^{2+} or Ca^{2+}. Physical Chemical Communication, 3, 42-55.

Schwarzenbach, R.P., Gschwend, P.M., Imboden, D.M., 1993. Environmental Organic Chemistry. John Wiley Science, Inc. New York, 255-260.

Simon, N.S. 2005. Loosely Bound Oxytetracycline in Riverine Sediments from Two Tributaries of the Chesapeake Bay. Environmental Science and Technology, 39, 3480-3487.

Sithole B.B., Guy, R.D., 1987a. Models for tetracycline in aquatic environments. I. Interaction with bentonite systems. Water, Air and Soil Pollution, 32, 303-314.

Sithole .B.B., Guy, R.D., 1987b. Models for tetracycline in aquatic environments. II. Interaction with humic substances. Water, Air and Soil Pollution, 32, 315-321.

Spaepen, K.R.I, Leemput, L.J.J., Wislosceke, P.G., Verschueren, C., 1997. A uniform procedure to estimate the predicted environmental concentrations of the residue of veterinary medicine in soil. Environmental Toxicology and Chemistry, 16, 1977-1982.

Stamatelatou, K., C., Frouda, M.S., Fountoulakis, P., Rdillia, M., Kornaros, Lyberatos, G., 2003. Pharmaceuticals and health care products in wastewater effluents: the example of carbazepine. Water Science and Technology, 3, 131-137.

Tamoseviç-Canoviç, M., Dakoviç, A., Rottinghaus, G., Matijaseviç, S., Duriciç, M., 2003. Surfactant modified zeolites-new efficient adsorbents for mycotoxins. Microporous and Mesoporous Materials, 61, 173-180.

Tavares, F.M.M., McGuffin, V., 1994. Seperation and characterization of tetracycline antibiotics by capillary electrophoresis. Journal of Chromotograpy A, 686, 129-142.

Terlaak, T.L., Gebbink, W.A., Tolls, J., 2006. The effect of pH and ionic strength on the sorption of sulfachloropyridazin, tylosin and oxytetracycline to soil. Environmental Toxicology and Chemistry, 25, 904-911.

Thiele-Bruhn, S., 2003. Pharmaceutical antibiotic compounds in soils-a review. Journal Plant, Nutrient, Soil Science, 166, 145-167.

Tolls, J., 2001. Sorption of veterinary pharmaceuticals in soils: Review. Environmental Science and Technology, 35, 3397-3406.

Tongraree, S., Flanagan, D.R., Poust., R., 1999a. The effects of pH and mixed solvent systems on the solubility of oxytetracycline. Pharmaceutical Development and Technology, 4, 571-580.

Tongraree, S., Flanagan, D.R., Poust., R, 1999b. The interaction between oxytetracycline and divalent metal ions in aqueous and mixed solvent systems. Pharmaceutical Development and Technology, 4, 581-591.

Tongraree, S., Goldberg, A.M., Flanagan, Poust., R., 2000. The effects of pH and PEG 400-water cosolvents on oxytetracycline- Magnesium complex formation. Pharmaceutical Development and Technology, 5, 189-199.

Vanderford, B.J., Pearson, R.A., Rexing, D.J., Snyder, S.A., 2003. Analysis of endocrine disruptors, pharmaceuticals, and personal care products in water using liquid chromatography/tandem mass spectrometry, Analytical Chemistry, 75, 6265-6274.

Violente, A., Gianfreda, L., 1993. Competition in adsorption between phosphate and oxalate on an aluminum hydroxide montmorillonite complex. Soil Science of Society of American Journal, 57, 1235-1247.

Vujakoviç, A.D., Tomasoviç-Canoviç, M.R., Dakoviç, A., Dondur, V.T., 2000. The adsorption of sulphate, hydrogenchromate and dihydogenphosphate anions on surfactant-modified clinoptilolite. Applied Clay Science, 17, 265-277.

Wang, Y., Liu, S., Xu, Z, Han, T, Chuan, S, Zhu, T., 2006. Ammonia removal from leachate solution using natural Chinese clinoptilolite. Journal of Hazardous Materials B, 136, 735-740.

Wessels, J.M., Ford, W.E., Szymczak, W., Schneider, S., 1998. The complexation of tetracycline and anhydrotetracycline with Mg^{2+} and Ca $^{2+}$: A spectroscopic study. Journal of Physical Chemistry, 102, 9323-9331.

Wiegel, S., Aulinger, A., Brokmeyer, R., Harms, H., Loffler, J., Reincke, H., Schmidt, R., Stachel, B., Tumpling, W., Wanke, A., 2004. Pharmaceuticals in the rier Elbe and its tributaries. Chemosphere, 57, 107-126.

Williamson, D.E., Everett, G.W.R., 1975. Proton nuclear magnetic resonance study of the site of metal binding in tetracycline. Journal of American Chemical Society, 97, 2397-2405.

Zwiener, C., Frimmel, F.H., 2000. Oxidative treatment of pharmaceuticals in water. Water Research, 34, 1881-1885.

http://www.epa.gov/epaoswer/hazwaste/test/pdfs/9081.pdf

http://www.fda.gov/cvm/FOI/038-439_EA.pdf

APPENDIX A

Calibration Curves of OTC

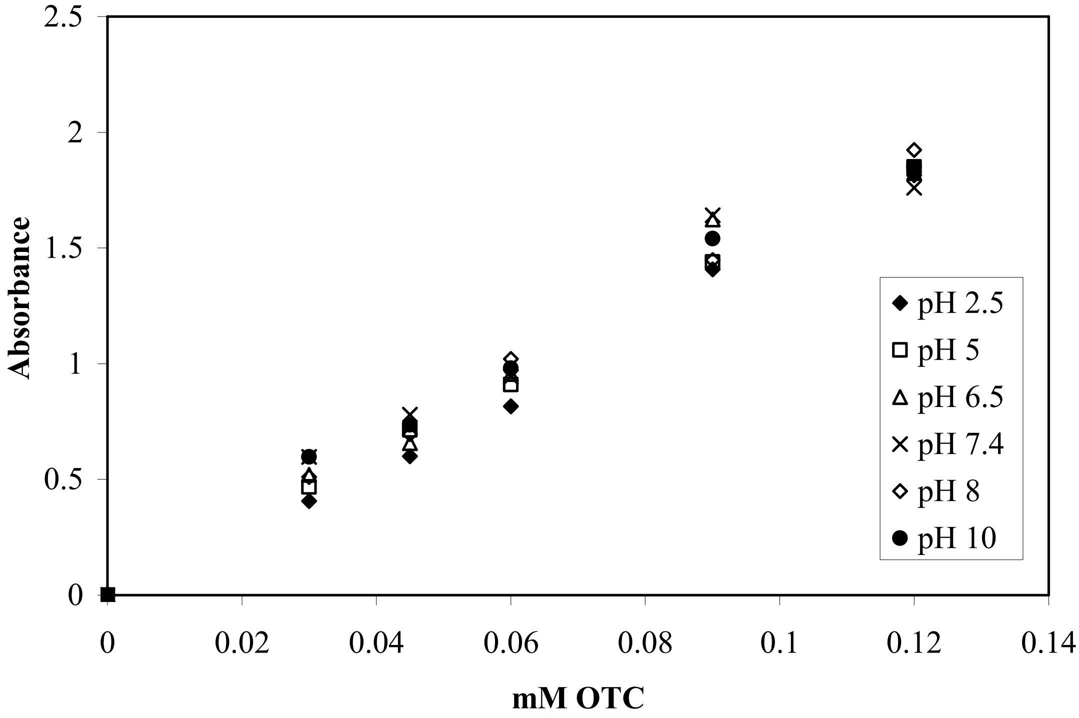

Figure A.1. Calibration curves of OTC at different pH.

Table A.1. Maximum absorption peak and extinction coefficient of OTC with different pH.

pH	λ (nm)	ε (R^2)
2.5	353	14.903 (0.992o)
5	354	15.583 (0.9988)
6.5	354	16.107 (0.9994)
7	362.5	16.144 (0.9938)
7.5	362.5	16.144 (0.9938)
8	364.5	16.159 (0.9981)
9.66	373	16.209 (0.9874)
10	373	16.209 (0.9874)

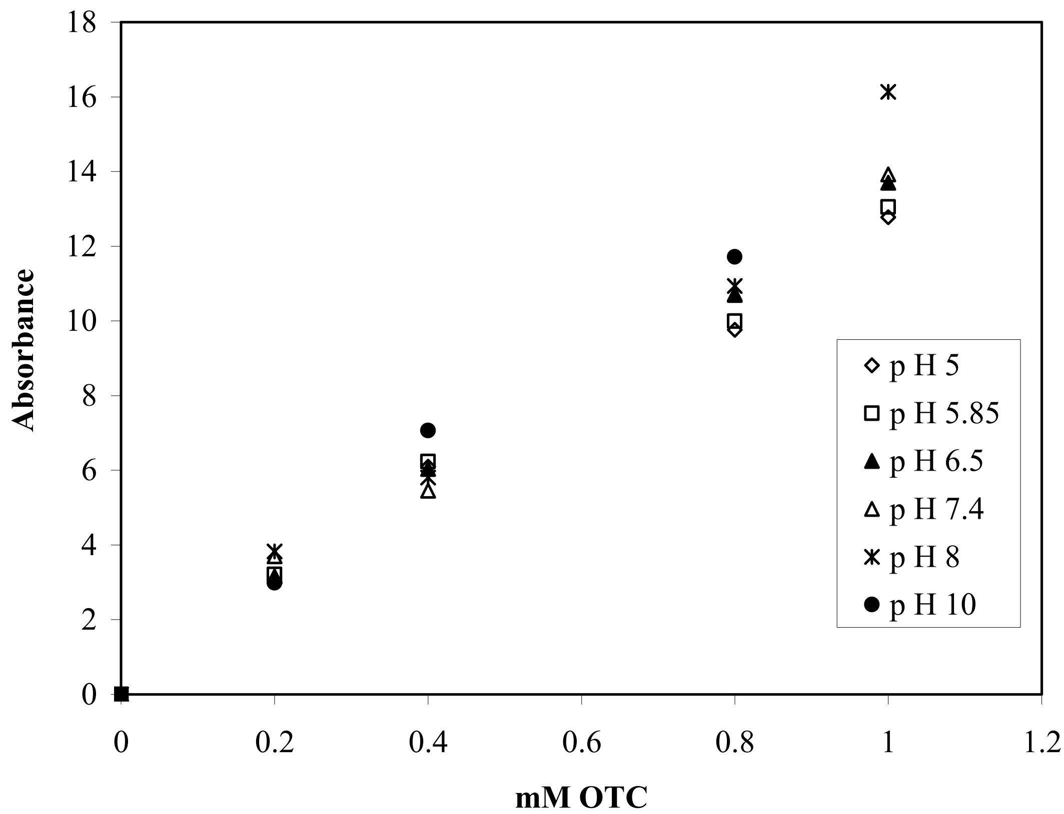

Figure A.2. Calibration curves of OTC with phosphate buffer at different pH values.

Table A.2. Maximum absorption peak and extinction coefficient of OTC with phosphate buffer at different pH.

pH	λ (nm)	ε (R^2)
5	354	12.844 (0.9868)
5.85	354	13.141 (0.9854)
6.5	354	13.712 (0.9958)
7.4	362.5	13.806 (0.9918)
8	364.5	15.199 (0.9807)
10	373	15.231 (0.9849)

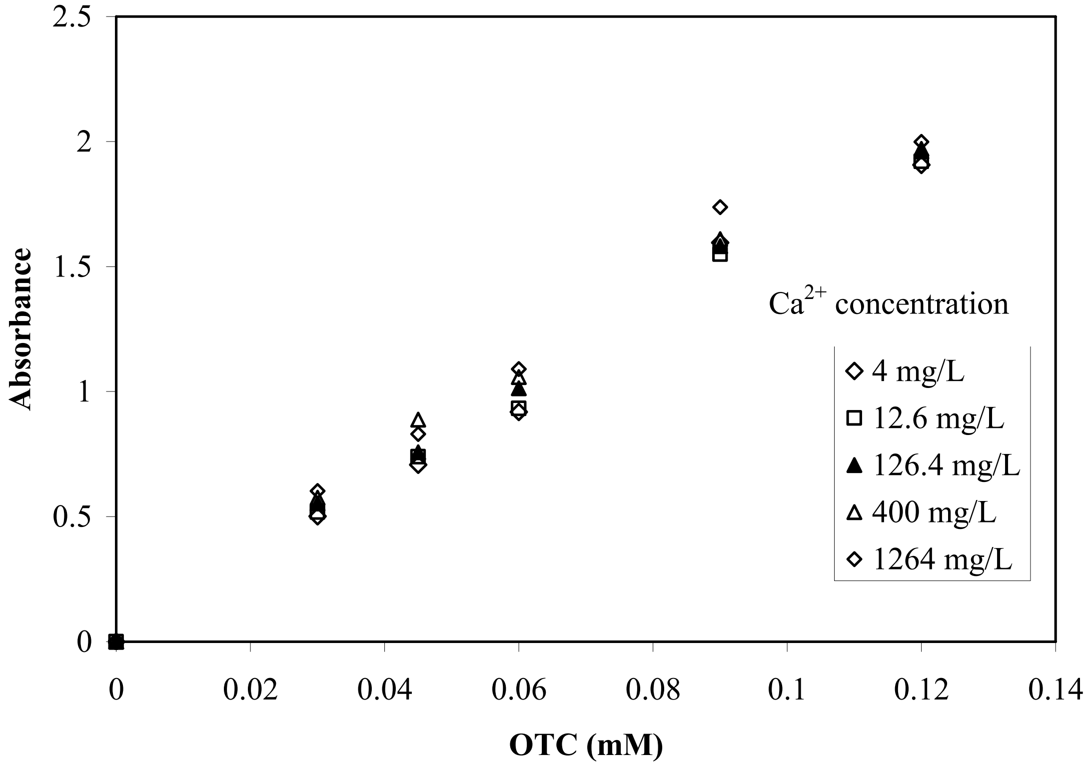

Figure A.3. Calibration curves of OTC with Ca^{2+} ions.

Table A.3. Maximum absorption peak and extinction coefficient of OTC in the presence and absence of Ca^{2+} ions.

Added Ca^{2+}(mg/L)	λ(nm)	ε (R^2)
0	354	16.107 (0.9798)
4	357	16.342 (0.9906)
12.6	360	16.356 (0.9955)
126.4	364.5	16.850 (0.9959)
400	364.5	17.296 (0.9982)
1264	364.5	17.812 (0.9840)

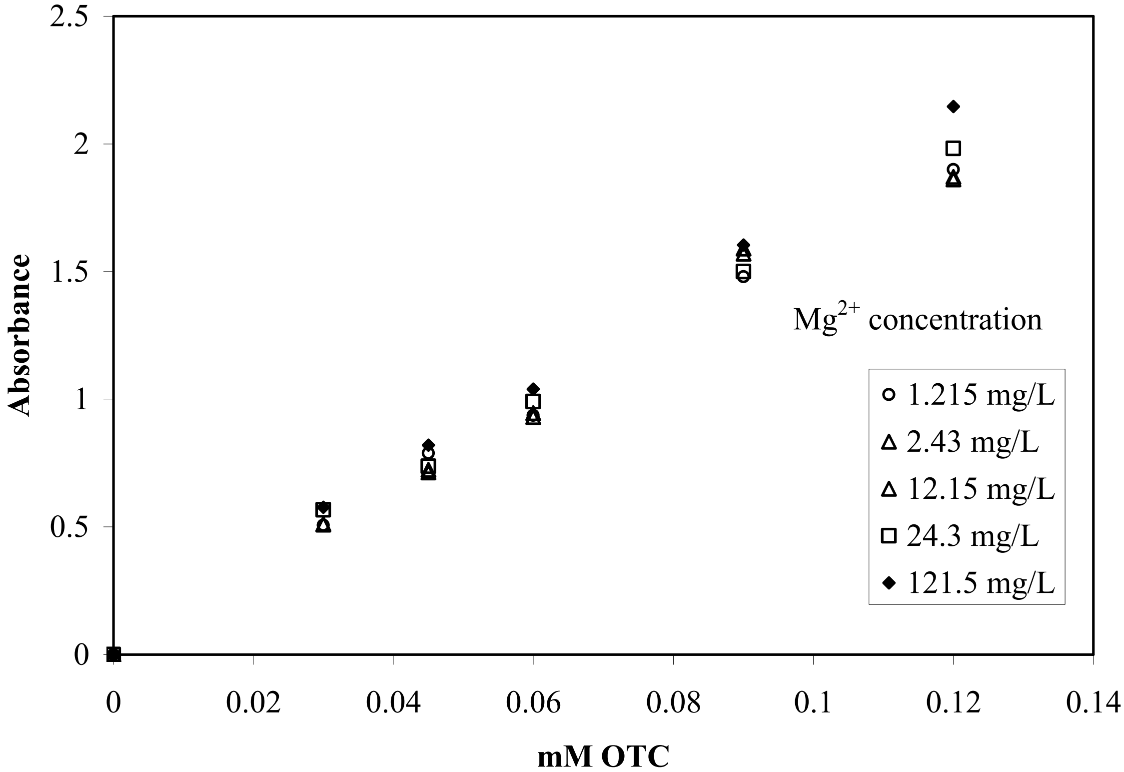

Figure A.4. Calibration curves of OTC with Mg^{2+} ions.

Table A.4. Maximum absorption peak and extinction coefficient of OTC in the presence and absence of Mg^{2+} ions.

Added Mg^{2+} (mg/L)	λ(nm)	ε (R^2)
0	354	16.107 (0.9798)
1.215	358	16.127 (0.9967)
2.43	358	16.155 (0.9914)
12.15	360	16.225 (0.9891)
24.3	363.5	16.621 (0.9980)
121.5	363.5	17.861 (0.9989)

APPENDIX B

Interlayer Spacings and Peak Intensities of Zeolites

Table B.1. Interlayer spacings and peak intensities of raw zeolite.

[raw.raw] raw — Peak ID Report

SCAN: 3.0/70.0/0.02/0.6(sec), Cu(40kV,40mA), I(max)=770, 09/29/06 12:04

PEAK: 21-pts/Parabolic Filter, Threshold=3.0, Cutoff=0.1%, BG=3/1.0, Peak-Top=Summit

NOTE: Intensity = Counts, 2T(0)=0.0(°), Wavelength to Compute d-Spacing = 1.54056Å (Cu/K-alpha1)

#	2-Theta	d(Å)	Height	Height%	Phase ID	d(Å)	I%	(h k l)	2-Theta	Delta
1	5.680	15.5469	68	9.4	Magadiite, syn - Na2Si14O29!10H2O	15.6815	77.0	(0 0 1)	5.631	-0.049
2	9.052	9.7616	196	27.2	Rb24Be24As24O96!3.2H2O - Zeolite Rho, (Rb...	9.7691	100.0	(1 1 0)	9.045	-0.007
3	9.940	8.8913	298	41.3	Clinoptilolite-Ca - KNa2Ca2(Si29Al7)O72!24H2O	8.8605	79.4	(0 2 0)	9.975	0.035
4	11.278	7.8391	148	20.5	Clinoptilolite-Ca - KNa2Ca2(Si29Al7)O72!24H2O	7.8597	10.3	(2 0 0)	11.248	-0.030
5	13.121	6.7417	105	14.6	Clinoptilolite-Ca - KNa2Ca2(Si29Al7)O72!24H2O	6.7287	7.1	(2 0-1)	13.147	0.026
6	17.001	5.2110	157	21.8	Clinoptilolite-Ca - KNa2Ca2(Si29Al7)O72!24H2O	5.2094	7.9	(3 1-1)	17.006	0.005
7	17.365	5.1026	157	21.8	Clinoptilolite-Ca - KNa2Ca2(Si29Al7)O72!24H2O	5.0908	9.5	(1 1 1)	17.405	0.040
8	19.176	4.6245	126	17.5	Clinoptilolite-Ca - KNa2Ca2(Si29Al7)O72!24H2O	4.6260	15.1	(1 3-1)	19.170	-0.006
9	20.504	4.3280	113	15.7	Clinoptilolite-Ca - KNa2Ca2(Si29Al7)O72!24H2O	4.3290	4.0	(4 0-1)	20.499	-0.005
10	20.857	4.2555	49	6.8	Magadiite, syn - Na2Si14O29!10H2O	4.2823	5.0	(0 1 3)	20.725	-0.132
11	21.782	4.0769	153	21.2	Magadiite, syn - Na2Si14O29!10H2O	4.0405	5.0	(1 0 3)	21.980	0.199
12	22.459	3.9555	721	100.0	Clinoptilolite-Ca - KNa2Ca2(Si29Al7)O72!24H2O	3.9585	48.4	(1 3 1)	22.441	-0.018
13	22.800	3.8970	445	61.7	Clinoptilolite-Ca - KNa2Ca2(Si29Al7)O72!24H2O	3.8881	38.1	(2 4 0)	22.853	0.053
14	23.718	3.7482	74	10.3	Rb24Be24As24O96!3.2H2O - Zeolite Rho, (Rb...	3.7234	32.3	(3 2 1)	23.879	0.160
15	24.176	3.6782	62	8.6	Clinoptilolite-Ca - KNa2Ca2(Si29Al7)O72!24H2O	3.6918	4.0	(0 4 1)	24.086	-0.090
16	25.181	3.5337	106	14.7	Clinoptilolite-Ca - KNa2Ca2(Si29Al7)O72!24H2O	3.5401	7.1	(3 1-2)	25.135	-0.046
17	25.781	3.4528	325	45.1	Magadiite, syn - Na2Si14O29!10H2O	3.4565	100.0	(2 0-2)	25.753	-0.028
18	26.120	3.4087	219	30.4	Clinoptilolite-Ca - KNa2Ca2(Si29Al7)O72!24H2O	3.4111	14.3	(2 2-2)	26.102	-0.019
19	26.397	3.3736	134	18.6	Clinoptilolite-Ca - KNa2Ca2(Si29Al7)O72!24H2O	3.3794	9.5	(4 0-2)	26.351	-0.046
20	26.779	3.3263	145	20.1	Magadiite, syn - Na2Si14O29!10H2O	3.3157	66.0	(0 2 2)	26.867	0.087
21	27.037	3.2952	238	33.0	Clinoptilolite-Ca - KNa2Ca2(Si29Al7)O72!24H2O	3.3039	4.8	(0 0 2)	26.964	-0.073
22	27.816	3.2046	190	26.4	Magadiite, syn - Na2Si14O29!10H2O	3.2141	14.0	(1 2-1)	27.733	-0.083
23	28.278	3.1533	225	31.2	Magadiite, syn - Na2Si14O29!10H2O	3.1587	98.0	(2 0-3)	28.229	-0.050
24	28.658	3.1124	107	14.8	Magadiite, syn - Na2Si14O29!10H2O	3.1105	1.0	(2 1-2)	28.676	0.018
25	29.122	3.0638	58	8.0	Clinoptilolite-Ca - KNa2Ca2(Si29Al7)O72!24H2O	3.0637	7.1	(1 3-2)	29.124	0.001
26	30.122	2.9644	284	39.4	Clinoptilolite-Ca - KNa2Ca2(Si29Al7)O72!24H2O	2.9614	37.3	(1 5 1)	30.153	0.031
27	32.043	2.7909	208	28.8	Clinoptilolite-Ca - KNa2Ca2(Si29Al7)O72!24H2O	2.7865	25.4	(5 3 0)	32.095	0.051
28	32.801	2.7281	85	11.8	Clinoptilolite-Ca - KNa2Ca2(Si29Al7)O72!24H2O	2.7219	12.7	(2 6-1)	32.878	0.076
29	33.498	2.6729	26	3.6	Clinoptilolite-Ca - KNa2Ca2(Si29Al7)O72!24H2O	2.6593	6.3	(2 0 2)	33.675	0.177

Materials Data, Inc.   [ARGE1|arge]<C:\Documents and Settings\arge\Desktop> Monday, Oct 02, 2006 05:01p (MDI/JADE6)

• Table B.1. Continued

[raw.raw] raw — **Peak ID Report**

SCAN: 3.0/70.0/0.02/0.6(sec), Cu(40kV,40mA), I(max)=770, 09/29/06 12:04

PEAK: 21-pts/Parabolic Filter, Threshold=3.0, Cutoff=0.1%, BG=3/1.0, Peak-Top=Summit

NOTE: Intensity = Counts, 2T(0)=0.0(°), Wavelength to Compute d-Spacing = 1.54056Å (Cu/K-alpha1)

#	2-Theta	d(Å)	Height	Height%	Phase ID	d(Å)	I%	(h k l)	2-Theta	Delta
30	35.522	2.5251	79	11.0	Clinoptilolite-Ca - KNa2Ca2(Si29Al7)O72!24H2O	2.5201	9.5	(6 2 0)	35.595	0.073
31	36.265	2.4750	49	6.8	Clinoptilolite-Ca - KNa2Ca2(Si29Al7)O72!24H2O	2.4784	4.8	(3 5 1)	36.215	-0.050
32	37.060	2.4238	70	9.7	Magadiite, syn - Na2Si14O29!10H2O	2.4200	1.0	(3 0 0)	37.120	0.060
33	38.310	2.3475	22	3.1	Magadiite, syn - Na2Si14O29!10H2O	2.3507	6.0	(3 0 1)	38.256	-0.055
34	46.199	1.9633	21	2.9	Clinoptilolite-Ca - KNa2Ca2(Si29Al7)O72!24H2O	1.9699	3.2	(1 9 0)	46.035	-0.164
35	46.830	1.9383	21	2.9	Magadiite, syn - Na2Si14O29!10H2O	1.9381	1.0	(2 1 6)	46.836	0.006
36	50.159	1.8172	103	14.3	Magadiite, syn - Na2Si14O29!10H2O	1.8267	24.0	(3 2 3)	49.880	-0.279
37	51.668	1.7677	59	8.2	Rb24Be24As24O96!3.2H2O - Zeolite Rho, (Rb...	1.7743	2.4	(2 3 7)	51.461	-0.206
38	55.566	1.6525	59	8.2	Rb24Be24As24O96!3.2H2O - Zeolite Rho, (Rb...	1.6468	2.6	(8 2 2)	55.777	0.211
39	65.866	1.4168	73	10.1	Rb24Be24As24O96!3.2H2O - Zeolite Rho, (Rb...	1.4120	5.3	(7 7 0)	66.119	0.253

Line Shifts of Individual Phases:

PDF#42-1350 - Magadiite, syn <2T(0) = -0.08, d/d(0) = 1.0>

PDF#39-1383 - Clinoptilolite-Ca <2T(0) = 0.1, d/d(0) = 1.0>

PDF#45-0129 - Zeolite Rho, (Rb,Be,As) <2T(0) = 0.12, d/d(0) = 1.0>

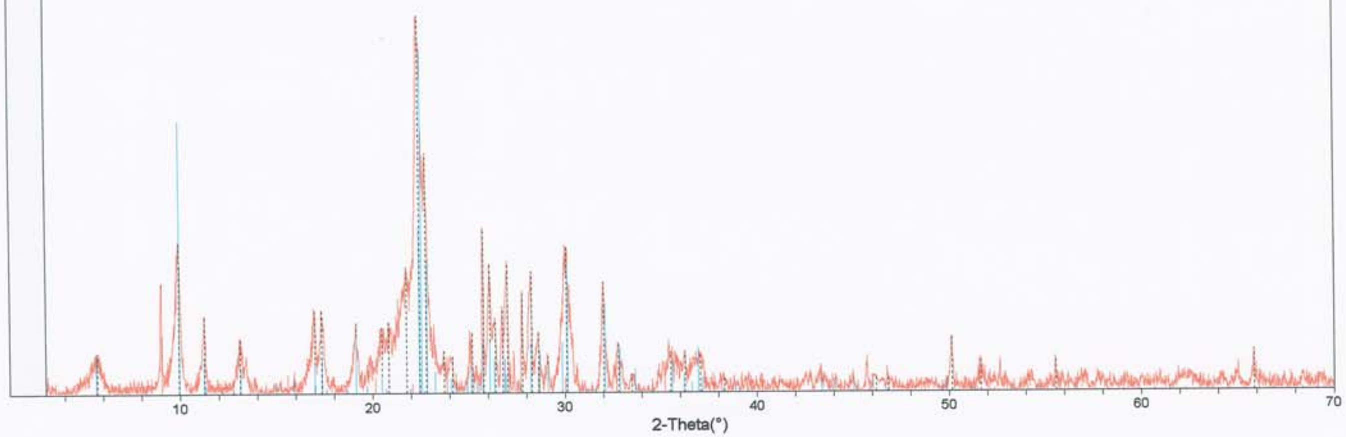

Table B.2. Interlayer spacings and peak intensities of Na zeolite.

[homoionic.raw] homoionic — Peak ID Report

SCAN: 3.0/70.0/0.02/0.6(sec), Cu(40kV,40mA), I(max)=1208, 09/29/06 14:26

PEAK: 23-pts/Parabolic Filter, Threshold=3.0, Cutoff=0.1%, BG=3/1.0, Peak-Top=Summit

NOTE: Intensity = Counts, 2T(0)=0.0(°), Wavelength to Compute d-Spacing = 1.54056Å (Cu/K-alpha1)

#	2-Theta	d(Å)	Height	Height%	Phase ID	d(Å)	I%	(h k l)	2-Theta	Delta
1	5.697	15.4988	141	12.7	Magadiite, syn - Na2Si14O29!10H2O	15.4081	77.0	(0 0 1)	5.731	0.034
2	9.020	9.7963	151	13.6	Rb24Be24As24O96!3.2H2O - Zeolite Rho, (Rb...	9.8124	100.0	(1 1 0)	9.005	-0.015
3	9.999	8.8389	423	38.0	Clinoptilolite-Ca - KNa2Ca2(Si29Al7)O72!24H2O	8.8783	79.4	(0 2 0)	9.955	-0.044
4	11.316	7.8127	217	19.5	Clinoptilolite-Ca - KNa2Ca2(Si29Al7)O72!24H2O	7.8737	10.3	(2 0 0)	11.228	-0.088
5	13.221	6.6912	143	12.8	Clinoptilolite-Ca - KNa2Ca2(Si29Al7)O72!24H2O	6.7389	7.1	(2 0-1)	13.127	-0.094
6	17.076	5.1883	209	18.8	Magadiite, syn - Na2Si14O29!10H2O	5.1700	15.0	(0 0 3)	17.137	0.061
7	17.440	5.0807	215	19.3	Clinoptilolite-Ca - KNa2Ca2(Si29Al7)O72!24H2O	5.0966	9.5	(1 1 1)	17.385	-0.055
8	19.217	4.6147	199	17.9	Clinoptilolite-Ca - KNa2Ca2(Si29Al7)O72!24H2O	4.6308	15.1	(1 3-1)	19.150	-0.067
9	19.960	4.4447	73	6.6	Magadiite, syn - Na2Si14O29!10H2O	4.4725	11.0	(1 0-3)	19.834	-0.126
10	20.543	4.3199	191	17.2	Clinoptilolite-Ca - KNa2Ca2(Si29Al7)O72!24H2O	4.3332	4.0	(4 0-1)	20.479	-0.064
11	21.019	4.2230	154	13.8	Magadiite, syn - Na2Si14O29!10H2O	4.2619	5.0	(0 1 3)	20.825	-0.194
12	22.520	3.9449	1113	100.0	Clinoptilolite-Ca - KNa2Ca2(Si29Al7)O72!24H2O	3.9411	100.0	(4 0 0)	22.542	0.022
13	22.899	3.8805	497	44.7	Clinoptilolite-Ca - KNa2Ca2(Si29Al7)O72!24H2O	3.8915	38.1	(2 4 0)	22.833	-0.066
14	24.194	3.6756	116	10.4	Clinoptilolite-Ca - KNa2Ca2(Si29Al7)O72!24H2O	3.6949	4.0	(0 4 1)	24.066	-0.128
15	25.198	3.5313	164	14.7	Clinoptilolite-Ca - KNa2Ca2(Si29Al7)O72!24H2O	3.5429	7.1	(3 1-2)	25.115	-0.084
16	26.161	3.4036	305	27.4	Clinoptilolite-Ca - KNa2Ca2(Si29Al7)O72!24H2O	3.4137	14.3	(2 2-2)	26.082	-0.079
17	26.401	3.3731	215	19.3	Clinoptilolite-Ca - KNa2Ca2(Si29Al7)O72!24H2O	3.3819	9.5	(4 0-2)	26.331	-0.070
18	26.838	3.3192	243	21.8	Clinoptilolite-Ca - KNa2Ca2(Si29Al7)O72!24H2O	3.3063	4.8	(0 0 2)	26.944	0.106
19	28.242	3.1572	310	27.9	Clinoptilolite-Ca - KNa2Ca2(Si29Al7)O72!24H2O	3.1612	12.7	(4 2-2)	28.206	-0.036
20	28.682	3.1098	132	11.9	Clinoptilolite-Ca - KNa2Ca2(Si29Al7)O72!24H2O	3.1115	11.9	(4 4-1)	28.666	-0.016
21	29.184	3.0575	79	7.1	Clinoptilolite-Ca - KNa2Ca2(Si29Al7)O72!24H2O	3.0657	7.1	(1 3-2)	29.104	-0.081
22	30.121	2.9645	446	40.1	Clinoptilolite-Ca - KNa2Ca2(Si29Al7)O72!24H2O	2.9633	37.3	(1 5 1)	30.133	0.012
23	32.119	2.7845	268	24.1	Clinoptilolite-Ca - KNa2Ca2(Si29Al7)O72!24H2O	2.7882	25.4	(5 3 0)	32.075	-0.044
24	32.920	2.7185	142	12.8	Clinoptilolite-Ca - KNa2Ca2(Si29Al7)O72!24H2O	2.7235	12.7	(2 6-1)	32.858	-0.063
25	33.556	2.6684	47	4.2	Clinoptilolite-Ca - KNa2Ca2(Si29Al7)O72!24H2O	2.6608	6.3	(2 0 2)	33.655	0.098
26	35.503	2.5265	109	9.8	Magadiite, syn - Na2Si14O29!10H2O	2.5246	1.0	(2 0 4)	35.529	0.027
27	36.077	2.4876	42	3.8	Clinoptilolite-Ca - KNa2Ca2(Si29Al7)O72!24H2O	2.4797	4.8	(3 5 1)	36.195	0.119
28	36.857	2.4367	112	10.1	Clinoptilolite-Ca - KNa2Ca2(Si29Al7)O72!24H2O	2.4319	12.7	(2 6 1)	36.932	0.075
29	37.159	2.4176	99	8.9	Clinoptilolite-Ca - KNa2Ca2(Si29Al7)O72!24H2O	2.4170	4.0	(4 4 1)	37.168	0.010

Materials Data, Inc.

[ARGE1|arge]<C:\Documents and Settings\arge\Desktop> Tuesday, Oct 03, 2006 10:34a (MDI/JADE6)

Table B.2. Continued

[homoionic.raw] homoionic — Peak ID Report

SCAN: 3.0/70.0/0.02/0.6(sec), Cu(40kV,40mA), I(max)=1208, 09/29/06 14:26

PEAK: 23-pts/Parabolic Filter, Threshold=3.0, Cutoff=0.1%, BG=3/1.0, Peak-Top=Summit

NOTE: Intensity = Counts, 2T(0)=0.0(°), Wavelength to Compute d-Spacing = 1.54056Å (Cu/K-alpha1)

#	2-Theta	d(Å)	Height	Height%	Phase ID	d(Å)	I%	(h k l)	2-Theta	Delta
30	38.324	2.3467	27	2.4	Magadiite, syn - Na2Si14O29!10H2O	2.3448	6.0	(3 0 1)	38.356	0.031
31	39.646	2.2714	73	6.6	Magadiite, syn - Na2Si14O29!10H2O	2.2719	4.0	(3 1-2)	39.638	-0.008
32	42.819	2.1102	39	3.5	Rb24Be24As24O96!3.2H2O - Zeolite Rho, (Rb...	2.1070	0.2	(6 2 2)	42.887	0.068
33	43.378	2.0843	48	4.3	Clinoptilolite-Ca - KNa2Ca2(Si29Al7)O72!24H2O	2.0853	4.8	(3 7-2)	43.355	-0.023
34	50.236	1.8146	46	4.1	Magadiite, syn - Na2Si14O29!10H2O	1.8233	24.0	(3 2 3)	49.980	-0.256
35	52.310	1.7474	24	2.2	Rb24Be24As24O96!3.2H2O - Zeolite Rho, (Rb...	1.7476	1.2	(8 0 0)	52.304	-0.006
36	54.339	1.6869	74	6.6	Rb24Be24As24O96!3.2H2O - Zeolite Rho, (Rb...	1.6955	4.0	(8 2 0)	54.039	-0.300
37	57.986	1.5892	38	3.4	Rb24Be24As24O96!3.2H2O - Zeolite Rho, (Rb...	1.5833	1.0	(7 5 2)	58.221	0.235
38	62.156	1.4922	52	4.7	Rb24Be24As24O96!3.2H2O - Zeolite Rho, (Rb...	1.4908	0.4	(6 6 4)	62.222	0.066
39	64.280	1.4479	36	3.2	Rb24Be24As24O96!3.2H2O - Zeolite Rho, (Rb...	1.4425	1.3	(2 3 9)	64.551	0.272

Line Shifts of Individual Phases:

PDF#39-1383 - Clinoptilolite-Ca <2T(0) = 0.08, d/d(0) = 1.0>
PDF#42-1350 - Magadiite, syn <2T(0) = 0.02, d/d(0) = 1.0>
PDF#45-0129 - Zeolite Rho, (Rb,Be,As) <2T(0) = 0.08, d/d(0) = 1.0>

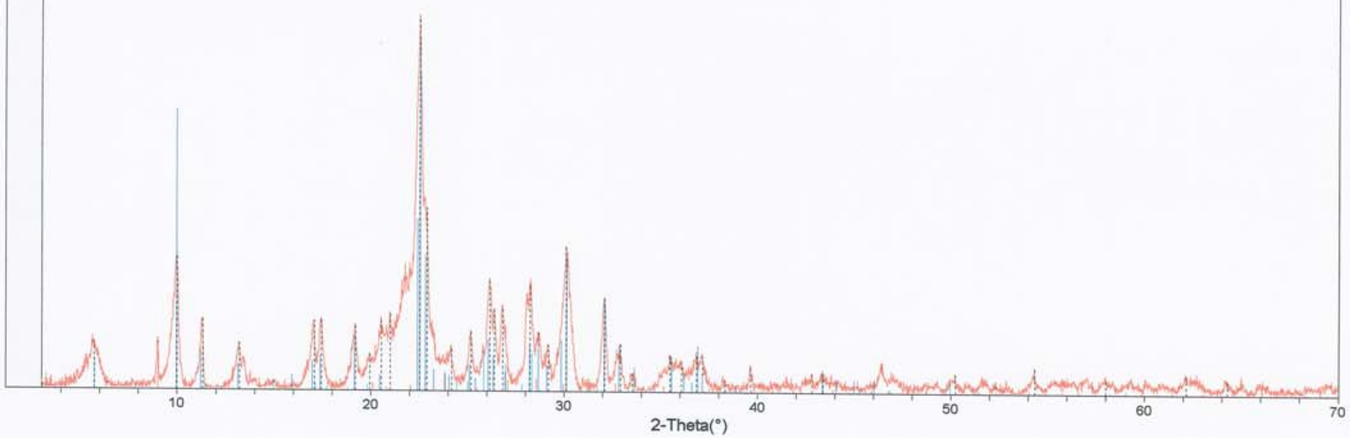

Materials Data, Inc.

[ARGE1|arge]<C:\Documents and Settings\arge\Desktop> Tuesday, Oct 03, 2006 10:34a (MDI/JADE6)

Table B.3. Interlayer spacings and peak intensities of HDTMA-modified zeolite.

[modified.raw] modified — Peak ID Report

SCAN: 3.0/70.0/0.02/0.6(sec), Cu(40kV,40mA), I(max)=681, 09/29/06 13:47

PEAK: 17-pts/Parabolic Filter, Threshold=3.0, Cutoff=0.1%, BG=3/1.0, Peak-Top=Summit

NOTE: Intensity = Counts, 2T(0)=0.0(°), Wavelength to Compute d-Spacing = 1.54056Å (Cu/K-alpha1)

#	2-Theta	d(Å)	Height	Height%	Phase ID	d(Å)	I%	(h k l)	2-Theta	Delta
1	5.760	15.3307	13	2.1	Magadiite, syn - Na2Si14O29!10H2O	15.3014	77.0	(0 0 1)	5.771	0.011
2	8.983	9.8357	41	6.6	(C17H13N)xSiO2 - RUB-3	9.7659	63.3	(1 1 0)	9.048	0.064
3	9.980	8.8560	242	38.8	Clinoptilolite-Ca - KNa2Ca2(Si29Al7)O72!24H2O	8.9140	79.4	(0 2 0)	9.915	-0.065
4	11.296	7.8265	141	22.6	Clinoptilolite-Ca - KNa2Ca2(Si29Al7)O72!24H2O	7.9017	10.3	(2 0 0)	11.188	-0.108
5	13.144	6.7300	86	13.8	Clinoptilolite-Ca - KNa2Ca2(Si29Al7)O72!24H2O	6.7594	7.1	(2 0-1)	13.087	-0.057
6	16.981	5.2170	129	20.7	Clinoptilolite-Ca - KNa2Ca2(Si29Al7)O72!24H2O	5.2277	7.9	(3 1-1)	16.946	-0.035
7	17.419	5.0869	143	22.9	Clinoptilolite-Ca - KNa2Ca2(Si29Al7)O72!24H2O	5.1083	9.5	(1 1 1)	17.345	-0.073
8	19.179	4.6240	124	19.9	Clinoptilolite-Ca - KNa2Ca2(Si29Al7)O72!24H2O	4.6404	15.1	(1 3-1)	19.110	-0.068
9	20.579	4.3124	110	17.6	(C17H13N)xSiO2 - RUB-3	4.3258	49.4	(1 3 0)	20.514	-0.064
10	21.000	4.2268	143	22.9	Magadiite, syn - Na2Si14O29!10H2O	4.2539	5.0	(0 1 3)	20.865	-0.135
11	22.461	3.9551	624	100.0	Clinoptilolite-Ca - KNa2Ca2(Si29Al7)O72!24H2O	3.9481	100.0	(4 0 0)	22.502	0.041
12	22.781	3.9003	354	56.7	Clinoptilolite-Ca - KNa2Ca2(Si29Al7)O72!24H2O	3.8982	38.1	(2 4 0)	22.793	0.012
13	23.275	3.8185	56	9.0	Clinoptilolite-Ca - KNa2Ca2(Si29Al7)O72!24H2O	3.8285	5.6	(2 2 1)	23.214	-0.061
14	23.716	3.7486	113	18.1	Clinoptilolite-Ca - KNa2Ca2(Si29Al7)O72!24H2O	3.7318	4.8	(2 4-1)	23.824	0.108
15	24.191	3.6760	53	8.5	Clinoptilolite-Ca - KNa2Ca2(Si29Al7)O72!24H2O	3.7009	4.0	(0 4 1)	24.026	-0.165
16	25.160	3.5366	94	15.1	(C17H13N)xSiO2 - RUB-3	3.5461	8.2	(2 0-2)	25.091	-0.069
17	26.102	3.4110	202	32.4	(C17H13N)xSiO2 - RUB-3	3.4132	14.6	(0 4 0)	26.085	-0.017
18	26.361	3.3782	182	29.2	Clinoptilolite-Ca - KNa2Ca2(Si29Al7)O72!24H2O	3.3869	9.5	(4 0-2)	26.291	-0.070
19	26.778	3.3264	482	77.2	Clinoptilolite-Ca - KNa2Ca2(Si29Al7)O72!24H2O	3.3112	4.8	(0 0 2)	26.904	0.126
20	27.820	3.2042	428	68.6	Magadiite, syn - Na2Si14O29!10H2O	3.1982	14.0	(1 2-1)	27.873	0.053
21	28.237	3.1578	223	35.7	Clinoptilolite-Ca - KNa2Ca2(Si29Al7)O72!24H2O	3.1656	12.7	(4 2-2)	28.166	-0.071
22	28.658	3.1124	91	14.6	Clinoptilolite-Ca - KNa2Ca2(Si29Al7)O72!24H2O	3.1157	11.9	(4 4-1)	28.626	-0.031
23	29.076	3.0686	50	8.0	Clinoptilolite-Ca - KNa2Ca2(Si29Al7)O72!24H2O	3.0699	7.1	(1 3-2)	29.064	-0.012
24	30.081	2.9683	261	41.8	Clinoptilolite-Ca - KNa2Ca2(Si29Al7)O72!24H2O	2.9671	37.3	(1 5 1)	30.093	0.012
25	32.042	2.7910	179	28.7	Clinoptilolite-Ca - KNa2Ca2(Si29Al7)O72!24H2O	2.7916	25.4	(5 3 0)	32.035	-0.007
26	32.835	2.7254	83	13.3	Clinoptilolite-Ca - KNa2Ca2(Si29Al7)O72!24H2O	2.7268	12.7	(2 6-1)	32.818	-0.017
27	35.425	2.5318	77	12.3	Clinoptilolite-Ca - KNa2Ca2(Si29Al7)O72!24H2O	2.5242	9.5	(6 2 0)	35.535	0.110
28	35.643	2.5168	65	10.4	Magadiite, syn - Na2Si14O29!10H2O	2.5219	1.0	(2 0 4)	35.569	-0.074
29	35.977	2.4942	43	6.9	Clinoptilolite-Ca - KNa2Ca2(Si29Al7)O72!24H2O	2.4823	4.8	(3 5 1)	36.155	0.178

Materials Data, Inc.

[ARGE1|arge]<C:\Documents and Settings\arge\Desktop> Tuesday, Oct 03, 2006 10:50a (MDI/JADE6)

• Table B. 3. Continued

[modified.raw] modified — Peak ID Report

SCAN: 3.0/70.0/0.02/0.6(sec), Cu(40kV,40mA), I(max)=681, 09/29/06 13:47

PEAK: 17-pts/Parabolic Filter, Threshold=3.0, Cutoff=0.1%, BG=3/1.0, Peak-Top=Summit

NOTE: Intensity = Counts, 2T(0)=0.0(°), Wavelength to Compute d-Spacing = 1.54056Å (Cu/K-alpha1)

#	2-Theta	d(Å)	Height	Height%	Phase ID	d(Å)	I%	(h k l)	2-Theta	Delta
30	36.714	2.4458	94	15.1	(C17H13N)xSiO2 - RUB-3	2.4408	1.3	(0 0 3)	36.792	0.078
31	37.101	2.4212	87	13.9	(C17H13N)xSiO2 - RUB-3	2.4203	2.5	(5 1-2)	37.116	0.015
32	39.509	2.2790	38	6.1	Magadiite, syn - Na2Si14O29!10H2O	2.2697	4.0	(3 1-2)	39.678	0.169
33	43.291	2.0883	39	6.3	Clinoptilolite-Ca - KNa2Ca2(Si29Al7)O72!24H2O	2.0872	4.8	(3 7-2)	43.315	0.024
34	45.034	2.0114	17	2.7	Clinoptilolite-Ca - KNa2Ca2(Si29Al7)O72!24H2O	2.0143	3.2	(6 4-3)	44.966	-0.069
35	46.704	1.9433	66	10.6	Magadiite, syn - Na2Si14O29!10H2O	1.9387	4.0	(1 0-8)	46.822	0.119
36	50.242	1.8144	101	16.2	Magadiite, syn - Na2Si14O29!10H2O	1.8220	24.0	(3 2 3)	50.020	-0.222

Line Shifts of Individual Phases:

PDF#39-1383 - Clinoptilolite-Ca <2T(0) = 0.04, d/d(0) = 1.0>
PDF#42-1350 - Magadiite, syn <2T(0) = 0.06, d/d(0) = 1.0>
PDF#50-1695 - RUB-3 <2T(0) = -0.1, d/d(0) = 1.0>

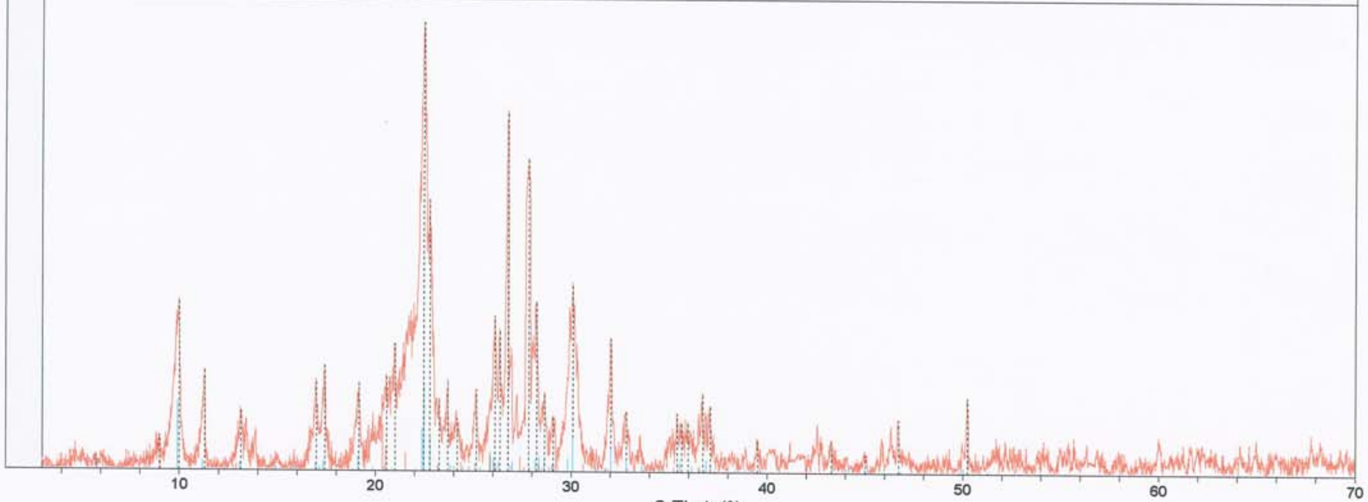

Table B.4. Interlayer spacings and peak intensities of Na zeolite equilibrated with OTC at pH 1.5.

[pH1-5.raw] pH1-5 — Peak ID Report

SCAN: 3.0/75.0/0.02/0.6(sec), Cu(40kV,40mA), I(max)=1164, 10/04/06 17:33

PEAK: 23-pts/Parabolic Filter, Threshold=3.0, Cutoff=0.1%, BG=3/1.0, Peak-Top=Summit

NOTE: Intensity = Counts, 2T(0)=0.0(°), Wavelength to Compute d-Spacing = 1.54056Å (Cu/K-alpha1)

#	2-Theta	d(Å)	Height	Height%	Phase ID	d(Å)	I%	(h k l)	2-Theta	Delta
1	5.773	15.2969	50	5.4	Magadiite, syn - Na2Si14O29!10H2O	15.6815	77.0	(0 0 1)	5.631	-0.142
2	9.980	8.8555	401	43.2	Clinoptilolite-Ca - KNa2Ca2(Si29Al7)O72!24H2O	8.8605	79.4	(0 2 0)	9.975	-0.006
3	11.302	7.8226	191	20.6	Magadiite, syn - Na2Si14O29!10H2O	7.7914	11.0	(0 0 2)	11.347	0.045
4	13.199	6.7022	131	14.1	Clinoptilolite-Ca - KNa2Ca2(Si29Al7)O72!24H2O	6.7287	7.1	(2 0-1)	13.147	-0.052
5	16.985	5.2158	138	14.9	Clinoptilolite-Ca - KNa2Ca2(Si29Al7)O72!24H2O	5.2094	7.9	(3 1-1)	17.006	0.021
6	17.478	5.0698	212	22.8	Clinoptilolite-Ca - KNa2Ca2(Si29Al7)O72!24H2O	5.0908	9.5	(1 1 1)	17.405	-0.073
7	19.180	4.6237	162	17.4	Clinoptilolite-Ca - KNa2Ca2(Si29Al7)O72!24H2O	4.6260	15.1	(1 3-1)	19.170	-0.009
8	20.542	4.3201	168	18.1	Clinoptilolite-Ca - KNa2Ca2(Si29Al7)O72!24H2O	4.3290	4.0	(4 0-1)	20.499	-0.043
9	22.520	3.9449	929	100.0	Clinoptilolite-Ca - KNa2Ca2(Si29Al7)O72!24H2O	3.9377	100.0	(4 0 0)	22.562	0.042
10	22.879	3.8838	497	53.5	Clinoptilolite-Ca - KNa2Ca2(Si29Al7)O72!24H2O	3.8881	38.1	(2 4 0)	22.853	-0.026
11	24.082	3.6924	67	7.2	Clinoptilolite-Ca - KNa2Ca2(Si29Al7)O72!24H2O	3.6918	4.0	(0 4 1)	24.086	0.003
12	25.200	3.5310	142	15.3	Clinoptilolite-Ca - KNa2Ca2(Si29Al7)O72!24H2O	3.5401	7.1	(3 1-2)	25.135	-0.066
13	26.180	3.4011	300	32.3	Clinoptilolite-Ca - KNa2Ca2(Si29Al7)O72!24H2O	3.4111	14.3	(2 2-2)	26.102	-0.079
14	26.833	3.3197	230	24.8	Magadiite, syn - Na2Si14O29!10H2O	3.3157	66.0	(0 2 2)	26.867	0.033
15	27.780	3.2088	291	31.3	Magadiite, syn - Na2Si14O29!10H2O	3.2141	14.0	(1 2-1)	27.733	-0.047
16	28.195	3.1625	426	45.9	Clinoptilolite-Ca - KNa2Ca2(Si29Al7)O72!24H2O	3.1590	12.7	(4 2-2)	28.226	0.032
17	28.776	3.0999	67	7.2	Clinoptilolite-Ca - KNa2Ca2(Si29Al7)O72!24H2O	3.1094	11.9	(4 4-1)	28.686	-0.090
18	29.219	3.0539	68	7.3	Clinoptilolite-Ca - KNa2Ca2(Si29Al7)O72!24H2O	3.0637	7.1	(1 3-2)	29.124	-0.096
19	30.161	2.9607	368	39.6	Clinoptilolite-Ca - KNa2Ca2(Si29Al7)O72!24H2O	2.9614	37.3	(1 5 1)	30.153	-0.007
20	32.139	2.7827	251	27.0	Clinoptilolite-Ca - KNa2Ca2(Si29Al7)O72!24H2O	2.7865	25.4	(5 3 0)	32.095	-0.045
21	32.943	2.7167	100	10.8	Clinoptilolite-Ca - KNa2Ca2(Si29Al7)O72!24H2O	2.7219	12.7	(2 6-1)	32.878	-0.065
22	33.623	2.6633	50	5.4	Clinoptilolite-Ca - KNa2Ca2(Si29Al7)O72!24H2O	2.6593	6.3	(2 0 2)	33.675	0.052
23	35.619	2.5184	64	6.9	Clinoptilolite-Ca - KNa2Ca2(Si29Al7)O72!24H2O	2.5201	9.5	(6 2 0)	35.595	-0.025
24	37.158	2.4176	84	9.0	Clinoptilolite-Ca - KNa2Ca2(Si29Al7)O72!24H2O	2.4157	4.0	(4 4 1)	37.188	0.030
25	43.301	2.0878	45	4.8	Clinoptilolite-Ca - KNa2Ca2(Si29Al7)O72!24H2O	2.0844	4.8	(3 7-2)	43.375	0.073
26	45.061	2.0103	39	4.2	Clinoptilolite-Ca - KNa2Ca2(Si29Al7)O72!24H2O	2.0118	3.2	(6 4-3)	45.026	-0.035
27	45.622	1.9868	40	4.3	Magadiite, syn - Na2Si14O29!10H2O	1.9793	1.0	(3 2 1)	45.806	0.184
28	46.404	1.9552	60	6.5	Magadiite, syn - Na2Si14O29!10H2O	1.9441	4.0	(1 0-8)	46.682	0.279
29	46.902	1.9355	38	4.1	Magadiite, syn - Na2Si14O29!10H2O	1.9381	1.0	(2 1 6)	46.836	-0.066

Materials Data, Inc.   [ARGE1|arge]<C:\Documents and Settings\arge\Desktop> Friday, Oct 06, 2006 10:09a (MDI/JADE6)

• Table B.5. Interlayer spacings and peak intensities of Na zeolite equilibrated with OTC at pH 10.

[pH10.raw] pH10 — Peak ID Report

SCAN: 3.0/75.0/0.02/0.6(sec), Cu(40kV,40mA), I(max)=1157, 10/04/06 19:32

PEAK: 23-pts/Parabolic Filter, Threshold=3.0, Cutoff=0.1%, BG=3/1.0, Peak-Top=Summit

NOTE: Intensity = Counts, 2T(0)=0.0(°), Wavelength to Compute d-Spacing = 1.54056Å (Cu/K-alpha1)

#	2-Theta	d(Å)	Height	Height%	Phase ID	d(Å)	I%	(h k l)	2-Theta	Delta
1	5.757	15.3379	63	6.2	Magadiite, syn - Na2Si14O29!10H2O	15.5710	77.0	(0 0 1)	5.671	-0.086
2	9.921	8.9081	442	43.7	Clinoptilolite-Ca - KNa2Ca2(Si29Al7)O72!24H2O	8.8783	79.4	(0 2 0)	9.955	0.033
3	11.261	7.8508	227	22.5	Clinoptilolite-Ca - KNa2Ca2(Si29Al7)O72!24H2O	7.8737	10.3	(2 0 0)	11.228	-0.033
4	13.143	6.7307	160	15.8	Clinoptilolite-Ca - KNa2Ca2(Si29Al7)O72!24H2O	6.7389	7.1	(2 0-1)	13.127	-0.016
5	16.982	5.2168	189	18.7	Clinoptilolite-Ca - KNa2Ca2(Si29Al7)O72!24H2O	5.2155	7.9	(3 1-1)	16.986	0.004
6	17.421	5.0864	264	26.1	Clinoptilolite-Ca - KNa2Ca2(Si29Al7)O72!24H2O	5.0966	9.5	(1 1 1)	17.385	-0.035
7	19.122	4.6375	175	17.3	Clinoptilolite-Ca - KNa2Ca2(Si29Al7)O72!24H2O	4.6308	15.1	(1 3-1)	19.150	0.028
8	19.859	4.4670	47	4.6	Magadiite, syn - Na2Si14O29!10H2O	4.4860	11.0	(1 0-3)	19.774	-0.085
9	20.521	4.3244	151	14.9	Clinoptilolite-Ca - KNa2Ca2(Si29Al7)O72!24H2O	4.3332	4.0	(4 0-1)	20.479	-0.042
10	22.520	3.9449	1011	100.0	Clinoptilolite-Ca - KNa2Ca2(Si29Al7)O72!24H2O	3.9411	100.0	(4 0 0)	22.542	0.022
11	22.820	3.8937	549	54.3	Clinoptilolite-Ca - KNa2Ca2(Si29Al7)O72!24H2O	3.8915	38.1	(2 4 0)	22.833	0.013
12	23.764	3.7411	84	8.3	Clinoptilolite-Ca - KNa2Ca2(Si29Al7)O72!24H2O	3.7256	4.8	(2 4-1)	23.864	0.100
13	24.103	3.6892	57	5.6	Clinoptilolite-Ca - KNa2Ca2(Si29Al7)O72!24H2O	3.6949	4.0	(0 4 1)	24.066	-0.037
14	25.212	3.5294	127	12.6	Clinoptilolite-Ca - KNa2Ca2(Si29Al7)O72!24H2O	3.5429	7.1	(3 1-2)	25.115	-0.097
15	26.121	3.4086	291	28.8	Clinoptilolite-Ca - KNa2Ca2(Si29Al7)O72!24H2O	3.4137	14.3	(2 2-2)	26.082	-0.039
16	27.081	3.2899	97	9.6	Clinoptilolite-Ca - KNa2Ca2(Si29Al7)O72!24H2O	3.3063	4.8	(0 0 2)	26.944	-0.137
17	27.660	3.2224	13	1.3	Magadiite, syn - Na2Si14O29!10H2O	3.2095	14.0	(1 2-1)	27.773	0.113
18	28.201	3.1618	256	25.3	Clinoptilolite-Ca - KNa2Ca2(Si29Al7)O72!24H2O	3.1612	12.7	(4 2-2)	28.206	0.005
19	28.662	3.1119	98	9.7	Clinoptilolite-Ca - KNa2Ca2(Si29Al7)O72!24H2O	3.1115	11.9	(4 4-1)	28.666	0.004
20	29.124	3.0636	86	8.5	Clinoptilolite-Ca - KNa2Ca2(Si29Al7)O72!24H2O	3.0657	7.1	(1 3-2)	29.104	-0.021
21	30.140	2.9626	421	41.6	Clinoptilolite-Ca - KNa2Ca2(Si29Al7)O72!24H2O	2.9633	37.3	(1 5 1)	30.133	-0.007
22	30.925	2.8892	178	17.6	Magadiite, syn - Na2Si14O29!10H2O	2.9017	1.0	(2 1 2)	30.789	-0.136
23	32.062	2.7893	252	24.9	Clinoptilolite-Ca - KNa2Ca2(Si29Al7)O72!24H2O	2.7882	25.4	(5 3 0)	32.075	0.013
24	32.821	2.7265	98	9.7	Clinoptilolite-Ca - KNa2Ca2(Si29Al7)O72!24H2O	2.7235	12.7	(2 6-1)	32.858	0.036
25	33.563	2.6679	47	4.6	Clinoptilolite-Ca - KNa2Ca2(Si29Al7)O72!24H2O	2.6608	6.3	(2 0 2)	33.655	0.091
26	35.559	2.5226	65	6.4	Clinoptilolite-Ca - KNa2Ca2(Si29Al7)O72!24H2O	2.5215	9.5	(6 2 0)	35.575	0.016
27	36.043	2.4898	52	5.1	Clinoptilolite-Ca - KNa2Ca2(Si29Al7)O72!24H2O	2.4797	4.8	(3 5 1)	36.195	0.153
28	36.738	2.4443	70	6.9	Clinoptilolite-Ca - KNa2Ca2(Si29Al7)O72!24H2O	2.4528	2.4	(6 4-1)	36.606	-0.132
29	37.102	2.4211	108	10.7	Magadiite, syn - Na2Si14O29!10H2O	2.4175	1.0	(3 0 0)	37.160	0.058

Materials Data, Inc. [ARGE1|arge]<C:\Documents and Settings\arge\Desktop> Tuesday, Oct 17, 2006 10:44a (MDI/JADE6)

Table B.5. Continued

[pH10.raw] pH10 — **Peak ID Report**

SCAN: 3.0/75.0/0.02/0.6(sec), Cu(40kV,40mA), I(max)=1157, 10/04/06 19:32

PEAK: 23-pts/Parabolic Filter, Threshold=3.0, Cutoff=0.1%, BG=3/1.0, Peak-Top=Summit

NOTE: Intensity = Counts, 2T(0)=0.0(°), Wavelength to Compute d-Spacing = 1.54056Å (Cu/K-alpha1)

#	2-Theta	d(Å)	Height	Height%	Phase ID	d(Å)	I%	(h k l)	2-Theta	Delta
30	46.435	1.9539	56	5.5	Magadiite, syn - Na2Si14O29!10H2O	1.9426	4.0	(1 0-8)	46.722	0.288

Line Shifts of Individual Phases:

PDF#39-1383 - Clinoptilolite-Ca <2T(0) = 0.08, d/d(0) = 1.0>

PDF#42-1350 - Magadiite, syn <2T(0) = -0.04, d/d(0) = 1.0>

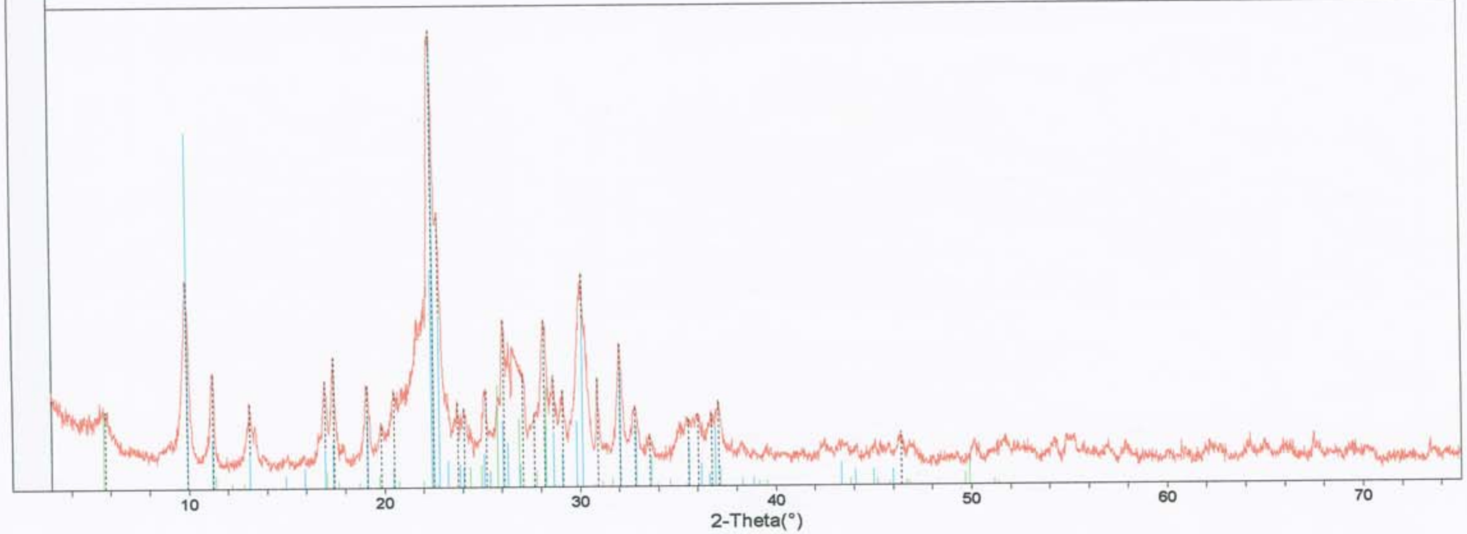

Materials Data, Inc. [ARGE1|arge]<C:\Documents and Settings\arge\Desktop> Tuesday, Oct 17, 2006 10:44a (MDI/JADE6)